

SGP-TR-99

Chelated Indium Activable Tracers
for Geothermal Reservoirs

Constantinos V. Chrysikopoulos
Paul Kruger

June 1986

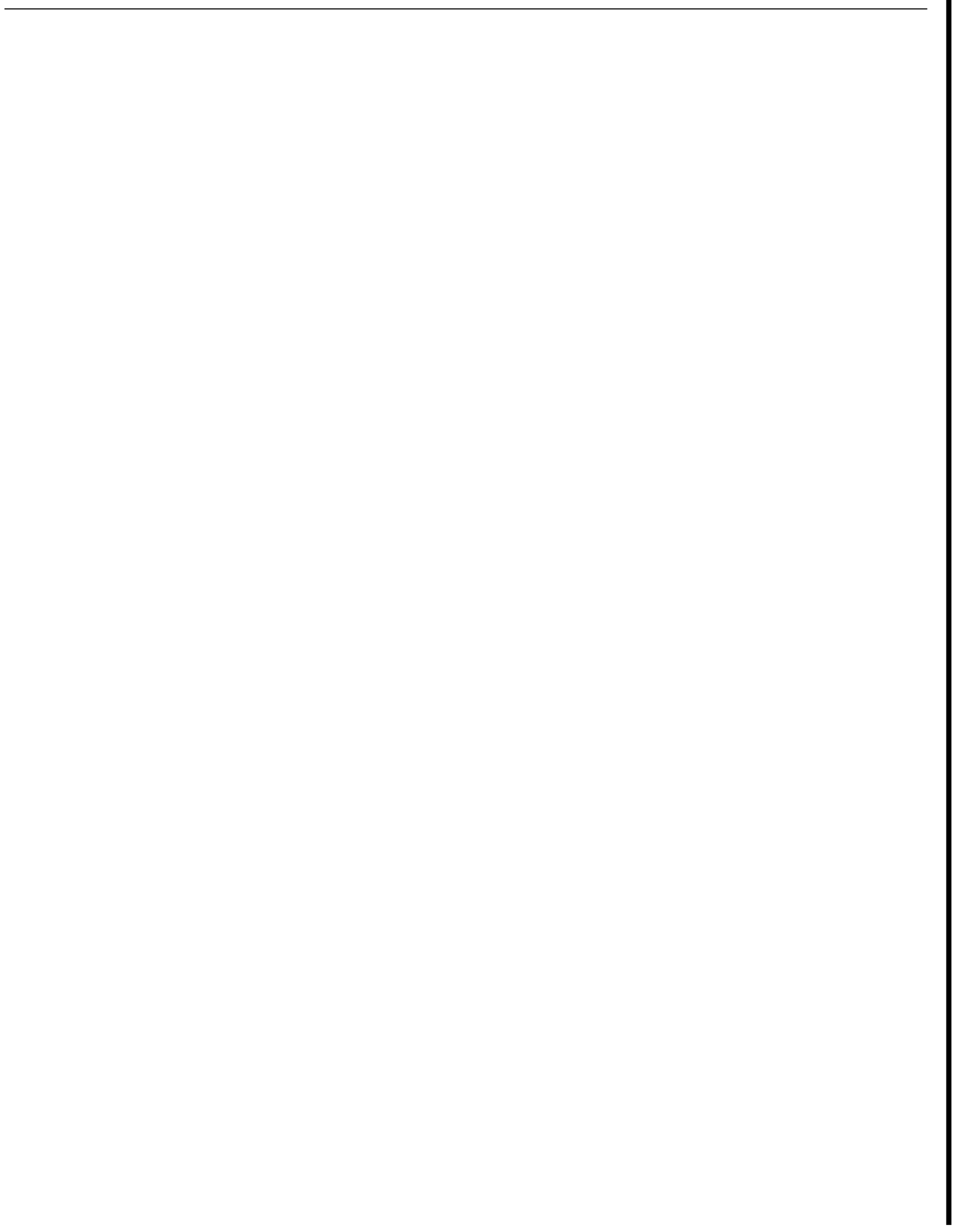
Financial support was provided through the Stanford Geothermal Program under Department of Energy Contract No. DE-AT03-80SF11459 and by the Department of Civil Engineering, Stanford University



Stanford Geothermal Program
Interdisciplinary Research in
Engineering and Earth Sciences
STANFORD UNIVERSITY
Stanford, California

ACKNOWLEDGEMENTS

The authors acknowledge Mike Thompson of U. S. Geological Survey (USGS), Menlo Park, for many stimulating discussions and permission to the high-temperature laboratory facilities; as well as Don Busick and *Gary* Warren of Health Physics, Stanford Linear Accelerator Center (SLAC), for providing the californium-252 neutron source. Appreciation is extended to Lew Semprini, Evangelos Voudrias and Yathrib Al-Riyami, for ~~their~~ friendly assistances to our research efforts. This investigation was made possible by U. S. Department of Energy Grant DE-AT03-80SF11459.



ABSTRACT

Sensitivity calculations for several potential activable tracers for geothermal fluids based on a 10-minute irradiation in a thermal flux of $2 \times 10^6 \text{ n/cm}^2 \text{ sec}$ and 30-minute delay time till measurement were performed. Indium was selected to be the most promising activable tracer. The thermal stability of indium tracer chelated with organic ligands ethylenediaminetetraacetic acid (EDTA) and nitrilotriacetic acid (NTA) was measured at several temperatures in the temperature range of geothermal interest. Measurement of the soluble indium concentration was made as a function of time by neutron activation analysis. From the data, thermal decomposition rates were estimated. The results indicated that the ability of EDTA to enhance indium solubility at elevated temperatures is superior compared to the ability of NTA. Adsorption experiments at geothermal reservoir temperatures were run to examine the effects of adsorbate concentration, rock size, and temperature on the tracer adsorption and thermal degradation. The rock employed for these measurements was graywacke, a prevalent rock **type** at The Geysers, California geothermal field. The results indicated that significant adsorption of InEDTA did not occur at temperatures up to 200°C. At higher temperatures a sharp reduction in soluble indium concentration was observed. The change in temperature behavior was caused by the thermal degradation of the organic ligand. The experimental results indicate that InEDTA and InNTA are excellent activable tracers for surface water and ground water systems, while InEDTA can be used effectively in geothermal reservoirs with temperatures up to 200°C.

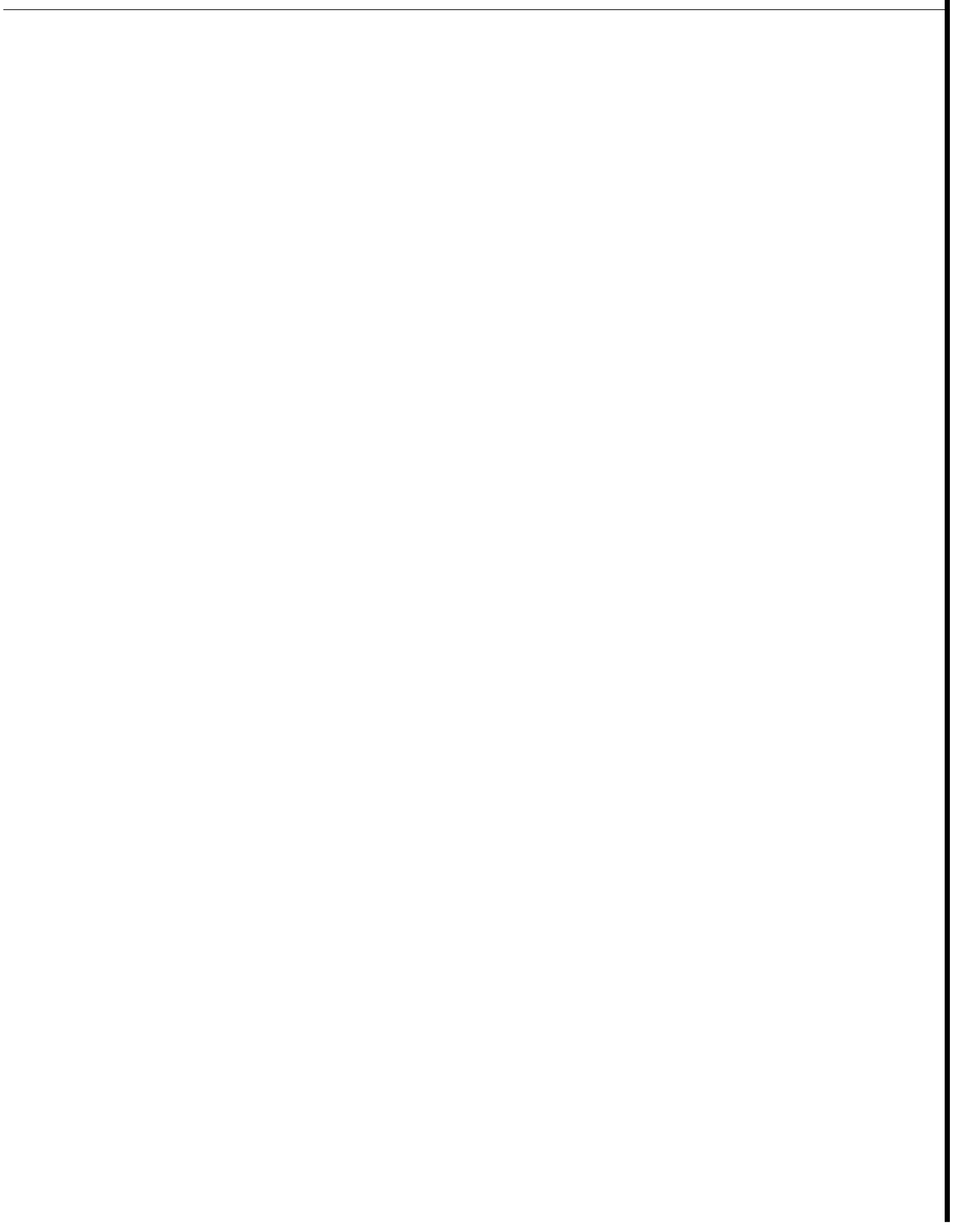


TABLE OF CONTENTS

	Page
Aknowledgements.....	iii
Abstract	v
List of Illustrations	ix
List of Tables	x
Nomenclature.....	.xi
 Chapter 1. INTRODUCTION	 1
1.1. Overview	1
1.2. Conventional Tracers.....	2
Internal Tracers	3
Chemical Tracers	3
Radioactive Tracers	4
Activable Tracers	5
1.3. Neutron Activation Analysis	5
1.4. Activable Tracer Requirements	8
1.5. Objectives of the Study.....	9
 Chapter 2. LITERATURE REVIEW	 11
2.1. Chemical Nature of Geothermal Systems	11
2.2. The Sensitivity Calculation.....	15
2.3. Indium	19
Occurrence and Geochemistry.....	19
Uses	22
Chemical Properties and Aqueous Chemistry	22
Liquid-Liquid Extraction	29
Ion Exchange Behavior	30
Detection Methods	32
Nuclear Properties.....	32
2.4. Chelates	35
Ethylenediaminetetraacetic Acid	36
Nitrilotriacetic Acid	41
 Chapter 3. EXPERIMENTAL PROCEDURES.....	 45
3.1. General Considerations.....	45

Reagent Preparation	45
Glassware Cleaning	45
3.2. Activation Facilities.....	46
Counting Apparatus	47
Gamma-Ray Scintillation Detector Calibrations.....	48
3.3. Statistical Considerations of Radioactivity Measurements	50
3.4. Concentration Determination	53
Irradiation and Counting Procedures.....	53
3.5. Tracer Stability Studies	55
Air Bath	55
Pressure Vessels.....	56
Experimental Design.....	57
3.6. Tracer Adsorption Studies.....	57
Rock Properties	58
Crushing and Sieving.....	59
Specific Surface Area	60
Experimental Design	61
 Chapter 4. RESULTS AND DISCUSSION	 63
4.1. Tracer Stability Results	64
Time Function of Tracer Solubility	64
Thermal Stability Behavior	64
4.2. Tracer Adsorption Results	69
Tracer Adsorption Evaluation at Room Temperature	69
Effect of Temperature.....	71
 Chapter 5. CONCLUSIONS AND RECOMMENDATIONS.....	 75
5.1. Conclusions	75
5.2. Recommendations	76
 APPENDICES	
A. Derivation of Radioactivity Correction Factors for Decay During Counting	77
B. Data Listings - Stability Experiments.....	81
C. Data Listings - Adsorption Experiments	83
D. Rate Constant Calculation.....	85
 REFERENCES	 87

LIST OF ILLUSTRATIONS

Figure	Page
I Distribution Diagram of Indium Hydrolysis	26
II Precipitation Region of In^{+3}	26
III Predominance Diagram for In^{+3} -OH-Cl Species	28
IV Gamma Spectra of Indium- 116m	34
V $p\alpha/p\text{H}$ Diagram for EDTA	38
VI Indium-EDTA Complex Formation	38
VII Thermal Decomposition Mechanism of EDTA	41
VIII $p\alpha/p\text{H}$ Diagram for NTA	42
IX Indium-NTA Complex Formation	42
X Gamma Spectra of Gold-198	47
XI Gamma-Ray Scintillation Detector Calibrations	49
XII Correction Applied to Observed Counts for Decay During Counting	52
XIII Calibration Curve	52
XIV Pulse-Height Spectrum of Indium-116m	54
XV Indium- 116m Decay Curve	54
XVI Schematic of a Pressure Vessel	56
XVII InEDTA Solubility Time Function	65
XVIII InNTA Solubility Time Function	65
XIX Effect of Temperature and Time on InEDTA Stability	66
XX Effect of Temperature and Time on InNTA Stability	67
XXI Effect of Initial InNTA Concentration on the Equilibrium Concentration at 200°C	69
XXII InEDTA Adsorption Onto 1.28, 0.94 and 0.46 mm Graywacke Sandstone Rock Sizes	71
XXIII Effect of T(°C) on InEDTA Adsorption Onto Graywacke Sandstone	73
A.1. Illustration of Activity Change During Irradiation and Decay Periods	78
D.1. Calculation of First Order Reaction Rate Constant	85

LIST OF TABLES

Table	Page
I Chemical Composition of Geothermal Waters	12
II Gas Composition of Geothermal Waters	12
III Activable Tracer Sensitivity	17
IV Laboratory Sensitivity for Potential Activable Tracers	17
V Indium Concentration in Selected Minerals and Rocks	20
VI Stability Constants of Indium(III) Complexes	28
VII Selected Nuclides of Indium	34
VIII Stability Constants of EDTA Complexes at 20°C	39
IX Stability Constants of NTA Complexes at 20°C	43
X ²⁵² Cf Source Flux Measurements.....	47
XI Average Rock Characteristics of Graywacke	58
XII Mineral Distribution of Graywacke Sandstone.....	59
XIII Size Distributions of Crushed Rocks	59
XIV Specific Surface Area Measurements.....	60
XV Effect of Potassium Phosphate Buffer On 500 ppm InEDTA Adsorption	72
B-1 InEDTA and InNTA Time Stability Data	81
B-2 InEDTA Thermal Stability Data	81
B-3 InNTA Thermal Stability Data	82
B-4 InNTA Thermal Stability Obtained at 200°C.....	82
C-1 Percent InEDTA in Solution for Adsorption Experiments	83
C-2 InEDTA Concentration as a Function of Temperature in Contact with 0.94 mm Rock	83

NOMENCLATURE

A	mass number
A	Counting rate (cps)
A_{bg}	Counting rate due to background (cps)
A_{net}	Net background rate (cps)
A_{obs}	Observed counting rate (cps)
A'	Avogadro's number (6.023×10^{23} atoms/g-mole)
cps	Counts per second
C	Counting correction factor
dps	Disintegrations per second
D	Radioactivity of product radionuclide at the end of irradiation (cps)
D_t	Radioactivity of product radionuclide at time T (cps)
D_{std}	Number of disintegrations of standard solution (dps)
D_{tr}	Number of disintegrations of tracer solution (dps)
f	Fractional isotopic abundance
I	Ionic strength (solution property)
k	Stability constant
k_{sp}	Solubility product
k_{obs}	Observed reaction rate constant (day^{-1})
M	Atomic weight (gr/gr-mole)
M	Molarity
n	Neutron
n	Amount of tracer isotope (atoms)
N_i	Number of counts of radiation i during counting interval (counts)
N_{corr}	Corrected number of counts (counts)
N_{min}	Minimum number of counts (counts)
N_{obs}	Observed number of counts (counts)
pH	Negative logarithm of the hydrogen ion concentration
pK	Negative logarithm of the ionization constant

ppm	Parts per million
t	Elapsed time from the end of irradiation to the start of counting (sec)
t'	Counting period (sec)
T	Temperature ($^{\circ}\text{C}$)
$T_{1/2}$	Half life (time)
w	Weight of target element (gr)
w_{\min}	Minimum weight of target element (gr)
w_{std}	Weight of target element in standard solution (gr)
w_{tr}	Weight of target element in tracer solution (gr)
Z	Atomic number

Greek Symbols

β^{-}	Beta particle
β_n	Overall stability constant
γ	Gamma radiation (MeV)
ϵ	Counting efficiency
σ	Neutron capture cross section (cm^2)
σ_N	Standard deviation
$\sigma_{\bar{N}}$	Standard error of the mean
τ	Length of irradiation period (sec)
λ	Decay constant (sec^{-1})
ξ	Degree of advancement
ϕ	Neutron flux (neutrons/ cm^2sec)

CHAPTER 1

INTRODUCTION

1.1. OVERVIEW

Reinjection of thermally spent geothermal brines is attractive for two distinct advantages. For environmental protection, it provides disposal of hazardous waste brines which cannot be discharged to surface waters. For operational efficiency, it serves to maintain reservoir pressure and enhance thermal energy recovery from the reservoir formation. However, uncertainties exist about the long-term potential of reinjection, such as the possibility of permeability reduction, inducement of seismic events, and the reduction of discharge enthalpy by initial breakthrough of cooled recharge fluid causing losses in steam production. Commercial scale reinjection in many of the existing liquid-dominated geothermal fields has proven that reinjection is a satisfactory means of disposal of geothermal effluents as well as beneficial for recycling both water and heat.

In a homogeneous reservoir, the advancing waste water can recover most of the heat stored in the formation rock. In a heterogeneous reservoir, the cold water may follow preferential flow paths. If the fluid residence time is small compared to the heat transfer time, much of the heat stored in the rock is bypassed causing colder water breakthrough to the production zone. Since most geothermal fields are highly fractured, detailed investigation of internal reservoir structure and flow paths are important, particularly, where reinjection is being used to sustain the reservoir pressure.

Traditional reservoir engineering tests identify fractures but cannot provide means of detection and evaluation of preferential path networks. Tracer tests, however, can accomplish this purpose successfully. The usual tracing procedure is to inject an external tracer into a reinjection well and to monitor tracer concentrations continuously in the geothermal fluid at the production wells. Such tests have been performed in Otake and Hatchobaru (Hayashi et al., 1978), Onuma (Ito et al., 1978), 'Be Geysers (Gulati et al., 1978), Kakkonda (Home, 1982), and Svartsengi (Gudmundsson et al., 1984).

The breakthrough time of the injected tracer and the long term tracer recovery are important information for determining flow characteristics of a geothermal reservoir. The first identification of the external tracer represents the arrival of reinjected fluid. The data are used to evaluate the speed of return as well as to estimate the geothermal reservoir permeability. For example, a slow return between injector and producer wells denotes a low formation permeability with no preferential flow path network. Early tracer arrival is attributed to dispersion caused primarily by the concentration gradient. If the produced tracer is recycled, the volume of the circulating fluid can be estimated from the long term dilution of the tracer (Home, 1981).

1.2. CONVENTIONAL TRACERS

The term *tracer* generally signifies a material whose property or characteristic that makes it possible to follow the dynamic behavior of a similar material in a flowing system. Tracers are categorized as either internal or external. Internal tracers are indigenous to the system under study, whereas external tracers are deliberately added. Tracers are categorized as: chemical, radioactive, and activable materials.

Internal Tracers

Internal tracers are stable or radioactive elements which occur naturally in the system being traced. Such tracers are ideal for geothermal systems but their direct

measurement is either difficult or impossible (Mazor, 1977; Mazor and Truesdell, 1984).

Radon-222, a radioactive noble gas element that originates from the radioactive decay of Radium-226, is naturally distributed in all geothermal fluids. Radon concentrations were measured in liquid-dominated geothermal fields in Wairakei, New Zealand and Cerro Prieto, Mexico, as well as in the vapor-dominated field The Geysers, U.S.A. The results of these studies were significant for the determination of flow and thermodynamic characteristics of the geothermal reservoirs (Semprini, 1981).

Chemical Tracers

Chemical tracers are detected by chemical analysis and have limitations of thermal instability, potential reactivity, and high natural background. Because of these limitations, large quantities are needed to assure detectable concentrations of tracer at the sampling location. Alkali halides, potassium iodide (KI) and potassium bromide (KBr) have less of a tendency for interaction with the reservoir formation, and have been used successfully in several Japanese geothermal reservoirs (Horne, 1982).

Fluorescent dyes are organic pigments whose molecules can be excited to fluorescence at wavelengths of 480-560 millimicrons. Preparation and handling of fluorescent tracers are simple and experiments with several colors can be performed simultaneously. Fluorescence detection can be achieved by fluorimeters with high sensitivity (Channell, 1970). The most reliable fluorescent tracers are Uranine, Eosine, Amidorhodamine, and Rhodamine WT. These dyes are useful under ground water reservoir conditions, but are likely to break down and lose their fluorescent properties at geothermal reservoir temperatures. The instability of Rhodamine WT at geothermal reservoir temperatures has been demonstrated experimentally by Al-Riyami (1986). Also, fluorescent tracers are sensitive to pH changes and are easily absorbed by reservoir formations. Fluorescein dyes were used at Hatchobaru for identification of possible reservoir thermal breakthrough problems (Horne, 1982). It was reported that the fluorescent tracer

tests provided important data on first arrival times, Rhodamine WT was used in a tracer test carried out in Klamath Falls, Oregon (Gudmundsson et al., 1983). The results were used to study the injection behavior of a geothermal reservoir known to be fractured.

Radioactive Tracers

Radioisotopes are available in wide selections according to material property, radiation energy, and half-life. The radioisotope can be incorporated into a wide variety of organic and inorganic compounds and so there is great flexibility of applications. Radioactive tracers are easy to measure continuously by their emitted gamma or beta radiation with great sensitivity and negligible interference. Theoretically, radioactive tracers are capable of providing all the results obtainable with fluorescent tracers, but the reverse is not true. The major drawback of the radioactive tracer technique is the safety hazard to the operators, population and environment. Although reasonable precautions may be taken for the use of radioactive tracers in subsurface reservoir testing, the public reaction has generally been one of fear and mistrust.

Tritium, in the form of tritiated water, is considered the best tracer available for vapor-dominated geothermal fields. Tritiated water travels with the same velocity, boils and changes phases like normal water. Tritium is less expensive than most radioisotopes but is more difficult to measure, because its low radiation energy requires sophisticated detection equipment. Tritium tracer surveys were conducted at The Geysers for the determination of regional flow pattern of reservoir fluid and efficiency of water vaporization (Gulati et al., 1978). Radioactive tracers, 8.04-day Iodine-131 and 35.4-hour Bromine-82, have been used effectively in geothermal studies in The Philippines, El Salvador and the U.S.A. (Home, 1984); as well as in Wairakei and Broadlands, New Zealand (McCabe, 1983).

Activable Tracers

Activable tracers are stable elements which in conjunction with activation analysis offer a reasonable compromise between retaining most of the advantages of radioactive tracers without the possibility of creating health and environmental hazards, such as those which may occur with the introduction of highly radioactive materials into the reinjected geothermal fluid. Activable tracers are readily obtained in large quantities and at a smaller cost compared with radioactive tracers. Activable tracers require convenient neutron irradiation facilities for the activation analysis. It is therefore troublesome, if there is no accessibility to a nearby neutron source. The quantity of the stable element used for the geothermal tracing is dependent upon the neutron flux available. The higher the neutron flux the smaller the quantity of stable element required for the activation analysis.

Activable tracers have been successfully used in many aspects of biological, medical, environmental, and industrial investigations. These investigations have demonstrated the important and frequently exclusive role of stable tracers. Experiments using activable tracers in geothermal systems have not yet been performed. Because of the peculiar advantages of activable tracers and the possibility of online activation analysis in geothermal systems, this tracing method is promising and requires further investigation.

1.3. NEUTRON ACTIVATION ANALYSIS

The technique of neutron activation analysis is a unique combination of nuclear and chemical processes selected to optimize the precision and accuracy of trace-element chemical analysis or a high-dilution tracer study. Very few analytical methods offer the versatility and sensitivity achievable by neutron activation analysis. Since neutrons activate the nucleus of an atom, not the electron shell, regardless of its oxidation state, chemical form or physical location, the technique allows both quantitative determination and qualitative identification of the elements from which the radiations

are monitored. The procedure for activation analysis for a tracer study is to select a suitable stable isotope with proper chemical and nuclear properties such that thermal neutron bombardment will produce the desired activation product. The amount of the activation product that is formed during neutron irradiation is proportional to the amount of the tracer isotope. After irradiation of the sample in a chosen irradiation facility (usually a low-power nuclear research reactor or a radioisotope source) for a period of time, the concentration of the tracer is measured by monitoring the characteristic radiation emitted by the product radionuclide. For more detailed description of the *Neutron Activation Analysis* technique and its applications refer to the following references: DeVoe and LaFleur (1969), Kruger (1971), Rakevic (1970), Ryan (1973), and Katz (1981).

Thermal neutrons are named so because of their average energy is the same as that of the molecules or atoms of the medium through which they travel. through which they travel. neutron capture cross sections are, in general, larger than any other projectile's cross sections, (b) there is wide diversity of devices with large thermal neutron fluxes, and (c) the uniform flux intensity provided by thermal neutrons assures a conservative sensitivity evaluation.

The duration of radioactivation is a relative parameter and depends upon the nuclear properties of the selected isotopic tracer as well as on the design characteristics of the activation analysis. When tracer concentrations are close to the limits of sensitivity, it is desirable to irradiate enough time for the tracer to approach the level of saturation activity. The saturation activity level is the steady state in which radioactive products disintegrate at the same rate at which they are formed. If the irradiation is terminated before the steady state is achieved, then the disintegration rate of the active nuclide is less than its rate of formation. For short-lived active nuclides the approach to saturation activity level is fast. On the other hand, for long-lived product nuclides a careful estimation of the minimum desired level of radioactivity reduces the time

period and cost of the activation process.

The energies and intensities of the gamma-rays emitted by the neutron activation products are selectively monitored with a radiation detector coupled to a multichannel analyzer system. Commercially available radiation detectors are the gas-filled, scintillation and semiconductor detectors. The solid state lithium-drifted germanium, Ge(Li) and the luminescence scintillation sodium-iodide thallium, NaI(Tl) counters are commonly used. Ge(Li) detectors have revolutionized neutron activation analysis because of their excellent resolution and sophistication. The major drawbacks of the Ge(Li) detectors are their low efficiency and low operating temperatures (Friedlander et al., 1981). NaI(Tl) detectors are most useful when sensitivity is the main concern or low levels of radioactivity are to be measured. Because of the high sensitivity of NaI(Tl) detectors, massive shielding can be effective in reducing background effects due to gamma-rays from surrounding materials and cosmic rays.

Geothermal fluids may contain major constituents whose activation would lead to high levels of radiation or to generation of radionuclides with gamma radiation perturbing the instrumental product nuclide determination. Such samples require chemical preconcentration of the tracer prior to neutron activation. Several techniques are available for separation of the interfering constituents. The most common separation techniques involve precipitation, solvent extraction, ion exchange chromatography, electro-deposition, and distillation. Rapid separation is always desirable so the fast ion exchange separation technique, if applicable, is favorable as the preconcentration step.

Occasionally and especially where the highest possible sensitivity is required, postirradiation separations are necessary. Postirradiation separations are simple and reliable because once the radioactive species are produced any chemical manipulation can be performed on the sample without contamination of the tracer material being measured. Interferences from radioisotopes of the same element cannot be reduced by any method. Consideration must be taken on the postirradiation separation time period so

that the particular radionuclide will not decay to unmeasurable levels. If preconcentration separation can accomplish the required sensitivity, elimination of the postirradiation step is preferred. Any postirradiation separation procedure increases the time period of the activation analysis and of greater importance results in undesirably higher exposure to ionizing radiation to the analyst.

1.4. ACTIVABLE TRACER REQUIREMENTS

An activable tracer for geothermal reservoirs must meet the requirements of external tracers as well as the necessary parameters demanded by the activation analysis technique. The cost of a tracer is a substantial fraction of the total cost of a tracer study, so for economic justification the tracer price must be attractive.

A major consideration of an external tracer is its conservation in the reinjected geothermal brine. An external tracer must be compatible with the chemistry of the geothermal fluid. The tracer should not be lost in the reservoir by such process as physical adsorption, chemisorption reactions, or ion exchange with the rock minerals. Also, it must be detectable in wellhead fluid after transport through a high-temperature reservoir. The tracer should not be susceptible to thermal degradation or phase changes during its transport.

Additional requirements for a suitable activable tracer are: (a) a background concentration as close as possible to the minimum detectable amount of tracer by available detection systems, (b) large natural isotopic abundance, (c) large neutron activation cross sections, (d) appropriate gamma radiation of the product radionuclide for measurement by gamma-ray spectrometry, and (e) optimum half-life of the product radionuclide.

The half-life of the product radionuclide should be long enough to permit distinguishable counting rate after a cooling period between the end of irradiation and measurement of the activity. The half-life of a few minutes is adequate when the irradiation

tion facility is close to the measurement equipment. When the samples must be transported from the selected irradiation reactor to a distant monitoring location, short lived product radionuclides may not be suitable. In these circumstances, it is often advantageous to use a local thermal neutron irradiator, because the time period of sample analysis will be reduced enough to outweigh the additional expenditure.

1.5. OBJECTIVES OF THE STUDY

The goal of this study is to develop an external-activable-tracer method with maximum sensitivity for measuring the early breakthrough time of reinjected geothermal brine at production wells and for extending the period of tracer recovery.

The specific objectives of the study are the following:

1. Identify potential activable tracers chemically stable and compatible with the chemistry of the geothermal fluid.
2. Evaluate the solubility as a function of time, and the thermal behavior at elevated reservoir temperatures of selected chelated activable tracers.
3. Investigate the effects of adsorbate concentration, particle size, and temperature on the adsorption of chelated tracer onto graywacke, a typical geothermal rock.



CHAPTER 2

LITERATURE REVIEW

2.1. CHEMICAL NATURE OF GEOTHERMAL SYSTEMS

High temperature geothermal systems are often associated with zones of volcanism and mountain building at the edge of crustal plates (Koenig, 1973). Molten mantle material is added to the crust in zones of plate divergence. This phenomenon occurs when the large mobile plates which make up the earth's crust move apart, thus thinning the crust. Hydrothermal systems also occur in convergence zones, such as the one stretching from Italy, Greece, and Turkey through the Caucasus to the Himalayas and south-west China (White, 1973). These zones are created when plates collide causing frictional heating. A third category of geothermal systems occurs at the areas where the motion of the plates causes a stretching and shattering of the continental plates. The junctions of the African, European, Asian, and Indian crustal plates belong to this classification.

The Larderello steam fields in Italy are in a region of metamorphic rocks, whereas The Geysers steam field in the U.S.A. is largely in fractured graywacke. In contrast, the wide spread hydrothermal activity in Iceland occurs in extensively fractured and predominantly basaltic rocks. Similar types of rock environments may produce different types of geothermal fields. For example, at Larderello, Italy, wells produce mainly dry steam, while at Kizildere, Turkey, in a zone of similar rocks, deep wells produce high temperature water (Ellis and Mahon, 1977). Geothermal fields are classified not only by the type of rock environment, but also by water availability,

reservoir pressure and temperature.

Geothermal reservoirs generally occur at depths ranging from 1 to 3 km, with temperatures varying from 60 to 300°C. The presence of hot rock alone is not sufficient because the heat must be extracted by circulating fluids. If the reservoir permeability is considerably low the fluids cannot permeate and circulate through the hot rock and geothermal energy cannot be adequately extracted. Therefore, suitable topographical location and optimum geological conditions are important factors for geothermal reservoir accessibility.

Isotopic studies in geothermal fields have shown that at least 90 percent of the geothermal water has meteoric origin (Gupta, 1980). Therefore, it is apparent that the aquifers have hydraulic continuity with rain-water recharge areas. The cold rain-water permeates through the surface of the recharge area into deeper formation boundaries where it is heated by conduction from hot rocks. The water expands upon heating and moves buoyantly upward through the water-filled rock strata. An impermeable cap rock overlying the aquifer is necessary to prevent the dissipation of the hot water and steam. If the heat of the rock is great enough to boil off more water than is being replaced, dry or superheated steam is produced. On the other hand, if the reservoir pressure is adequate to maintain a pressure-controlling liquid phase, a liquid-dominated geothermal field results. *

Tsai et al. (1978) conducted a literature survey on the chemical composition of geothermal effluents. Tables I & II show the chemical constituents reported in geothermal effluents with their minimum and maximum concentrations. The major constituents of geothermal fluids are: chloride, sulfate, sodium, calcium, magnesium, potassium, and bicarbonate. Geothermal waters are usually categorized according to their

* For extensive discussions of the *Geothermal Systems* the readers are referred to the following references: Kruger and Otte (1973); Collie (1978); Gupta (1980); Butler and Pick (1982); Edwards et al. (1982) and Armstead (1983).

TABLE I. Chemical Composition of Geothermal Waters
[From Tsai et al. (1978)]

Constituent	Conc. (ppm)	Constituent	Conc. (ppm)
Aluminum (Al)	0 - 7,140	Lead (Pb)	0 - 200
Ammonium (NH ₄)	0 - 1,400	Lithium (Li)	0 - 300
Arsenic (As)	0 - 12	Magnesium (Mg)	0 - 39,200
Barium (Ba)	0 - 250	Manganese (Mn)	0 - 2,000
Boron (B)	0 - 1,200	Mercury (Hg)	0 - 10
(HBO)	13.6 - 4,800	Molybdenum (Mo)	0.029 - 0.074
Bromide (Br)	0.1 - 3,030	Nickel (Ni)	0.005 - 2
Cadmium (Cd)	0 - 1	Nitrate (NO ₃)	0 - 35
Calcium (Ca)	0 - 62,900	Nitrite (NO ₂)	0 - 1
Carbon Dioxide (HCO ₃)	0 - 490	Oxygen (O ₂)	0 - 10
(CO ₂) ³	0 - 10,150	Phosphate (PO ₄)	0 - 0.3
Cesium (Cs)	0 - 1,653	Potassium (K) ⁴	0.6 - 29,900
Chloride (Cl)	0.002 - 22	Rubidium (Rb)	0 - 169
Cobalt (Co)	0 - 241,000	Silica (SiO ₂)	3 - 1,441
Copper (Cu)	0.014 - 0.018	Silver (Ag) ²	0 - 2
Fluoride (F)	0 - 10	Sodium (Na)	2 - 79,800
Germanium (Ge)	0 - 35	Sroutium (Sr)	0.133 - 2,000
Hydrogen Sulfide	0.037 - 0.068	Sulfate (SO ₄)	0 - 84,000
Iodide (I)	0.2 - 74	Sulfur (S) ⁴	0 - 30
Iron (Fe)	0 - 105	TDS	47 - 387,500
	0 - 4,200	Zinc (Zn)	0.004 - 970

TABLE II. Gas Composition of Geothermal Vapors
[From Tsai et al. (1978)]

Constituent	Concentration (Vol. %)
Ammonia (NH ₃)	0 - 5.36
Argon (Ar)	0 - 6.3
Arsenic (As)	0.002 - 0.05
Boric Acid (HBO)	0 - 0.45
Carbon Dioxide (CO ₂)	0 - 99
Carbon monoxide (CO)	0 - 3
Helium (He)	0 - 0.3
Hydrocarbons	0 - 18.3
Hydrogen (H ₂)	0 - 39
Hydrogen Fluoride (HF)	0.00002
Hydrogen Sulfide (H ₂ S)	0 - 42
(H ₂ + H ₂ S)	0.2 - 6
Methane (CH ₄)	0 - 99.8
Nitrogen (N ₂) ⁴	0 - 97.1
(N ₂ + Ar)	0.6 - 96.2
Oxygen (O ₂)	0 - 64
Sulfide Oxide (SO ₂)	0 - 31

major constituents into four principal types:

- (1) Sodium chloride
- (2) Acid sulfate
- (3) Acid sulfate-chloride
- (4) Calcium bicarbonate.

There is a close relationship between the concentration of many minor metals and the salinity of geothermal water (Ellis and Mahon, 1977). In the low salinity, high temperature waters which are most frequently encountered, trace metals seldom exceed the order of tens of parts per billion. For highly saline geothermal waters, even those of moderate temperatures, heavy metal concentrations become appreciable. Minor metal concentrations in geothermal waters separated at atmospheric pressure differ from the concentrations in the deep waters. Also, due to steam formation which occurs when high temperature water flashes at atmospheric pressure into a mixture of water and steam, waters collected at the surface are at a higher pH than the deep high temperature waters. The concentrations of such gases as CO_2 , H_2S , CH_4 , H_2 , and N_2 in the steam are inversely related to the percentage of steam flashed from the water and therefore to the separation pressure at which the steam is collected from the discharge. D'Amore et al. (1983) discussed the effect of natural recharge on gas composition. They observed that H_2S content in the gas at Castelnuovo, Italy, geothermal field decreased with increased recharge. The decrease in H_2S concentration was attributed to dissolution in liquid water and oxidation. Gas concentration in geothermal fluids varies widely between areas. The etiology for this phenomenon is the reservoir environment, the formation lithology, rock interaction, and rock mineral chemical equilibria. For example, when high temperature waters come into contact with organic rich sediment rocks, the gas concentration in the steam increases considerably.

2.2. THE SENSITIVITY CALCULATION

In thermal neutron activation reactions, termed n-gamma (n, γ) reactions, neutrons react with the target nuclei and release photons of electromagnetic radiation. This electromagnetic radiation with energies in the range of 0.01 to 10-MeV (Connolly, 1978), is called prompt gamma radiation and is not generally associated with neutron activation analysis. The activation reaction for a target element X with atomic number Z and mass number A, can be written as:



or in abbreviated form as:



The activation product has the same atomic number Z but mass number (A+1). The activation product is almost always a radioactive isotope of element X, decaying by β^- emission to the next element in the periodic table X^o of atomic number (Z+1) and mass number (A+1):



Occasionally, product nuclides of the form ${}^{(A+1)m}_Z X$, where m stands for metastable, decay by γ -emission from an excited state to the ground state. This process is called isomeric transition (IT) and the energy of the emitted γ -radiation is the energy difference between the two isomeric states:



The disintegration rate of the radioisotope produced at the end of irradiation period is given by the *radioactivation* equation:

$$D_o = n \sigma \phi (1 - e^{-\lambda \tau}) \quad (2.5)$$

where

D_o = amount of radioactivity of the product radionuclide at the end of irradiation, disintegrations per second (dps)

ϕ = incident neutron flux, n/cm² sec

σ = neutron capture cross section, cm²

n = number of atoms present in the sample which can give rise to the product activity, atoms

λ = decay constant of the product radionuclide, sec⁻¹

τ = length of irradiation, sec

After the end of irradiation, the activity of the product radionuclide decreases according to the *radioactivity decay* equation:

$$D_t = D_o e^{-\lambda t} \quad (2.6)$$

where

t = the elapsed time from the end of irradiation to the start of counting

D_t = amount of radioactivity of the product radionuclide at time t

For a particular isotopic tracer the value of n can be obtained from:

$$n = \frac{w f A'}{M} \quad (2.7)$$

where

w = weight of target element, grams

f = fractional isotopic abundance

A' = Avogadro's number, 6.023×10^{23} atoms/gram-mole

M = atomic weight of the element, grams/gram-mole

An important parameter for the sensitivity calculation is the counting efficiency of the detector system:

$$\epsilon = \frac{N_i}{D} \quad (2.8)$$

where

ϵ = counting efficiency

N_i = number of counts of radiation i during counting time interval, (cps)

The over-all counting efficiency is adjusted for the decay scheme which relates the fraction of the radionuclide's disintegration rate represented by the measured γ -ray transitions.

The sensitivity calculation is an estimation of the minimum amount of a tracer element required for efficient detection under given irradiation and counting conditions. Therefore, summarizing all the parameters that have been considered, the sensitivity equation can be expressed as:

$$w_{\min} = \frac{N_{\min} M}{\epsilon \sigma \phi A' f (1 - e^{-\lambda \tau}) e^{-\lambda t}} \quad (2.9)$$

Other parameters, such as chemical yield if chemical separations are required, can be included in the sensitivity equation. For similar irradiation and measurement conditions of the tracer and known standard, the activable tracer measurement reduces to the simple form of:

$$w_{tr} = w_{std} \frac{D_{tr}}{D_{std}} \quad (2.10)$$

Where w is the weight of the target element, D is the number of disintegrations of the samples in the same time-interval, and subscripts tr and std indicate tracer and comparator standard respectively.

Kruger (1983) identified several potential activable tracers for liquid-dominated reservoirs, based on sensitivity calculations for all stable isotopes of the elements which meet the initial criteria of low background concentration in geothermal fluids and appropriate nuclear properties. Table III summarizes the elements and their minimum detectable concentrations. These calculations were based on product half-lives of 6 or less hours and irradiation time of 24 or less hours in the U. C. Berkeley

TABLE III. Activable Tracer Sensitivity
[From Kruger (1983)]

Tracer	MDL* (ng)	Tracer	MDL(ng)	Tracer	MDL(ng)
¹¹⁵ In	0.18	⁸¹ Br	4.03	⁶⁵ Cu	71.50
⁵⁹ Co	0.22	¹²⁷ I	13.10	¹⁹³ Ir	106.66
¹⁶⁴ Dy	0.76	¹⁷⁵ Lu	15.12	¹⁰⁸ Pb	109.84
⁵¹ V	0.78	¹⁹⁷ Au	31.00	⁵⁰ Ti	347.59
¹⁸⁶ W	1.91	¹⁰⁷ Ag	31.49	²⁰⁴ Hg	473.58
⁵⁵ Mn	2.66	¹⁰³ Rn	32.69	¹⁰⁴ Ru	1455.26
¹³⁹ La	2.89	¹³³ Cs	33.42	⁶⁹ Ga	1519.10
²³² Th	3.68	¹⁵¹ Eu	34.00	⁴⁵ Sc	22216.31

* MDL = Minimum Detectable Level

TABLE IV. Laboratory Sensitivity for the Potential Activable Tracers

TARGET NUCLIDE**				
Element	Conc. (ppb)*	Isotope	f	$\sigma_{(n, \gamma)}$
V	< 5	⁵¹ V	0.997	4.88
Co	< 60	⁵⁹ Co	1.000	19
In	< 100	¹¹⁵ In	0.957	70
Dy	< 2000	¹⁶⁴ Dy	0.281	900
PRODUCT NUCLIDE**				
Isotope	T _{1/2}	Major- γ	ϵ	Sensitivity***
⁵² V	3.75 m	1.434	2.15	126.06
^{60m} Co	10.47 m	0.059	1.73	2.24
^{116m} In	54.12 m	1.294	2.93	0.59
¹⁶⁵ Dy	2.33 h	0.095	12.38	0.10

* Concentrations in geothermal fluids, from Cosner and Apps (1978). Values are in micrograms per liter and they are neither exact nor representative of every geothermal fluid.

** The nuclear data have been adapted from Lederer and Shirley (1978). f = isotopic abundance; $\sigma_{(n, \gamma)}$ = thermal neutron cross section in barns; ϵ = over-all counting efficiency (d/c).

*** Minimum weight (mg) of the element necessary to obtain 60 cpm after 10-minute irradiation in a thermal neutron flux of 2×10^6 n/cm²-sec and 30-minute delay time till measurement.

multi-sample rotating Lazy-Susan irradiation site. The sensitivity data showed that ^{51}V , ^{59}Co , ^{115}In and ^{164}Dy should be considered as potential activable tracers for geothermal reservoirs.

The four promising activable tracers and their sensitivity calculations based on a 10-minute irradiation in the Stanford Linear Accelerator Center (SLAC) ^{252}Cf facility and 30-minute delay time till measurement are shown in Table IV. The minimum value of $N = 60$ cpm at the measurement time was set as an additional sensitivity requirement. This arbitrary counting rate value is high enough to permit efficient detection of the γ -ray of interest. Indium is considered to be the most promising of the four potential activable tracers (see Table IV), because of its unique combination of good detection sensitivity and relatively high energy of major γ -ray emission. High energy γ -rays are preferred when interfering radionuclides with low γ -energy are present because their Compton scattering contribution to the tracer full-energy peak is negligible. However, the counting efficiency decreases with increasing γ -ray energy.

2.3. INDIUM

Indium has atomic number 49, atomic weight 114.82 and is a member of the Group-III A elements of the periodic table along with boron, aluminum, gallium and thallium. Indium was discovered in 1863 by F. Reich and T. Richter, during the examination of a sphalerite ore. Because of the indigo-blue color of its spectrum they gave the name indium to the metal. In appearance indium is silver-white and lustrous, resembling platinum. It is easily shaped by pressure and does not become compressed or brittle when it is deformed. The metal has melting point 156.17°C and boiling point 2075°C .

Occurrence and Geochemistry

Indium is a relatively rare metal and it is never found uncombined in nature or in concentrated deposits, but it is widely distributed. Indium has been reported to occur

in several countries including Sweden, Finland, Germany, Italy, Peru, Russia, Canada and the United States.

Indium occurs in minerals either as an isomorphous replacement for other elements of similar ionic radii or as structural member of the principal mineral. Indium is concentrated up to 0.1 percent in some minerals of zinc, copper, iron as well as in several hydrothermal minerals. Also It becomes concentrated in various byproducts during recovery of other metals, principally zinc and lead. Indium content in minerals which are structurally dominated by iron has been observed to be higher than its normal abundance. The higher the iron concentration the higher the degree of indium concentration. However any given mineral, even from the same deposit, could contain different indium content if formed under different conditions. Therefore, indium mineral content is strongly affected by depositional conditions (Linn and Schmitt, 1972).

Numerous investigators have detected indium in minerals and rocks. The most complete study of indium distribution has been conducted by Shaw, D. M. (1952), who examined specimens from different geological materials. A spectrochemical method of analysis was used with sensitivity of the order of 0.02 ppm and $\pm 20\%$ precision. Selected minerals and rocks with their indium concentrations are presented in Table V for comparative purposes. The uniformly poor concentration of indium in all of the common minerals and rocks confirms its low crustal abundance of 0.11 ppm.

The concentration of indium in soils ranges from 0.01 to 4 ppm. Indium concentration in ambient air ranges from 5.3×10^{-5} ng/m³ to 43 ng/m³ depending on the site's mining activity and industrialization. Rain waters from nonindustrial areas have been found to contain 0.002 to 2 ppb indium. Hot spring waters in Bulgaria were reported to contain up to 40 ppb indium (Smith et al., 1978). Indium concentration in Pacific Ocean water was found to be 4 ppt (Chow and Snyder, 1969), while its concentration

TABLE V. Indium Concentration in Selected Minerals **and** Rocks
[From Shaw (1952)]

MINERALS		
Sample	Locality	In(ppm)
Opal	Grand Manan Is., New Brunswick, Canada	
Magnetite	Seabrook Lake, Mississagi Reserve, Ont.	0.07 1
Iron Oxides	Sappi, Luvia, Finland	0.12
Pyrite	Crystal Falls, Michigan	
Pyrrhotite	Creighton Mine, Sudbury, Ontario	
Chalcopyrite	Creighton Mine, Sudbury, Ontario	4.8
Galena	Sakkijarvi, Finland	0.9 1
Olivine rock	S. Massif, Khabozero, Kola Peninsula, U.S.S.R.	-
Garnet	N. Stromfjord, Greenland	0.18
Titanite	Eganville, Renfrew Co., Ontario	
Hypersthene	Rifkol, W. Greenland	0.038
Muscovite	Kuutelokallio, Kaatiala, Kuortane, Finland	4.5
Kaolin	Werran Hills, Nigeria	0.12
Leucite	Civita Castellano, Italy	
ROCKS		
Sample	Locality	In(ppm)
IGNEOUS ROCKS		
Basalt	Tolstoi Point, St George, Aleutian Is.	0.32
Hornblendite	Kaalamo, Finland	0.053
Gabbro	Sudbury, Ontario	
Olivine-Diabase	Sappi, Luvia, Finland	0.078
Monzonite	San Juan Co., Colorado	
Granite	Bomarsund, Ahvenanmaa, Finland	2.0
Granite	Bambole, Vehkalahti, Finland	0.14
Obsidian	Millard Co., Utah	
Lamprophyre	Seabrook Lake, Mississagi Reserve, Ont.	0.071
SEDIMENTARY ROCKS		
Limestone	Limberg, Parainen, Finland	
Bauxite	Tennessee	0.17
Laterite	Funchal, Madeira	0.058
Graywacke	Manitou Lake, Ontario	0.049
Graywacke	Mena, Arkansas	0.033
Graywacke	Washington State	0.23
Shale	Tallinn, Estonia	0.18
Porcellanite	Iron Co., Michigan	0.27
Anthraxolite	Sudbury, Ontario	0.21
METAMORPHIC ROCKS		
Granodiorite Gneiss	Albany Co., Wyoming	0.88
Garnet Gneiss	N. Isortog, Greenland	1.8
Olive Slate	Glove Quadr., New York	
Black Phyllitic Slate	Glove Quadr., New York	0.050
Biotite-Muscovite Phyllite	Glove Quadr., New York	0.066

* The symbol "-" indicates an indium concentration below the limits of detection.

in Atlantic Ocean water was reported to be 0.1 ppt (Matthews and Riley, 1970).

Uses

The first commercial use of indium was in 1934 as an ingredient of dental alloys. Small amounts of indium increase the strength and ductility of dental solders and orthodontic wires. Jewelry coatings and decorative arts have been using indium because of its color. Bearing manufacturing for military airplanes during the World War II was a major consumer of indium. Indium bearings showed scarcely any corrosion and good fatigue resistance (Forrester, 1964). Low-melting alloys of indium are used in meltable safety devices such as heat regulators, sprinklers, and other fire safety systems. Some indium alloys have the ability to wet glass and are being used for glass-to-glass seals. Indium has found applications in semiconductors, transistors, microwave oscillators, amplifiers, piezoelectric units, infrared detectors, Touch Tone telephones, and in several other products of the electronics industry (Rees and Gray, 1976; Chynoweth, 1976). In the field of nuclear energy indium is employed in control rods for nuclear reactors because of its large thermal neutron cross-section (Belous, 1974). Petroleum industries use indium in some conventional catalysts to increase the concentration of aromatics of gasoline and thus to reduce the knocking tendency of petroleum products in internal combustion engines (Burke, 1972).

Chemical Properties and Aqueous Chemistry

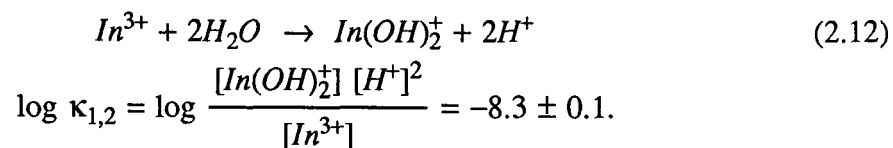
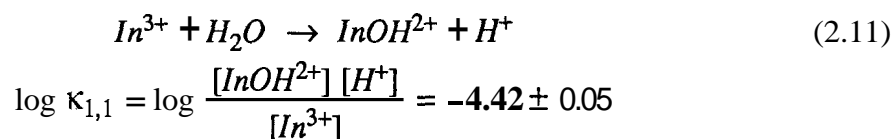
The electron configuration of indium is $1s^2 2s^2 2p^6 3s^2 3p^6 3d^{10} 4s^2 4p^6 4d^{10} 5s^2 5p^1$. Its first, second and third ionization potentials are 5.79, 18.79 and 57.8 eV, respectively. The element exhibits positive oxidation states from one through three, but the common valence is three.

Indium(III) is stable in aqueous systems, while the monovalent and divalent indium may exist in aqueous solutions at low concentrations but they are more often found as solid halide compounds. In acidic solutions In^{3+} is coordinated by six water

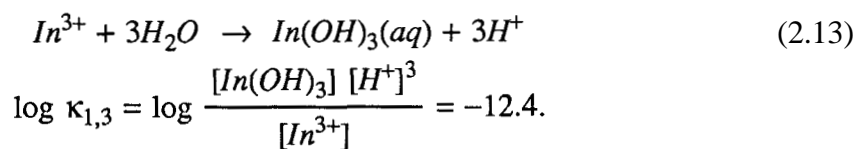
molecules. The anhydrous InF_3 is not affected by water, while the anhydrous InCl_3 and InBr_3 are quite soluble in both water and organic solvents. The binary compounds of monovalent indium are insoluble solids and in aqueous solutions undergo disproportionation to give indium metal and In^{3+} (Carty and Tuck, 1975).

Weak mineral acid solutions dissolve indium slightly. The dissolution rate is increased by heating the mineral acid, but this causes indium salt formation and evolution of hydrogen. Cold nitric acid dissolves the metal slowly, rapidly when heated with formation of nitrogen oxides. Cold sulfuric acid dissolves the metal with evolution of hydrogen and precipitation of anhydrous indium. With hot sulfuric acid, sulfur dioxide is evolved. Hydrochloric and oxalic acid dissolve the metal rapidly with evolution of hydrogen. The metal is not affected by dry air at normal temperatures, but when in contact with water, some hydroxide formation occurs.

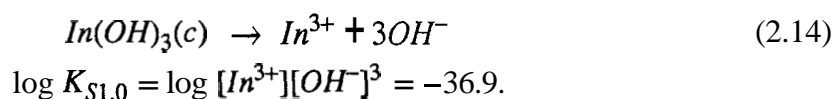
Indium(III) appears to form all of its hydrolysis products rapidly and reversibly. According to Biedermann (1956) the hydrolysis of the hydrated In^{3+} can be described by the following equations:



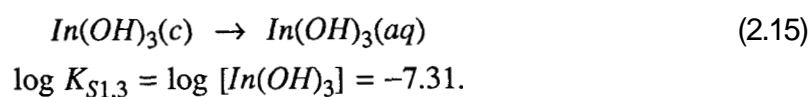
Rossotti and Rossotti (1956) determined the mononuclear hydrolysis constants of indium by examining the distribution of **indium-2-thenoyltrifluoroacetone** complex between benzene and aqueous 3M sodium perchlorate solutions. The reported values of the hydrolysis constants are in agreement with those obtained potentiometrically by Biedermann (1956), and their value of $\kappa_{1,2} = 10^{-8.8}$ seems more realistic. Baes and Mesmer (1976) obtained a value of $\kappa_{1,3}$:



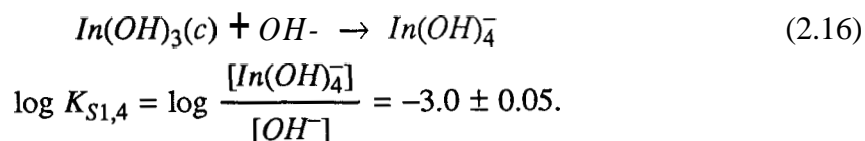
$\text{In}(\text{OH})_3$ is fairly stable and only slightly soluble in excess base. The solubility product of $\text{In}(\text{OH})_3$ has been recommended by Feitknecht and Schindler (1963) to be:



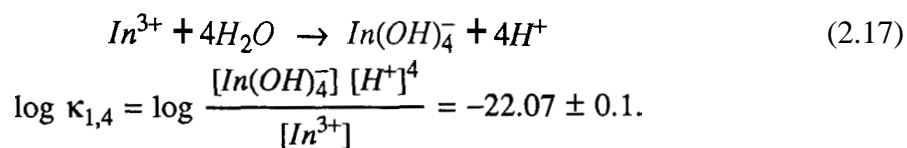
According to Baes and Mesmer (1976) the minimum solubility of $\text{In}(\text{OH})_3$ is:



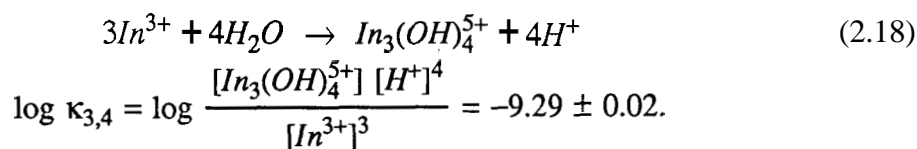
While the solubility of $\text{In}(\text{OH})_3$ in dilute NaOH was found by Thompson and Pacer (1963) to be proportional to the NaOH concentration



Baes and Mesmer (1976) calculated that very high alkali concentrations give soluble indates in accordance with the following reaction:

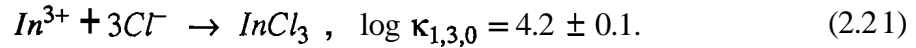
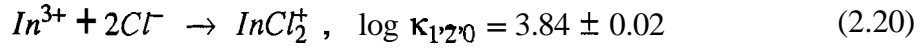
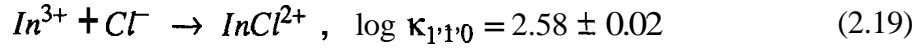


Biedermann (1956) claimed, but without presentation of detailed compositional identification, that in addition to mononuclear species InOH^{2+} and $\text{In}(\text{OH})_2^+$ several polynuclear hydrolytic species form, such as $\text{In}[\text{In}(\text{OH})_2]_n^{(3+n)+}$. Where n is an integer which may take an unlimited series of values. These polynuclear series of species have been represented sufficiently by $\text{In}_3(\text{OH})^{5+}$

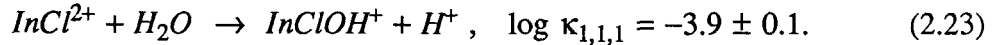
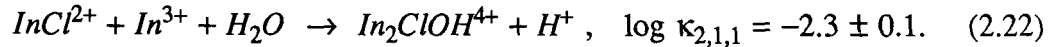


The hydrolysis distribution-diagram for a solution saturated with In(OH) is shown in Figure I. The diagram was constructed with the use of Equations 2.11 through 2.17. The corresponding formation and solubility constants have been adjusted at ionic strength $I = 1M$. The heavy curve corresponds to the total indium concentration.

Ferri (1972a) studied the complex formation equilibria between indium(III) and chloride ions. The author found no evidence for the formation of indium bearing species containing more than three chloride ions. At 25°C and 3M NaClO₄ ionic medium the following values for the formation constants were reported:



From a subsequent study, Ferri (1972b) investigated the hydrolysis equilibria of the indium chloride complex species. The chloride bearing products in the pH range 2.7 - 3.4, where hydrolysis occurs, were attributed to the formation of the following equilibria



The main hydrolysis product were assumed to be the species In₂ClOH⁴⁺. This suggestion was criticized by Baes and Besmer (1976) who have estimated that InOHCl⁺ dominate over a wide range of chloride concentrations near pH 5.

According to Biryuk et al. (1969) [as cited by Smith et al. (1978)] In(OH)₃ species in aqueous solution of ionic strength 0.1 begin to precipitate above pH 3.4. This precipitation phenomenon has been verified experimentally by the present author and the results are shown in Figure 11. The pH of precipitation increases considerably in the presence of complexing species. From the predominance diagram (Figure 11) for In³⁺-OH⁻-Cl⁻ species at 25°C in 3M NaClO₄ drawn by Baes and Mesmer (1976), it

FIGURE I. Distribution Diagram of Indium Hydrolysis

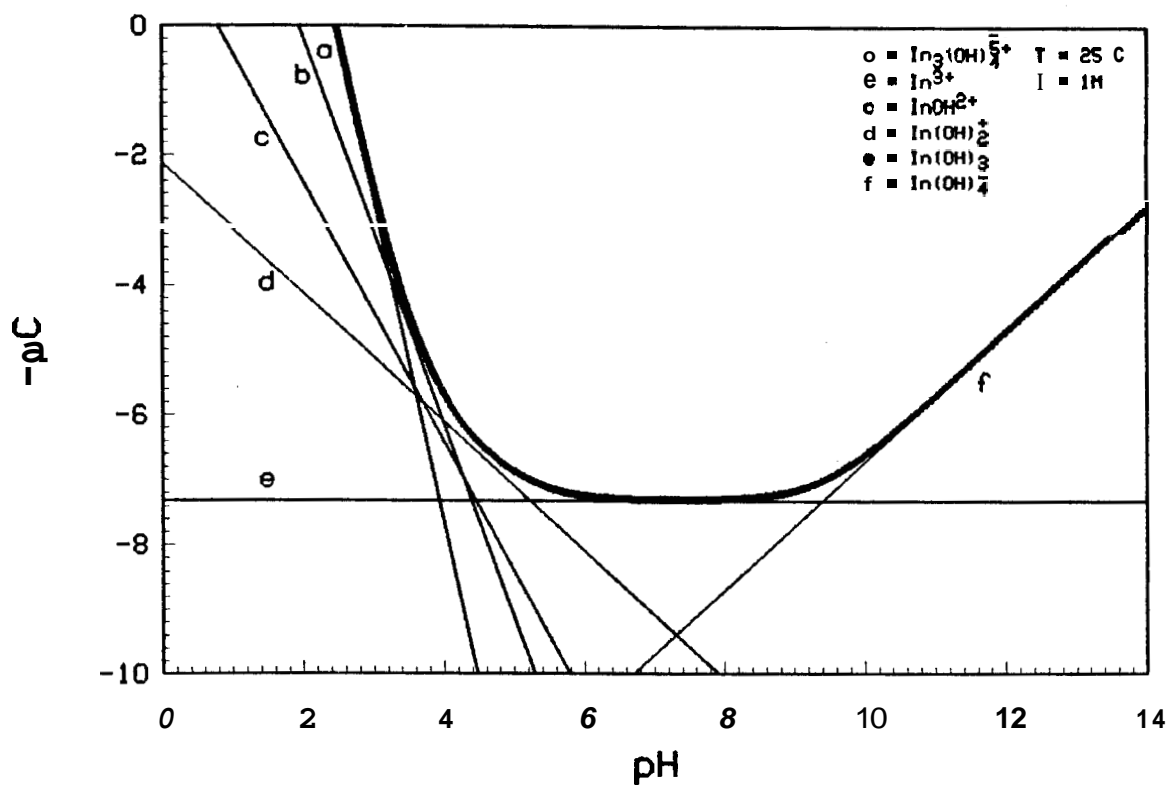
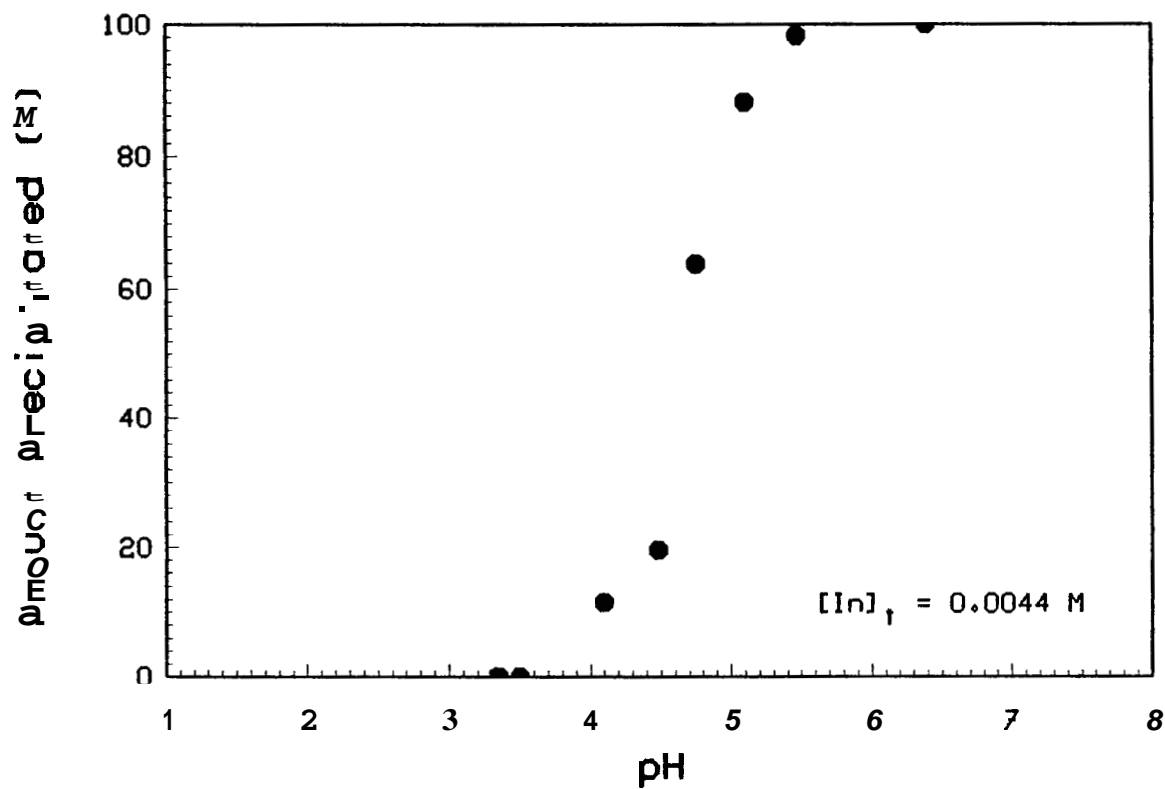


FIGURE 11. Precipitation Region of In^{3+}



is clear that chloride retards hydrolysis, and precipitation occurs in the pH range 5.5 - 9.8. In concentrated chloride solutions polynuclear species of unknown composition are formed. These species are assumed to be $\text{In}_2(\text{OH})_2\text{Cl}_2^{2+}$.

The most common insoluble indium compounds are In_2S_3 , $\text{In}(\text{OH})_3$, $\text{In}_2(\text{CO}_3)_3$, $\text{In}_4[\text{Fe}(\text{CN})_6]_3$, $\text{In}(\text{CN})_3$, $\text{In}_2(\text{C}_2\text{O}_4)_3$, $\text{InOH}(\text{C}_2\text{H}_3\text{O}_2)$, InIO_3 , InPO_4 and $\text{In}(\text{oxinate})_3$. There are two modifications of indium(III) sulfide. $\alpha\text{-In}_2\text{S}_3$ which is stable up to $\sim 330^\circ\text{C}$ and the fairly stable $\beta\text{-In}_2\text{S}_3$ which dissolves in strong mineral acids in excess of ammonium and alkali metal sulfides (Smith et al., 1978).

Separation of indium by sulfide precipitation has very limited applicability in radiochemical separations because of its high contamination from other tracer activities (Sunderman and Townley, 1960). Indium hydroxide is precipitated when NH_4OH is added into the solution, but this process carries along traces of metals which are soluble in dilute ammonia. Ferric, magnesium and bismuth hydroxides can be used as carriers for indium. Behrens et al. (1977) investigated groundwater flows with indium-EDTA tracer. They used bismuth hydroxide as coprecipitation carrier as well as a displacing reactant. They observed that 99% of the indium was found in the precipitate when 1 ml of concentrated H_2SO_4 and 2 ml bismuth solution were added in 100 ml water sample in addition to 10 ml 5 N ammonia. Indium basic acetate is precipitated when sodium acetate is added into a boiling indium solution. Also, 8-hydroxyquinoline precipitates indium from a neutral solution as $\text{In}(\text{oxinate})_3$. This precipitation method has been used in several radiochemical procedures for indium concentration prior to counting (Sunderman and Townley, 1960).

Several complexes of indium have been reported in the literature. Some of the most widely used complexes of indium(III) with organic ligands and their stability constants in aqueous solutions are given in Table VI. Insoluble indium chelates are employed in precipitation reactions, while other chelates soluble in organic solvents are employed in solvent extraction procedures,

FIGURE III. Predominance Diagram for $\text{In}^{+3}\text{-OH}^{-}\text{-Cl}^{-}$ species
 [From Baes and Mesmer (1976)]

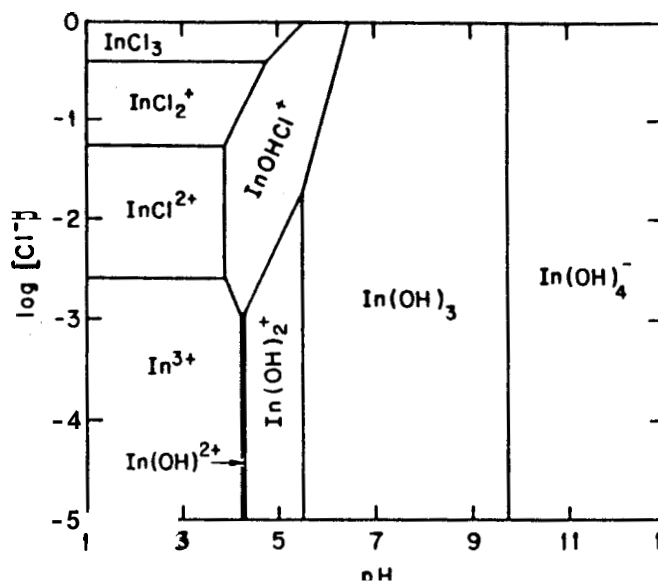


TABLE VI. Stability Constants of Indium(III) Complexes
 [From Smith et al. (1978)]

Ligand	Log of Stability Constant
Acetic acid	$k_1 = 3.50$
Acetylacetone	$k_1 = 8.0, k_2 = 7.1$
Citric acid	$k_1 = 6.18$
CDTA *	$k_1 = 27$
EDTA **	$k_1 = 24.95$
Formic acid	$k_1 = 2.74, k_2 = 1.98, k_3 = 0.98, k_4 = 1.0$
Glycolic acid	$k_1 = 2.93, k_2 = 2.59, k_3 = 1.78, k_4 = 0.65$
HEDTA ***	$k_1 = 17.2$
8-Hydroxyquinoline	$k_{so} = -31.34$
Maleic acid	$k_1 = 5.0$
Nitrilotriacetic acid (NTA)	$k_1 = 15.9$
Propanoic acid	$k_1 = 3.57, k_2 = 2.79, k_3 = 1.79, k_4 = 0.93$
Tartaric acid	$k_1 = 4.48$

*

CDTA = *t*-Cyclohexane-1,2-diaminetetraacetic acid

**

EDTA = Ethylenediaminetetraacetic acid

HEDTA = (2-Hydroxyl) ethylenediaminetriacetic acid

Liquid-Liquid Extraction

Extraction is the process of transferring a solute between two immiscible solvents. In inorganic chemical analysis, one solvent is usually water and the other solvent is a suitable organic liquid.

Solvent extraction has been convenient and effective means for separating indium from aqueous solutions. Sunderman and Townley (1960) summarized the early work of several investigators involving extraction of indium halides in diethyl-ether and isopropyl-ether, extraction separation of indium from gallium with cyclohexanone, as well as extraction of chelate complexes of indium-acetylacetone into acetylacetone and indium-diethyldi-carbamine into chloroform or carbon tetrachloride.

According to De and Sen (1967) indium is completely extracted with 100 percent tributylphosphate (**TBP**) from 6-8M hydrochloric acid. Most of the coextracted ions can be removed by repeated scrubbing with 6M hydrochloric acid. Irving and Damodaran (1970) reported that indium is extracted with 1,2-dichloroethane from tetra-n-hexylammonium. Lee and Burrell (1972) extracted trifluoroacetylacetone metal chelates from sea water medium. They reported that iron and indium form coordination saturated chelates with trifluoroacetylacetone and that they extract excellently into toluene from sea water. The major drawback of chelate extraction of indium into organic solvents is that a number of other metals extract as well under the same conditions.

Stary and Hladky (1963) found that trivalent indium is quantitatively extracted by 0.1M solutions of acetylacetone, benzoylacetone and dibenzoylmethane in benzene. The extraction constants and the two-phase stability constants of 30 metal β -diketonates were calculated by the investigators. These constants are useful for the selection of the required separation conditions for the removal of indium from other interfering metals. Similarly, indium can be extracted from hydrochloric acid into binary solvent mixtures containing isobutyl methyl ketone and any common diluent (Irving

and Lewis, 1967). According to Lyle and Shendrikar (1965), indium up to 1000 ppm can be extracted with **n-benzoyl-n-phenylhydroxylamine** (BPHA) and chloroform from 0.05M acetic acid-acetate buffered solutions. Also, it has been reported that chloroform can extract efficiently indium-1-(2-pyridylazo)-2-naphthol chelate (usually abbreviated as In-PAN) (Shibata, 1961).

Ion Exchange Behavior

The general behavior of the ion exchange of indium is not available, but its main ion exchange characteristics can be demonstrated by the numerous applications involving indium ions found in literature.

It has been demonstrated that anion exchange of metal complexes is a powerful tool for the separation of ions, as well as for the study of complexing reactions. Andersen and Knutsen (1962) studied the adsorption of indium to anion exchanger Dowex 1 (200-400 mesh) from HBr and HCl solutions. It was found that In is adsorbed strongly in HBr solutions contrary to HCl solutions. Also, the adsorption of In in HBr rises rapidly with increasing acid concentration. Detailed analysis of the species involved was not presented but it was concluded that indium prefers to form bromo-complexes rather than chloro-complexes, and that bromide ions are adsorbed more strongly than chloride ions on the Dowex 1 resin. The anion exchanger Dowex 1 has also been used by Korkisch and Hazan (1964) for the chromatographic separation of Al, Ga and In in hydrochloric acid-acetone and hydrochloric acid-2-methoxyethanol mixtures. Since the distribution coefficients are not very high under the experimental conditions employed, long columns have to be used. Wodkiewicz and Dybczynski (1974) found that indium is adsorbed on anion exchanger Amberlite IRA-68 only at HBr concentrations greater than 4M. The calculated adsorbability of indium on Amberlite IRA-68 in the bromide system is lower than the reported adsorbability on Dowex 1 resin in a similar system. Dybczynski et al. (1977) investigated the effect of degree of resin crosslinking on the anion exchange of indium phosphate complex,

$[\text{In}(\text{HPO}_4)_3]^{3-}$, on Dowex 1. It was concluded that lightly crosslinked resins are best for separations of large ionic complexes.

Less information has been reported concerning cation exchange than anion exchange separations of indium. According to Strelow and Victor (1971) Al, Ga, In and Tl can be separated without tailing with 100 percent recoveries from AG50W-X8 (200-400 mesh) cation exchange resin with hydrochloric acid-acetone mixtures. The reported cation exchange distribution coefficients compare favorably with analogous coefficients obtained with Dowex 1 anion exchange resin. From a subsequent study, Strelow (1980) prepared an elution curve for a mixture of In, Ga and Co. The author claimed that indium and other elements which have a strong tendency to bromide complex formation can be eluted with 0.5M hydrobromic acid in 86 percent acetone from AG50W-X4 cation exchange resin. Riley and Taylor (1968) conducted studies on trace element concentration from sea water. They achieved 100 percent total recovery of indium with Chelex-100 (50-100 mesh) ion exchange column and 2 N nitric acid as eluant. Muzzarelli et al. (1970) conducted separations of trace elements from sea water brine and sodium and magnesium salt solutions by the natural chelating polymer Chitosan. The eluting agent used was 0.1 N EDTA and indium recovery was estimated approximately 70 percent. This chelating polymer has the advantage that it does not appreciably collect sodium and magnesium but its capability for indium recovery cannot be favorably compared with the indium recoveries obtained by Dowex A1 or Chelex-100 resins.

Cation exchange followed by anion exchange separation was employed by Matthews and Riley (1970) for the determined indium in sea water. Since the concentration of indium in sea water is low, a preconcentration stage is essential. They selected Dowex A1 (50-100 mesh) chelating ion exchange resin in the sodium form to investigate the absorbability of indium. It was found that 20 percent of the indium was retained at pH 7.0, but the efficiency of the retention increased rapidly as the pH

was raised. The indium was eluted with 3 M hydrochloric acid. In addition to indium the eluate contained milligram amounts of sodium, potassium, magnesium and calcium. These trace elements were removed by passing the eluate from the Dowex A1 column through a Dowex AG2-X8 (200-400 mesh) column where indium chloro-anions were retained completely. The column was washed with 3 M hydrochloric acid which removed 98 percent of the alkali and alkaline earth elements present in the original eluate. No indium was removed from the column because its adsorption is optimum at high acid concentration. The adsorbed indium was recovered by elution of the anion exchanger with 0.1 M hydrochloric acid. The authors claimed that the two ion exchange procedures achieved an overall indium recovery exceeding 98 percent at concentration levels of the order of nanograms per liter.

Amphoteric ion exchange resins can also be employed in radiochemical and analytical separations of indium. Dybczynski and Sterlinska (1974) achieved separations of Ga-In-Tl mixtures with the amphoteric ion exchange resin, Retardion 11A8. This resin contains carboxylic and quaternary ammonium exchange groups, and can be effectively used with metals that can exist both as cations and as anions in solution.

Detection Methods

Several methods have been described in the literature for the determination of indium. The most common detection methods involve anodic stripping voltametry (Florence et al., 1974), spectrophotometry (Shibata, 1960), polarography (Lin and Feng, 1984), mass spectrometry (Chow and Snyder, 1969), atomic absorption (Riley and Taylor, 1968; Rattonetti, 1974; Busheina and Headridge, 1981), and the very sensitive method of neutron activation (Matthews and Riley, 1970; Behrens et al., 1977; Navada et al., 1981; Drabaek, 1982).

Nuclear Properties

The only two naturally occurring isotopes of indium are with mass numbers 113

and **115**; over **30** radionuclides of indium are known. Several of these isotopes are formed during the thermal neutron fission of ^{235}U and it is estimated that the uranium fission in the United States produces approximately 0.05 tons of indium annually. The percentage isotopic abundances of the natural isotopes of indium are given in Table VII, together with their products upon neutron irradiation, their half-lives, some details of the decay modes, and the radiation emitted with energies in MeV. The cross sections for $^{113}_{49}\text{In}(n,\gamma)^{114}_{49}\text{In}$ and $^{113}_{49}\text{In}(n,\gamma)^{114m}_{49}\text{In}$ reactions are relatively small, **3** and **5** barns respectively. Also, ^{114}In has considerably short half-life (**71.9** seconds), while ^{114m}In has a half-life of **49.5** days which is very long for an activable tracer. In addition to these unfavorable properties, ^{113}In has a small isotopic abundance (**4.3%**); therefore, this natural isotope of indium is not useful for geothermal tracing. On the other hand, the cross sections for $^{115}_{49}\text{In}(n,\gamma)^{116}_{49}\text{In}$ and $^{115}_{49}\text{In}(n,\gamma)^{116m}_{49}\text{In}$ reactions are quite large, **41** and **70** barns respectively. The **14.1** second ^{116}In is easily excluded from any tracing applications because of its extremely short half-life. The unique combination of good isotopic abundance of $^{115}_{49}\text{In}$ (**95.7%**) and the fairly good half-life of its activation product (**54.12** minute- ^{116m}In) is the chief reason that makes indium an excellent activable tracer. The beta particles emitted from ^{116m}In have energies of **1.00 (51%)**, **0.87 (28%)**, **0.60 (21%)** MeV and may be radioassayed with a proportional counter. The gamma spectrum of this isotope (see Figure IV) consists of several gamma rays ranging from **0.138** to **2.225** MeV. Its major gamma ray is **1.2935** MeV with an absolute intensity of 85 percent, which **makes** its detection entirely tractable by scintillation detectors.

TABLE VII. Selected Nuclides of Indium

[From Lederer and Shirley (1978)]

Nuclide	$f(\%)$	$T_{1/2}$	Decay Modes	σ
^{113}In	4.3			$^{114}\text{In}:3, ^{114m}\text{In}:5$
^{114}In		71.9s	β^- (98.1%); EC; γ :1.3	
^{114m}In		49.5d	IT:0.1902(96.7%); EC	
^{115}In	95.7	$5.1 \times 10^{14}\text{y}$	β^-	In-116:41, In-116m:70
^{116}In		14.1s	β^- ; γ :1.294 (1.3%)	
^{116m}In		54.12m	β^- ; γ :1.2935 (85%)	

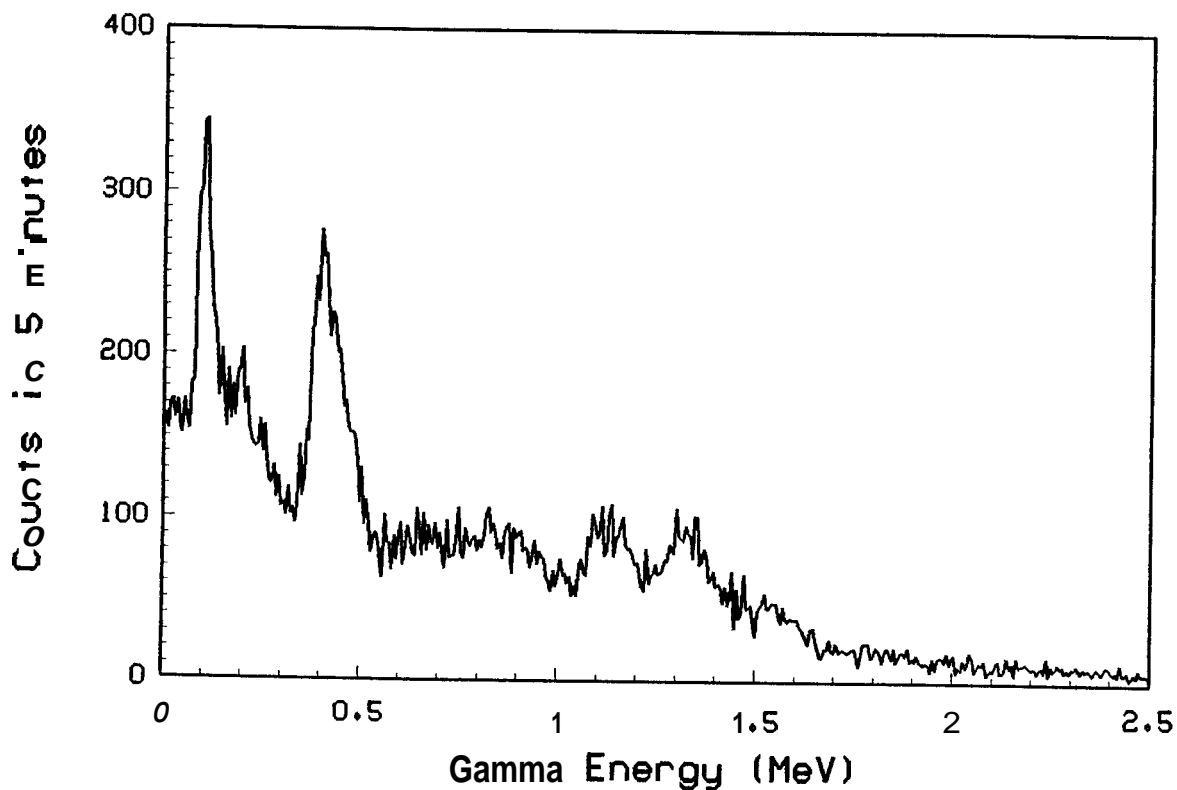
*

IT = isomeric transition; EC = electron capture; γ energies in MeV

**

σ = cross section (barns)

FIGURE IV. Gamma Spectra of Indium-116m



2.4. CHELATES

Most metal ions are capable of sharing electron pairs with a nonmetal atom having a free electron pair to form a coordination bond. However, it isn't uncommon for metal ions to contribute electrons to the bond as they do in π bonding. Therefore for simplicity purposes, any negative ion bound to a metal atom is customarily called a *ligand* and the bond between them a *metal-ligand* bond. If a specie is capable of attaching itself to a metal ion through more than one donor atom to produce a cyclic ring type of arrangement, it is known as *chelating agent* (Brady and Humiston, 1975). The complex is called a *chelate* and its properties are influenced to a considerable extent by the nature and oxidation state of the central metal atom.

Chelating agents are polyprotic acids, and usually only the fully deprotonated form of the acid gives complexes with the metal ion. This implies that the formation of chelate complexes is affected by the acidity of the solution, and that the chelate stability is strongly enhanced in basic solutions. In such solutions most metals precipitate. Therefore, a buffer medium acting as a subsidiary complexing agent must be provided in order to prevent the precipitation of the hydroxide (Butler, 1964).

Metal chelates are inherently more stable than closely related nonchelate complexes and their equilibrium relationships are written as formation rather than as dissociation reactions. Chelates are usually developed by combination of stepwise reactions:



where

M = metal

L = ligand.

The overall stability constant, β_n , is the product of the step formation constants

$$\beta_n = \frac{[ML]}{[M][L]} \frac{[ML_2]}{[ML][L]} \cdots \frac{[ML_n]}{[ML_{n-1}][L]} = \frac{[ML_n]}{[M][L]^n} \quad (2.25)$$

The reciprocal of the overall formation constant is known as the *instability constant* and it is analogous to the dissociation constant.

Dwyer and Mellor (1964) suggest that the principal factors influencing the stability of metal chelates are: (a) the ring size, because big rings are unstable especially in aqueous solutions where the competition between the water molecules and chelate of the metal ion favors completely the hydrated form of the ion, (b) the number of rings or more specifically the stability of the metal complex increases with increasing number of chelate rings, (c) the basic strength of the chelating molecule, (d) the effect of substitution in the chelating molecule, (e) the nature of the donor atoms, and (f) the influence of the central atom.

Chelating agents such as nitrilotriacetic acid (NTA), diethylenetriaminepentaacetic acid (DTPA) and ethylenediaminetetraacetic acid (EDTA) have been extensively employed in wide variety of applications, such as prevention of normal hardness deposits in industrial equipment; decontamination of nuclear facilities; stabilization of fatty acids; prevention of turbidity formation in wine; as well as in the therapeutic removal of poisonous metals ingested by humans (Jacklin, 1965; Sniegowski and Venezky, 1974; Means et al., 1980). These chelating agents form extremely strong complexes with rare earths and actinides, and have been considered as principal contributors in the mobilization of radionuclides from radioactive waste burial sites (Means et al., 1978).

Ethylenediaminetetraacetic Acid

*

Ethylenediaminetetraacetic acid, usually abbreviated EDTA, is one of the most

* EDTA is sold under a variety of trade names: Calcol, Chelaton, Complexone 111, Iminol D, Nervanaid, Nullapon, Sequestrene, Idranal 111, Titra Ver, Trilon B and Versene.

common chelating agents used in analytical chemistry as a titrant for metal ions, EDTA is a white anhydrous crystalline solid with a melting point of 240°C . It is almost insoluble in water as well as in absolute acetone, ethanol and ether, but it is readily soluble in inorganic acid solutions (Garvan, 1964). However, the mono-, di-, tri- and tetrasodium salts of EDTA increase in water solubility with increasing temperature.

EDTA is a tetraprotic acid since each of its carboxyl groups is ionizable, and it is characterized by the following pK values: $\text{pK}_1 = 2.0$, $\text{pK}_2 = 2.67$, $\text{pK}_3 = 6.16$ and $\text{pK}_4 = 10.26$. Figure V shows the pH-dependent ionization of EDTA in the form of a distribution diagram, where the heavy curve corresponds to the fully deprotonated form of the acid. EDTA can form coordination bonds at six sites, the four oxygen and the two nitrogen sites, and 1:1 water soluble complexes with most metal ions. In general the metal complexes of EDTA form five five-membered rings and reduce the charge on the central atom by four (see Figure VI).

A list containing most of the stability constants of EDTA complexes with metal ions is provided in Table VIII. From this table it can be observed that V^{3+} possesses the highest stability constant with EDTA, while In^{3+} possesses slightly less stable EDTA complex than the ferric cation does. The greater the stability constant the more tightly the metal ion is bound in the chelate. This implies that Fe^{3+} could possibly act as a displacing reactant releasing the cation In^{3+} from its EDTA complex. The total iron concentration of geothermal fluids is quite high ranging from 0 to 4,200 ppm (see Table I). Since geothermal reservoirs resemble the conditions of a reducing environment containing very little dissolved oxygen, the ferric cation is expected to constitute a very small fraction, if any, of the total iron concentration of geothermal liquids. Therefore, it is believed that the displacing ability of Fe^{3+} can not seriously perturb the InEDTA tracer. Also, from Table VIII it is apparent that the ferrous cation can not replace indium from the InEDTA complex due to its weaker stability constant.

FIGURE V. $p\alpha/pH$ Diagram for EDTA

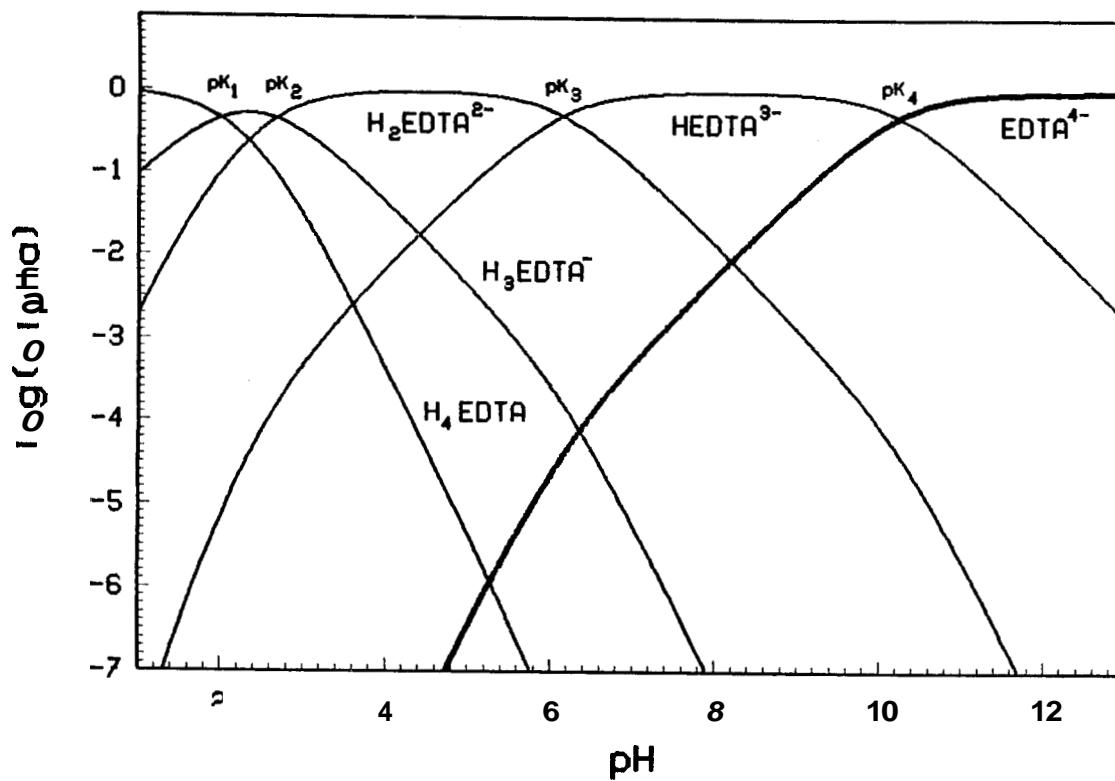


FIGURE VI. Indium-EDTA Complex Formation

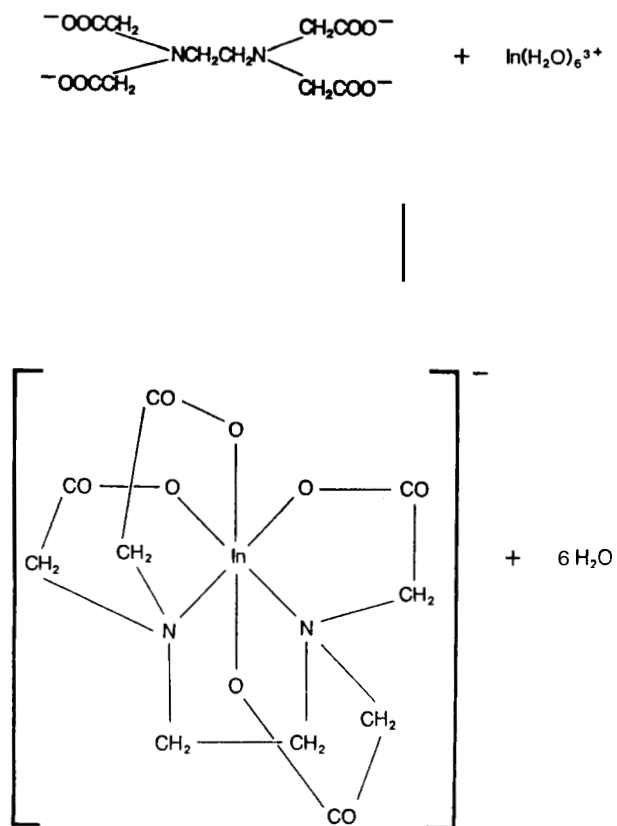


TABLE VIII. Stability Constants of EDTA Complexes at 20°C in KNO_3
 [From Pribil (1972) ³

Cation	Log of Stability Constant	Cation	Log of Stability Constant
V^{3+}	25.90	Eu^{3+}	17.35
Fe^{3+}	25.10	Sm^{3+}	17.14
In^{3+}	24.90	Na^{3+}	16.61
Th^{3+}	23.20	Zn^{3+}	16.50
Bi^{3+} *	22.80	Ca^{3+}	16.46
Hg^{2+}	21.80	Pr^{3+}	16.40
Ga^{3+}	20.30	Co^{2+}	16.31
Lu^{3+}	19.83	Al^{3+}	16.13
Yb^{3+}	19.51	Ce^{3+}	15.98
Tm^{3+}	19.32	La^{3+}	15.50
EP^+	18.85	Fe^{2+} **	14.33
Cu^{2+}	18.80	Mn^{2+}	14.04
VO^{2+}	18.77	V^{2+}	12.70
Ho^{3+}	18.74	Ca^{2+} **	10.96
Ni^{2+}	18.62	Mg^{2+} **	8.69
Dy^{3+}	18.30	Sr^{2+} **	8.63
Y^{3+}	18.09	Ba^{2+} **	7.76
Pb^{2+}	18.04	Ag^+	7.20
Tb^{3+}	17.93	Li^+ **	2.79
Gd^{3+}	17.37	Na^+ **	1.66

* From Behrens et al. (1977)

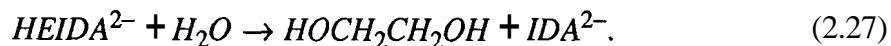
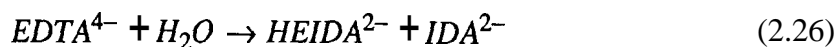
** Stability constants measured at 20°C in 0.1 M KCl.

The ability of EDTA to form stable, water-soluble complexes with most of metal ions is the characteristic that contributes to undesirable environmental consequences such as mobilization of radioactive rare earths, transition metals, and transuranics. Since EDTA is rather slowly biodegradable (Tiedje, 1977), it is expected to be very persistent in the natural environment. Indeed, EDTA has been observed in twelve years old industrial wastes (Means et al., 1978). Therefore wherever EDTA is being used, waste solutions should be treated prior to final disposal in the ground. Thermal degradation treatment has been considered a suitable solution to the environmental problem.

The properties of EDTA at elevated temperatures have been studied by several investigators. Wendlandt (1960) examined by thermogravimetric and differential thermal

analysis the thermal stability of uncomplexed EDTA and its derivatives. The reported decomposition temperatures of EDTA ranged from 250 to 265°C, but the degradation products were not identified. The thermal behavior studies of EDTA were extended by Venezky and Moniz (1969) who claimed that the decomposition of H_4EDTA at 200°C occurs rapidly with a stepwise loss of $(-CH_2CO_2^-)$ groups. The authors indicated without experimental justification that a secondary degradation takes place at this temperature in which the degradation products retain chelating ability.

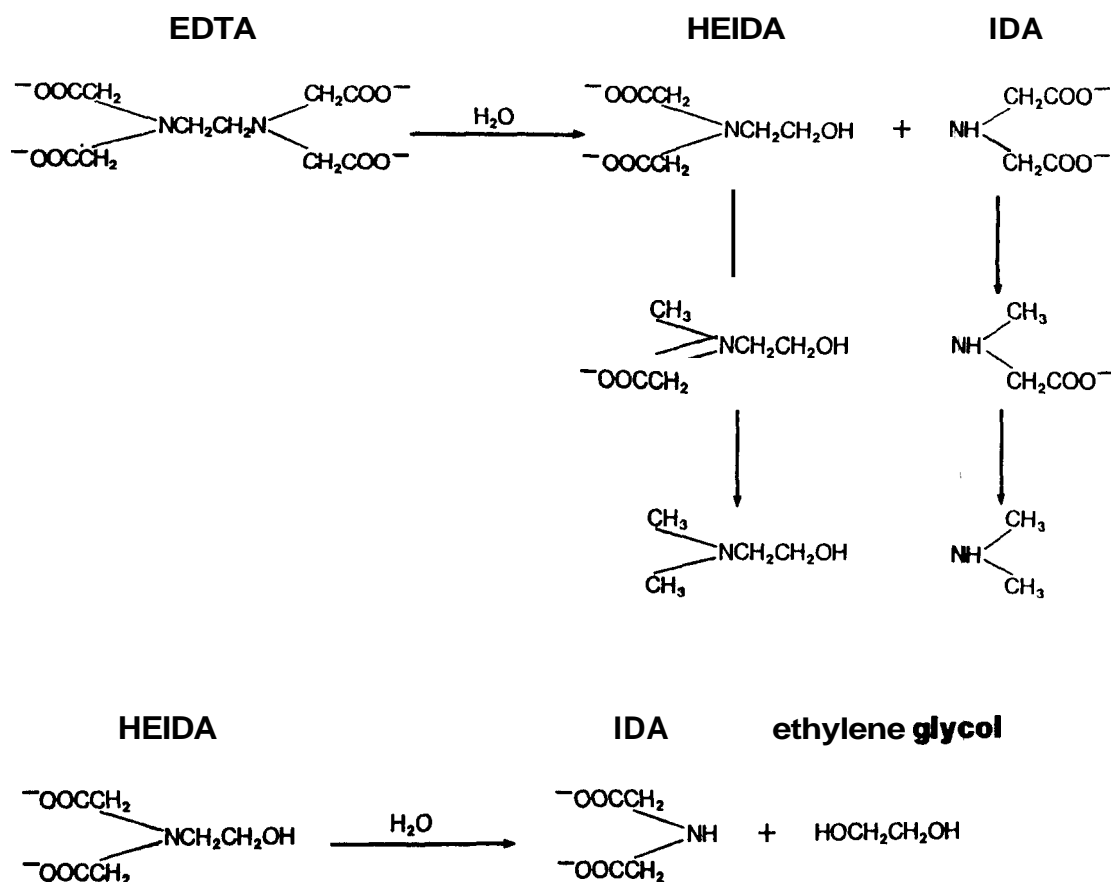
Sniegowski and Venezky (1974) developed a gas chromatographic method for the analysis of EDTA, IDA (iminodiacetic acid), and HEIDA (N-2-hydroxyethyl iminodiacetic acid). This new method of analysis was employed in the investigation of EDTA decomposition at high temperature and pressure. The reported decomposition reaction involves the hydrolytic cleavage of the ethylenic C-N bond and the proposed decomposition mechanism is:



Investigation of the thermal stability of EDTA was also performed by Martell et al. (1975). The decomposition rates and products of EDTA in water solution at 200 and 260°C were determined by nuclear magnetic resonance at pH 9.5. They reported that the decomposition reaction of EDTA involves the hydrolytic cleavage of the ethylenic C-N link to produce the stable pair: HEIDA and IDA. At 260°C these decomposition products appeared after about 31 minutes. At higher temperatures further breakdown of the primary products of EDTA occurred with the loss of CO_2 producing the corresponding methylamines. Furthermore, hydrolytic cleavage of the remaining CH_2CH_2-N link was observed giving ethylene glycol. The reported EDTA thermal degradation mechanism is comparable with the one proposed by Sniegowski and Venezky (1974) and it is illustrated in Figure VII.

FIGURE VII. Thermal Decomposition Mechanism of EDTA

[From Martell et al. (1975)]



Nitrilotriacetic Acid

*

Nitrilotriacetic acid or NTA is another member of the amino carboxylic acid family of chelating agents. It is a white crystalline solid, barely soluble in water. NTA is a tribasic acid with the ability of ionizing each one of its carboxyl groups, and it is characterized by the following pK values: $\text{pK}_1 = 1.89$; $\text{pK}_2 = 2.49$; and $\text{pK}_3 = 9.73$. Figure VIII shows the pH-dependent ionization of NTA in the form of a distribution diagram, where the heavy curve corresponds to the fully deprotonated form of the acid. NTA can form coordination bonds at four sites, the three oxygen and one nitrogen sites. The acid is of great analytical significance, because it forms stable water

* NTA is also called Trilon A, Trimethylamine tricarboxylic acid, or Complexione I.

FIGURE VIII. α/pH Diagram for NTA

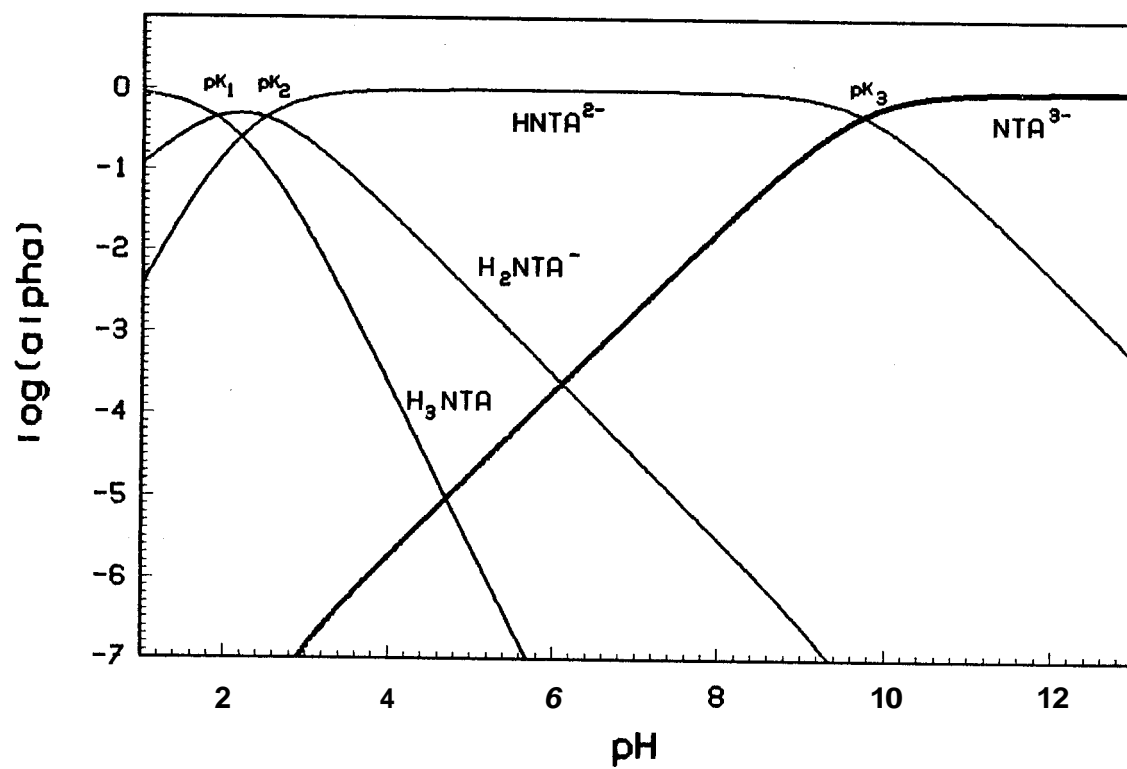
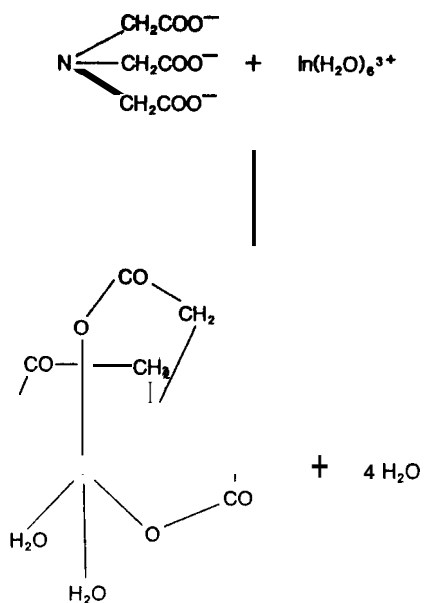


FIGURE IX. Indium-NTA Complex Formation



soluble complexes with most metal ions. In general the **NTA** metal complexes form three five-membered rings and reduce the charge on the metal atom by three (see Figure IX).

A list containing some of the stability constants of **NTA** complexes with metal ions is provided in Table IX. From this table it can be observed that the **InNTA** complex is very strong. Only Bi^{3+} forms an **NTA** metal chelate of higher stability constant. Since the Bi^{3+} concentration of geothermal fluids is at trace levels, it is anticipated that Bi^{3+} will not displace quantitatively In^{3+} from the **InNTA** chelate.

NTA has been used extensively as a phosphate substitute in heavy-duty detergents. Since the detergents become components of wastewater, the detergent industry and others concerned with wastewater treatment and water supply have focused their studies on the biodegradability of **NTA**. The investigations have shown that the degradation of **NTA** is essentially complete to end products of CO_2 and inorganic **N**; in river water (Warren and Malec, 1972), sea water (Erickson et al., 1970),

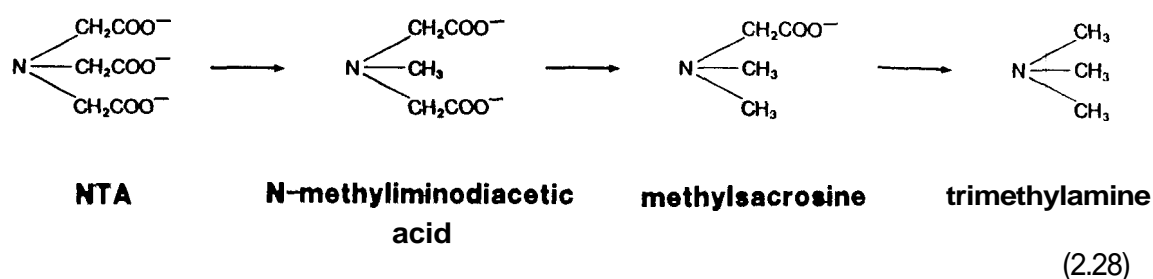
TABLE IX. Stability Constants of **NTA** Complexes Measured at 20°C
[From Pribil (1972)]

Cation	Log of Stability Constant	Cation	Log of Stability Constant
Bi^{3+} *	17.50	La^{3+}	10.48
In^{3+} **	15.90	Ca^{2+}	9.83
Fe^{3+}	15.87	Fe^{2+}	8.83
V^{3+} *	13.41	Mn^{2+}	7.44
Cu^{2+}	12.96	Ca^{2+}	6.41
Dy^{3+} ***	11.74	Mg^{2+}	5.41
Ni^{2+}	11.53	Ag^+	5.40
Y^{3+}	11.41	Sr^{2+}	4.98
Pd^{2+}	11.39	Ba^{2+}	4.82
Zn^{2+}	10.67	Li^+	2.30
Co^{2+} ****	10.60	Na^+	1.50

- * from Martell and Smith (1974)
- ** from Smith et al. (1978)
- *** from Smith and Carson (1981)
- **** from Moeller (1975)

activated sludge (Shumate et al., 1970), and sewage lagoons (Rudd and Hamilton, 1972). Because NTA is biodegradable, it would not be present in high concentrations in groundwater systems and therefore it should not be considered as an environmental hazard.

Attention has also been given to the thermal properties of NTA. Martell et al. (1975) studied the decomposition of NTA in aqueous solution at 260 and 293°C. The decomposition rates and products were determined by nuclear magnetic resonance at pH 9.3. They reported that NTA does not undergo hydrolytic cleavage below 260°C, but decomposes at about 290°C and above through a stepwise decarboxylation to N-methyliminodiacetic acid, methylsacrosine, and trimethylamine.



The half life of NTA at 293°C was estimated to be **4.0** hours. Also, it has been reported by Venezky and Moniz (1970) that at the lower temperature of 200°C, the half life of NTA³⁻ and HNTA²⁻ are both greater than 1000 hours.

Most of the published information on properties of organic ligands at elevated temperatures is based on uncomplexed EDTA and NTA rather than their indium chelates which are of considerable practical value and essential to this study. The lowest temperature at which decomposition of InEDTA and InNTA metal chelates proceed at any significant rate should be obtained experimentally. However, there is good reason to suspect that the metal chelates will breakdown at temperatures close to the decomposition temperature-range of their organic ligands.

CHAPTER 3

EXPERIMENTAL, PROCEDURES

3.1. GENERAL CONSIDERATIONS

Reagent Preparation

All reagents used in this investigation were of analytical reagent grade. The metals used for the laboratory activable tracer sensitivity measurements were as follows: vanadium and indium: Aldrich Chemical Co.; dysprosium and cobalt: Alfa Products. Baker Analyzed disodium salts of EDTA and NTA were used for the ligand standard solutions. Tracer stock solutions were prepared by dissolving the corresponding metal reagent powder in concentrated nitric acid. Milli-Q reagent grade deionized water was used as solvent. The tracer stock solutions were acidified to reduce adsorption onto container walls and stored in glass volumetric-flasks with ground glass stoppers. The pH of the organic ligand solutions was adjusted to a pH slightly above the last pK value of the corresponding ligand, because chelating agents are polyprotic acids and usually only the fully deprotonated form of the acid gives complexes with the metal ion. The indium tracer solutions were formed with a chelon to metal mole ratio of 10 to increase the stability of the indium chelate complex.

Glassware Cleaning

To ensure that contamination does not occur from improperly cleaned labware, all laboratory vessels and equipment were thoroughly cleaned. Glassware were soaked overnight in either acid or base dilute cleaning bath, depending on the solution stored

in the container. After removal from the cleaning solution, the glassware were rinsed several times with deionized tap water. Finally, the glassware were rinsed with Milli-Q water and stored in drawers or covered until use. Cleaning bath solutions were changed frequently. Glassware such as flasks and pipettes used for storing or transferring concentrated stock solutions were labeled and segregated from those used for dilute solutions. This precaution is necessary when working with low concentration tracer solutions. An additional consideration was to use low background capsules with sorbate-free interiors assuring reliable and consistent results. Therefore, disposable Wheaton scintillation capsules were employed for neutron irradiation and gamma-ray spectroscopy. Also to reduce the amount of labware cleaning, disposable polystyrene centrifuge tubes were used throughout the procedure.

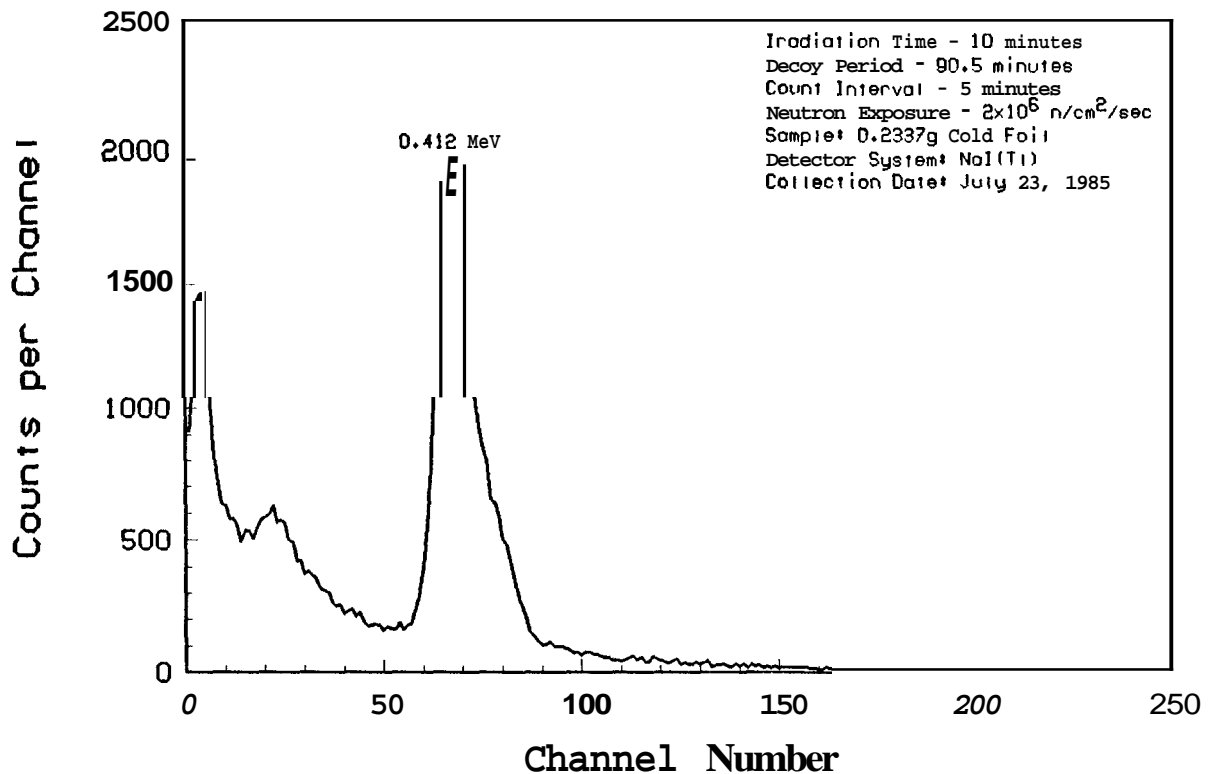
3.2. ACTIVATION FACILITIES

A ^{252}Cf neutron source located at the Stanford Linear Accelerator Center (SLAC) was used for the procedure development. The ^{252}Cf is encapsulated in a helium atmosphere and it is assumed to decay with an effective half-life of **2.646** years. The effective ^{252}Cf content was calculated from its neutron emission rate and is given in equivalent weight units assuming 2.311×10^6 neutrons per second per microgram of ^{252}Cf . The thermal neutron flux was calibrated with gold foils provided by SLAC. The thermal neutron flux was calculated from the area under the characteristic photopeak (0.412 MeV) of ^{198}Au shown by the sample spectra in Figure X. Several flux measurements of the ^{252}Cf source have been obtained and presented as a function of time in Table X. A neutron flux of the order of 10^6 thermal n/cm²sec is considered adequate for procedure development, but for natural background measurements a device with larger neutron flux is necessary.

TABLE X. ²⁵²Cf Source Flux Measurements

Date	Thermal Neutron Flux (n/cm ² s)
May 25, 1984	2.84x 10 ⁶
July 2, 1984	2.64x 10 ⁶
April 3, 1985	1.89x10 ⁶
May 23, 1985	1.79x10 ⁶
Sep. 25, 1985	1.75x 10 ⁶

FIGURE X. Gamma Spectra of Gold-198



Counting Apparatus

Sample activities were measured with a Baird-Atomic Model 810C Well Scintillation detector coupled to a Canberra Series 30 Multichannel Analyzer. The Model 810C well scintillation detector makes possible the detection of gamma and beta ray emissions from radioactive materials and provides an electrical output in suitable form for the multichannel analyzer. The Model 810C is supplied with a well crystal assembly for 5 ml samples. This assembly includes a 1.75 inch diameter by 2 inch thick

sodium-iodide thallium crystal, photomultiplier tube and metal shield. The Canberra series 30 analyzer consists of 1024 data channels, each with a capacity of 10^6-1 counts. The data may be stored in either Pulse Height Analysis (PHA) or Multichannel Scaling (MCS) mode. The data were displayed on a 9 inch screen while full memory readout and integral of preselected regions of interest were collected with a Newport 810 digital printer.

Gamma-Ray Scintillation Detector Calibrations

Studies were made of the correction factors necessary to relate the counting rate obtained from the multichannel analyzer to concentrations of tracer in the sample. Because of the high sensitivity of NaI(Tl) detectors, massive shielding can be effective in reducing background effects due to gamma rays from surrounding materials and cosmic rays. Since all materials contain some naturally occurring radioactivity, the background count rate obtained with the absence of tracer must be subtracted from the total sample count rate. The average background count rate for the Baird-Atomic Model 810C well scintillation detector was estimated with a blank sample counted for 24 hours. The background activity plotted as a function of channel number is shown in Figure XI-(A).

Another important characteristic of scintillation detectors is the variation of counting efficiency with gamma ray energy. An experimental efficiency curve was prepared for the Model 810C scintillation detector and is shown in Figure XI-(B). The counting efficiencies of the radionuclides of interest are obtained from this calibration curve. The calibration standards used for the construction of the counting efficiency curve were provided by the Stanford Health Physics facility.

Because the counting efficiency is dependent on the sample volume and its geometric position in the well, it is necessary to make corrections to the sample activity measurement. The relation of counting efficiency and sample volume can be obtained by diluting a sample of known activity by a constant factor, and monitoring

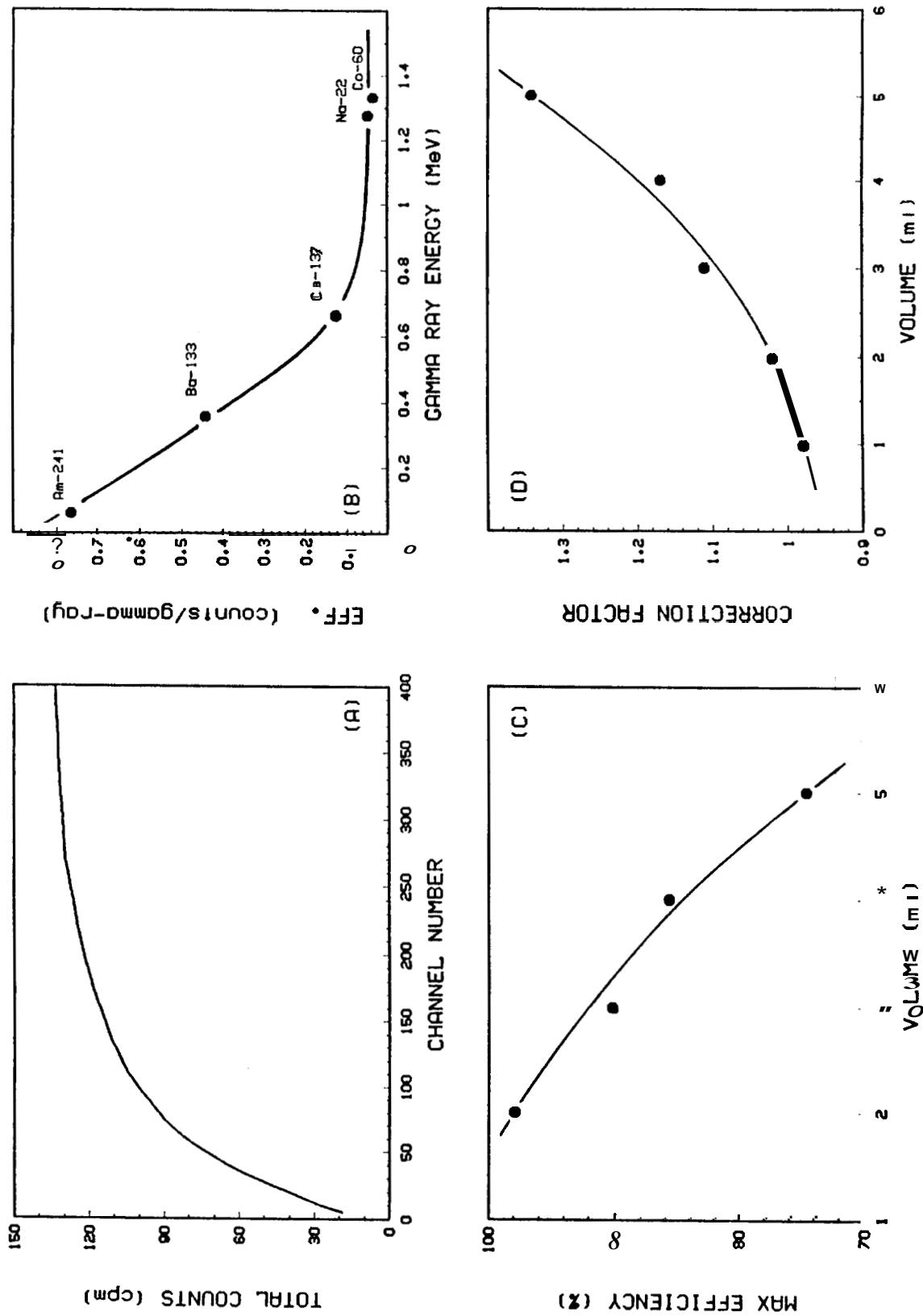


FIGURE XI. Gamma-Ray Scintillation Detector Calibrations. (A) Background activity as a function of channel number, (B) Experimental efficiency curve, (C) Counting efficiency relationship, (D) Counting efficiency correction factor curve.

the activity fluctuations per dilution. The counting efficiency relationship for the Baird-Atomic Model 810C well scintillation detector is shown in Figure XI-(C) while the counting efficiency correction factors have been calculated and presented in a graphical form in Figure XI-(D).

3.3. STATISTICAL CONSIDERATIONS OF RADIOACTIVITY

MEASUREMENTS

The laws governing radioactive decay are probability functions, and can be described accurately only when they are applied to a large number of events. Measurements of radioactivity, are like all physical measurements, subject to both random and systematic error. The precision of radiation measurements by counting is usually expressed in terms of variance and the standard deviation of an individual observation or the analogous quantities for the mean of several observations (Wylie, 1984). For a number of decays, N , occurring over n equal finite time intervals Δt , the measure of the precision is given by the quantity called *variance* of N :

$$\text{Var}(N) = E[E(N) - N] = E[(\bar{N} - N)^2] = \sigma_N^2 \quad (3.1)$$

Where \bar{N} is the arithmetic mean of the measured values, $E[f(N)] = \int f(x)P_N(x)dx$ is a parameter of the distribution function, P_N , denoting the expected value of any function of N (DeGroot, 1975), and σ_N is the standard deviation:

$$\sigma_N = \pm \left[\frac{\sum_{i=1}^n (\bar{N} - N_i)^2}{n - 1} \right]^{1/2} \quad (3.2)$$

The mean value of a large number of events is presumably the true value. The standard error of the mean of a single measurement from its true value is given by:

$$\sigma_{\bar{N}} = \pm \frac{\sigma_N}{\sqrt{n}} \quad (3.3)$$

In radioactivity observations by counting, a Poisson distribution of observed values is followed. Thus, the standard deviation of the accumulated counts can be

approximated by the relation:

$$\sigma_{\bar{N}} = \pm \sqrt{\bar{N}} \approx \pm \sqrt{N} \quad (3.4)$$

For sufficiently large number of counts the Poisson distribution becomes equivalent to the well-known normal distribution, the Gaussian error curve. In the normal distribution the probability that the observed value will deviate from the true value by more than the standard deviation is 31.7 per cent (Holman, 1978). Although the absolute deviation increases with an increase of the accumulated counts, the relative error diminishes.

The observed counting rate, A , over the total time $n\Delta t$, is given by the expression:

$$A = \frac{N}{n\Delta t} \pm \left[\frac{N}{(n\Delta t)^2} \right]^{1/2} \quad (3.5)$$

For low count rates it is significant to obtain the net count rate, A_{net} , as the difference between observed count rate, A_{obs} , and background count rate, A_{bg} :

$$A_{net} = (A_{obs} - A_{bg}) \pm \left[\sigma_{\bar{N}_{obs}}^2 + \sigma_{\bar{N}_{bg}}^2 \right]^{1/2} \quad (3.6)$$

It is clear that the results are significantly reliable only when $A_{obs} \gg A_{bg}$.

When the half-life of radioactive atoms is short compared to the counting time t' , the activity can not be treated as constant because decay occurs during the period of measurement. Therefore, corrections must be made to the observed counts. The magnitude of the necessary correction, C , is given by the expression:

$$N_{corr} = CN_{obs} = \frac{N_{obs}}{1 - \exp\left(-\frac{\ln 2}{T_{1/2}} t'\right)} \left[\frac{\ln 2}{T_{1/2}} \right] t' \quad (3.7)$$

The derivation of the above expression is included in Appendix A, while the correction factor for counting times t' as a function of $T_{1/2}$ is graphically presented in Figure XII.

FIGURE XII. Correction Applied to Observed Counts for Decay During Counting

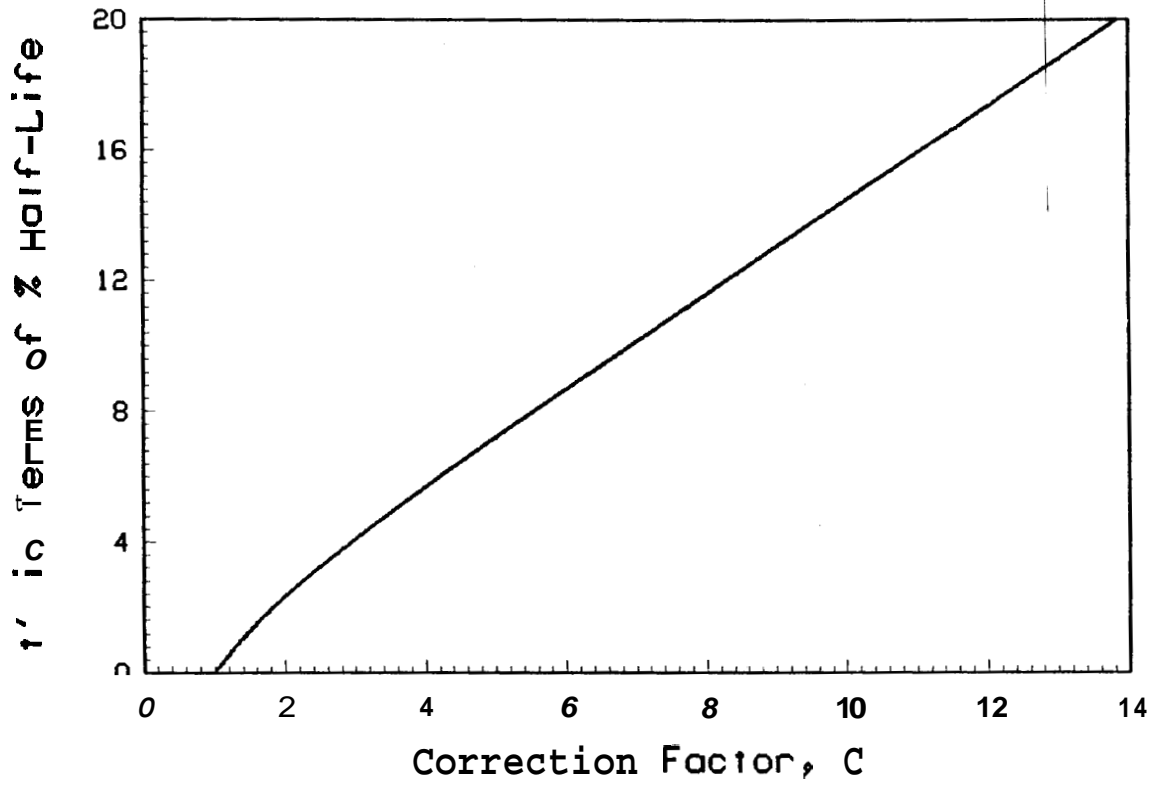
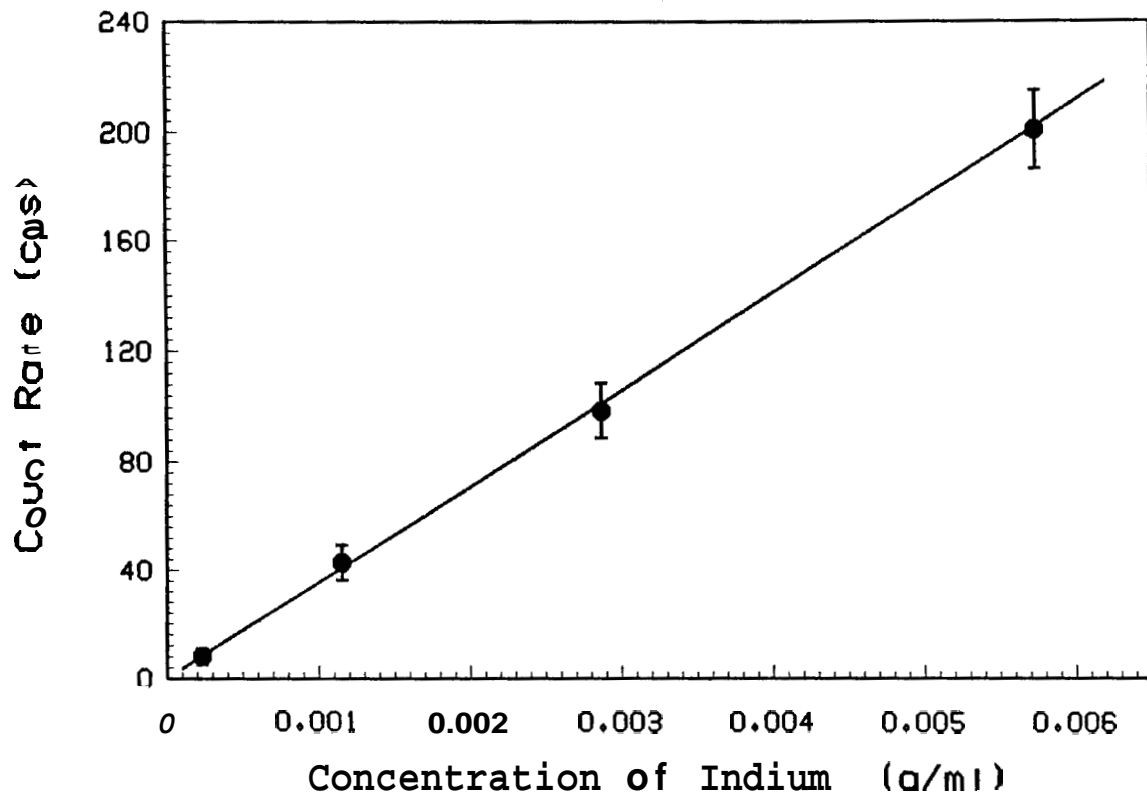


FIGURE XIII. Calibration Curve



3.4. CONCENTRATION DETERMINATION

The calibration curve required to convert count-rates (cps) per sample to tracer concentrations is presented in Figure XIII. The curve was constructed by recording the count-rates obtained at 30-minute decay period for various concentrations of indium in the range of 2×10^{-4} to 7×10^{-3} g/ml. Since a neutron flux may vary during the irradiation period, an evaluation of unknown tracer concentration by absolute gamma-ray counting or by interpolation of the calibration data, creates evident problems in precision and accuracy. Therefore, the comparator method of radioactivation analysis is employed throughout the procedure. This method requires only relative measurements and it is based on identical irradiation and counting treatment of known and tracer samples. Under such conditions the activable tracer measurement is described by Equation 2.10:

$$w_{tr} = w_{std} \frac{D_{tr}}{D_{str}} \quad (2.10)$$

Irradiation and Counting Procedures

The tracer and comparator standard enclosed in scintillation capsules were simultaneously irradiated with the ^{252}Cf neutron source for a ten-minute period. Following activation the tracer and comparator standard were placed, one at a time, in a NaI(Tl) well crystal for a five-minute count interval. The gamma irradiations detected by the crystal were recorded on a 1024-channel analyzer. The multichannel analyzer calibration settings were adjusted such as the ^{137}Cs photopeak (0.66 MeV) was registered in channel 113. Only the count-integral of the 1.29 MeV ^{115}In peak (channels 209-245) was collected. A typical pulse-height spectrum of a neutron activated indium sample is shown in Figure XIV. Where the heavy shaded area corresponds to the count-integral of the 209-245 channel region, and the lower spectrum corresponds to background effects from the well crystal surrounding materials and cosmic rays. It was

FIGURE XIV. Pulse-Height Spectrum of Indium-116m

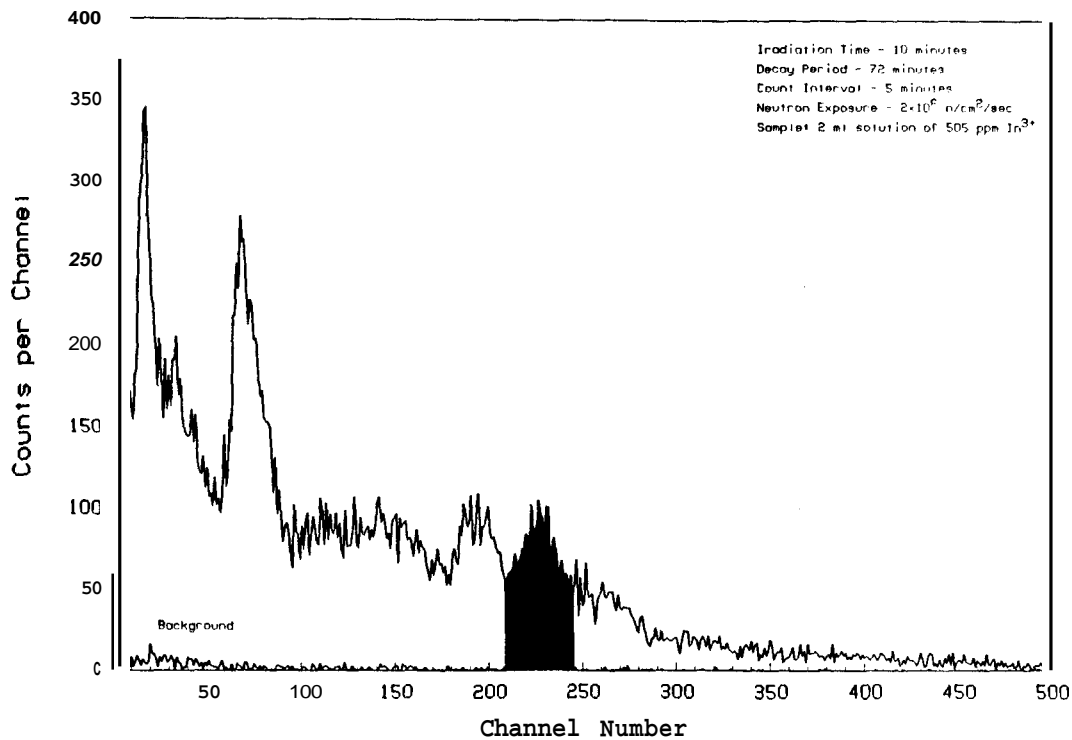
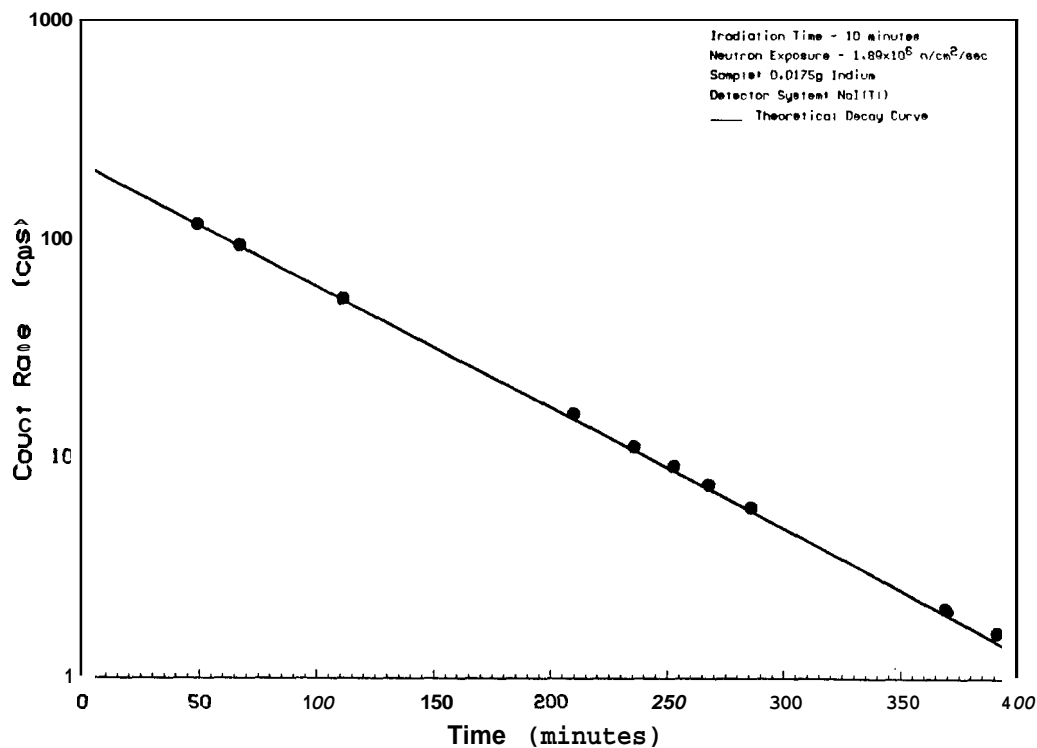


FIGURE XV. Indium-116m Decay Curve



observed that background count-rate within the preselected channel region was less than 4 cpm. The ^{116m}In activity of tracer and comparator standard in channels 209-245 was extrapolated to 30-minute decay period and tracer concentrations were calculated by the relationship of Equation 2.10. The graph of count rate (counts per second) versus decay-time (minutes) of an indium activated sample is shown in Figure XV, The collected experimental data match the theoretical curve; this verifies the expected first-order decay and assures the reliability of activity extrapolations.

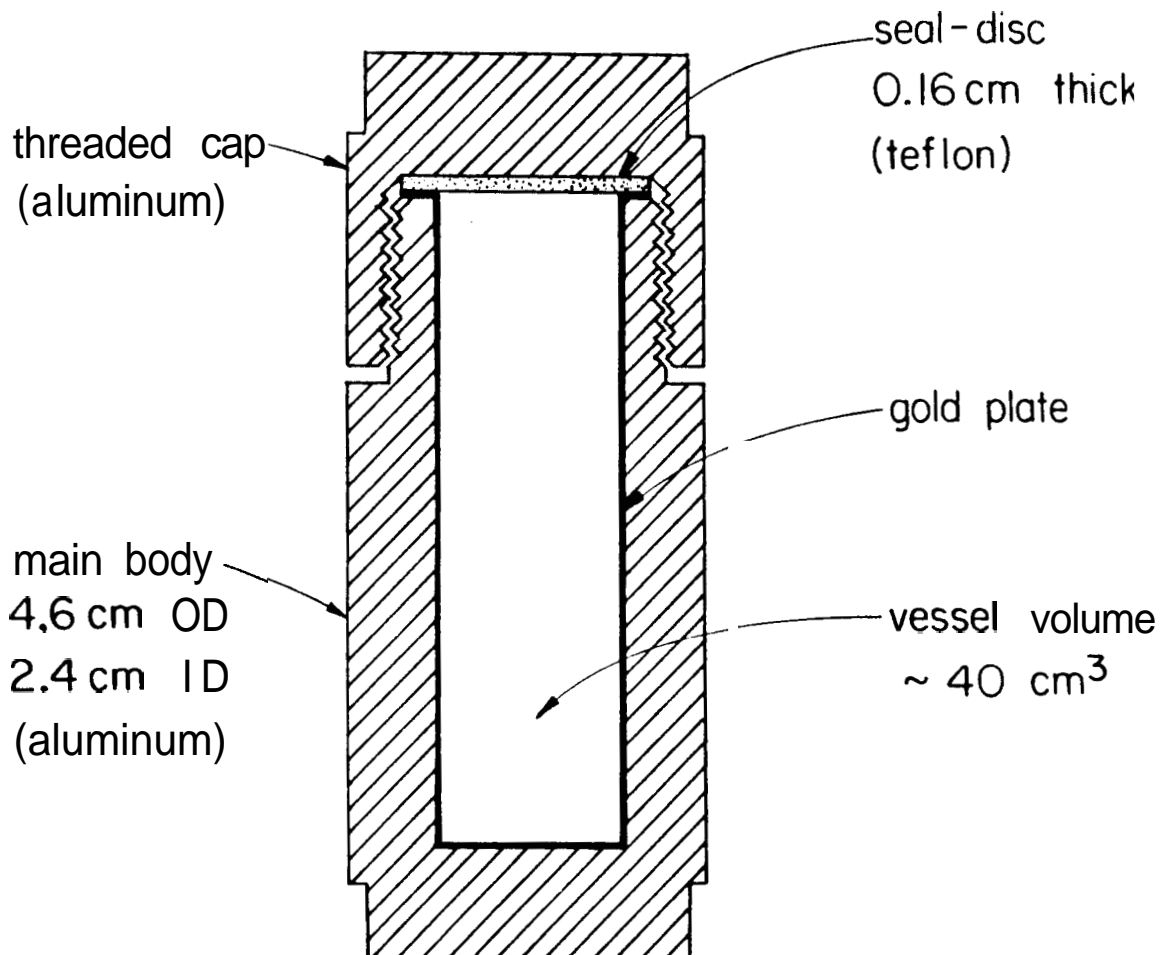
3.5. TRACER STABILITY STUDIES

The experimental work consisted of two parts. First, batch experiments were carried out at room temperature to evaluate and compare the time stability of indium solubility as EDTA and NTA complexed ions. Second, thermal stability measurements of the indium chelates were performed for reservoir temperatures of 150, 200, and 240°C, to determine thermal decomposition rates from the experimental data. A brief description of the equipment used in the high temperature experiments is as follows:

Air Bath

Elevated temperatures are obtained with a Blue-M mechanical convection oven. The oven's temperature range is from 15°C above ambient to 343°C, and it is automatically controlled with a variable potentiometer, maintaining constant temperature within $\pm 0.5^\circ\text{C}$. Temperature uniformity is obtained with recirculating horizontal airflow. The oven is constructed with double wall stainless steel interior, insulated with fiberglass. Two nickel-plated steel shelves, removable and adjustable, are used as vessel holders.

FIGURE XVI. Schematic of a Pressure Vessel



Pressure Vessels

Figure XVI shows a detailed schematic of the pressure vessel. Each pressure vessel is constructed of aluminum with gold plated interior wall. The choice of gold plated pressure vessels was dictated by the desire to minimize interactions between tracer solution and vessel wall. The outside diameter is **4.6 cm**; the overall height is 11.5 cm and the total empty volume is **40 ml**. The vessel is closed with a threaded aluminum cap and sample leakage is prevented by a 0.16 cm thick teflon-disc seal. The pressure vessels were provided by the U.S. Geological Survey, Menlo Park.

Experimental Design

The time stability experiments at room temperature (20-22°C) were conducted over a two month period. Stock solutions of indium chelated tracers at a concentration of 505 ppm were prepared and stored in glass containers with ground glass stoppers. At regular intervals two 5-ml samples of tracer solution were transferred by pipette from each glass container to **15-ml** polystyrene centrifuge tubes. After centrifugation at 3500 rpm for ten minutes, **2-ml** of the supernatant liquid were removed from each centrifuge tube to a **6-ml** Wheaton scintillation capsules for neutron irradiation and gamma-ray spectroscopy. Comparator standards were prepared and encapsulated with the unknown samples and were treated identically under the same irradiation flux conditions.

The thermal stability high temperature experiments were conducted over 20 to 30 day periods. The pressure vessels were filled with **10-ml** tracer solution. Geothermal reservoir temperatures were simulated with an air-bath. At the end of heating period, the vessels were taken from the air-bath and quickly quenched by immersion in a cool water-bath. As soon as the pressure vessels were quenched, the samples were transferred to centrifuge tubes. The detection of the soluble indium concentration was performed with the same analytical procedure as the one described for the room temperature experiments.

3.6. TRACER ADSORPTION STUDIES

This work investigates the effects of tracer adsorption in geothermal reservoirs. The tests include studies on adsorbate concentration, particle size, and temperature as variables on the adsorption of InEDTA onto graywacke sandstone. Two sets of experiments were conducted. First, batch experiments were carried out at room temperature to characterize the tracer adsorption-process. Second, experiments at elevated temperatures were implemented to provide linkage between temperature effects on tracer adsorption and thermal degradation.

Rock Properties

Graywacke is a dark coarse-grained sandstone that consists of poorly sorted and extremely angular grains of quartz and feldspar with an abundant variety of small, dark rock and mineral fragments bounded together by a clay matrix or a chert cement that imparts a great toughness and hardness to the rock. Graywacke is very abundant within the sedimentary section, usually occurring as a thick and extensive body. Graywackes are typically interbedded with marine shales or slates and associated with submarine lava flows and bedded cherts (Gary et al., 1972).

The rock used for the entire set of adsorption experiments was an igneous metamorphic, graywacke rock of Western California. The exact source of the rock is not available, but it is known to be prevalent at the geothermal field The Geysers, California. The average characteristics of a representative sample of 300 rocks were measured by Macias-Chapa (1981) and have been listed in Table XI.

TABLE XI. Average **Rock** Characteristics of Graywacke
[From Macias-Chapa (1981)]

Length	1.85±0.40 cm
Width	1.2±0.25 cm
Thickness	0.67±0.22 cm
Surface Area/Rock *	4.85±0.90 cm ² /g
Mean Surface Area **	2.65±1.03 cm ² /g
Specific Surface Area ***	2.80±0.11 m ² /g
Density ***	2.78±0.73 g/cm ³
Porosity	4.90±1.30 (%)
Weight	1.83±0.80 g/rock

* by the method of Hunsbedt et al., (1975).

** by the B.E.T. method.

*** by a fluid displacement method.

According to the microscopic observations of Satomi (1982), this graywacke sandstone consists of grain sizes ranging from 0.05 to 1-mm in diameter with an average of 0.3-mm. The reported mineral distributions of the rock is shown in Table XII. The cementing constituents are mainly clay minerals such as montmorillonite, illite, Kaoline-like minerals, mixed-layer clay and fine-grained smectitic and chloritic

minerals.

TABLE XII. Mineral Distribution of Graywacke Sandstone
[From Satomi (1981)]

Mineral	Mode (%)
Quartz	29.4
Feldspar	30.4
Epidote	trace
Apatite	trace
Sphene	trace
Rock Fragments (Shale Metabasalt)	5.8
Cementing Materials (clays)	34.4

Crushing and Sieving

The original graywacke sandstones were crushed in a single-runner rock grinder. The rocks were rubbed between the vertical grooved-faces of two circular disks. One disk was stationary and one rotating at high speed. The rocks were fed through an opening in the hub of the stationary disk and were passed outward through the narrow gap between the disks. The reduced solids were discharged from the periphery into a stationary casing. The discharge size was controlled by adjusting the width of the gap between the disks. The crushed rocks were separated into mesh size ranges through Tyler sieves. The sieve screen scale equivalent mesh-sizes employed and the resulting rock size distributions are listed in Table XIII. The average rock size of each grounded rock-range was assumed to be the average of the lower and upper sieve sizes.

TABLE XIII. Size Distributions of Crushed Rocks

Sieve Mesh-Range	Size Range (mm)	Average Rock Size (mm)
12-14	1.397- 1.168	1.283
14-24	1.168-0.701	0.935
24-65	0.701-0.208	0.455
>65	<0.208	(Powder)

Specific Surface Area

The specific surface area of the crushed rock size-distributions were measured with the Micromeritics AccuSorb 2100E surface-area pore-volume analyzer. The instrument utilizes the Brunauer, Emmett, Teller (1938) low temperature multilayer gas adsorption technique, known as the B.E.T. method from the surnames of its discoverers. The B.E.T. model assumes that a number of layers of adsorbate molecules form at the solid surface and that a given layer need not complete formation prior to initiation of subsequent layers.

For the surface area measurements, approximately 2g of each rock size-distribution were loaded into sample flasks attached to the instrument. The samples were heated at 115°C and outgassed simultaneously. After an overnight evacuation, the samples were exposed in a series of steps to inert gas, krypton, at 77.5°K. The low temperature obtained with liquid nitrogen, enhanced the physical adsorption of krypton to the solid surface. Finally, the specific surface area of the samples was calculated by using 21.3 Å as the cross-sectional area of a krypton molecule at -195.5°C. The results indicate that the total surface area available for adsorption is greater for the more finely divided rock particles. The actual surface-area measurements are shown in Table XIV, and they compare favorably with the 2.8 m²/g surface-area reported by Macias-Chapa (1981); who has obtained this measurement by the B.E.T. method using nitrogen adsorbate and 20g sample of the same graywacke sandstone with undetermined size distribution.

TABLE XIV. Specific Surface Area Measurements

Average Rock Size (mm)	Surface Area (m ² /g)
1.283	1,905
0.935	2,026
0.455	2,191
<0.208	3,510

Experimental Design

The adsorption experiments were designed using graywacke sandstone, a typical geothermal rock of high cation exchange capacity. The major clay constituents of a graywacke, montmorillonite and illite, possess cation exchange capacities of 0.81 and 0.16 meq/g respectively (Stumm and Morgan, 1981). Several InEDTA stock solutions were prepared with concentrations spanning two orders of magnitude. The concentrations used allowed for good sensitivity at the low end of the detection range. The solutions were buffered at pH 6.9 with potassium phosphate (KH_2PO_4). Phosphate buffer was added in an amount sufficient to obtain an ionic strength of 0.2 M after the addition of all reagents.

At room temperature, experiments were run for the first three rock size distributions and every one of the InEDTA tracer concentrations. The graywacke in powder form was excluded from the adsorption experiments, because it is not representative of a geothermal reservoir environment. *Oak Ridge* type 50-ml capacity polycarbonate centrifuge tubes were filled with 5g of rock and 40-ml of buffered tracer solution. The tubes were connected to a rotating rack for a 3-day period to provide adequate reaction time for the attainment of equilibrium in all samples. At the end of equilibration period the centrifuge tubes were removed from the rack and were spun at approximately 3,000 rpm for thirty minutes at room temperature (20-22°C). After centrifugation, two 2-ml aliquots of the supernatant liquid were removed from each centrifuge tube with a pipette and transferred to 6-ml Wheaton scintillation capsules for neutron irradiation and gamma-ray spectroscopy.

For the elevated temperature investigations, the pressure vessels employed in the tracer thermal stability studies were filled with 2.5g of 0.45-mm diameter rock and 20-ml of 500 ppm-InEDTA buffered tracer solution. The experiments were conducted at temperatures ranging from 22" to 255°C. Since the available Blue-M oven was not equipped with a rotating rack, the pressure vessels were shaken manually at regular

intervals for a 3-day equilibration period. After equilibration, the pressure vessels were removed from the oven and quenched by immersion in a cool water-bath. As soon as the vessels were cool, the slurries were transferred to centrifuge tubes and measurement of soluble indium concentration was obtained with the prescribed analytical procedure.

CHAPTER 4

RESULTS AND DISCUSSION

The data collected from the experimental investigations were classified into two major categories: tracer stability, and tracer adsorption data. The first category contains results from the solubility time function investigations at room temperature, and from the thermal stability experimentations of indium chelates. The second category includes the results obtained from the adsorption investigations of InEDTA in contact with graywacke sandstone at room and elevated temperatures. The experimental data presented throughout this chapter in graphical form are compiled in Appendices B (stability concentrations) and C (adsorption concentrations).

Potential sources of error in the obtained measurements include volumetry, gravimetry, interfering reactions, self-shielding, anisotropic neutron flux, and counting statistics. Errors in volumetry and gravimetry are easily evaluated and they were less than ± 0.3 percent. Errors due to interfering nuclear reactions may occur from contamination of sample containers and chemical reagent impurities. Sample contamination was avoided with proper labware cleaning and utilization of contaminant-free reagents. Furthermore, errors from interfering nuclear reactions were eliminated during counting by collecting only a small fraction of the pulse-height spectrum corresponding to the highest energy **peak**. Therefore, the contribution to the tracer full-energy peak from interfering radionuclides with lower gamma-ray energy was negligible. Self-shielding errors can result from the flux perturbation caused by the insertion of a condensed material or a large sample containing nuclides with high thermal neutron cross-section

area into the volume of the neutron flux. As neutrons are absorbed within the interior of the sample the neutron flux is suppressed. Self-shielding effects were eliminated by employment of dilute homogeneous samples. Irradiation in an anisotropic neutron flux can also lead to significant errors. Neutron flux gradients were excluded from potential error sources because samples and standards were irradiated simultaneously. The most significant error was introduced during counting. The error associated with counting statistics was calculated for every measurement according to the procedure presented in section 3.3.

4.1. TRACER STABILITY RESULTS

Time Function of Tracer Solubility

The results of the time stability investigations are shown in Figures XVII and XVIII. The slight scatter of the solubility data is attributed to the fair precision of the analytical technique used to measure the soluble indium concentration. Since the tracer solutions were adjusted to pH 7, any unchelated indium ions would be expected to adsorb onto container walls and to precipitate as indium hydroxide. Although it has been suggested by Tyree (1967) that metal-chelate tracers may degrade slowly, the data indicate that there was no alteration in tracer concentration during the two month experimental period. Therefore, it is apparent that the organic ligands EDTA and NTA form stable complexes with indium at room temperature.

Thermal Stability Behavior

The results of the InEDTA and InNTA thermal stability investigations are shown in Figures XIX and XX respectively. The data obtained at 150°C indicate that both of the chelated tracer-concentrations remained constant over the experimental period of 20 days. The calculated standard error of the mean of tracer concentration, $\sigma_{\bar{x}}$, is ± 5.2 ppm for InEDTA and ± 4.9 ppm for InNTA. Therefore, 150°C temperature has little effect on the InEDTA and InNTA chelate stability.

FIGURE XVII. InEDTA Solubility Time Function

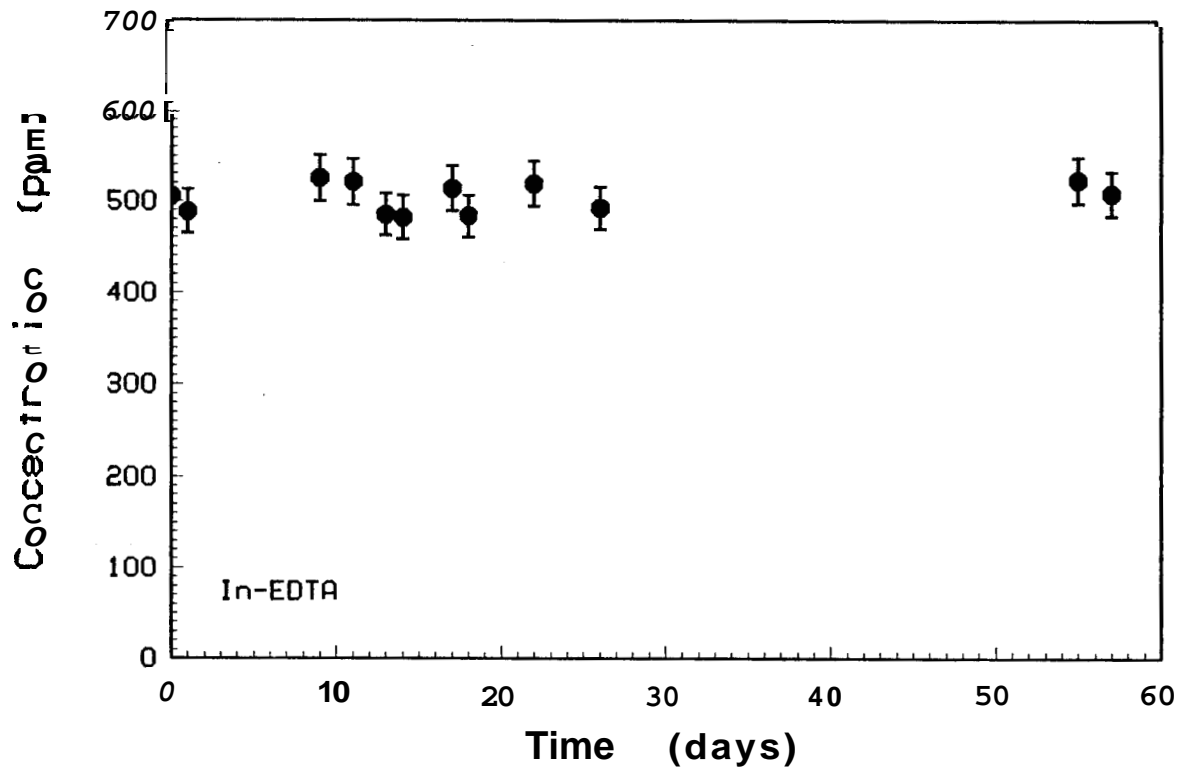
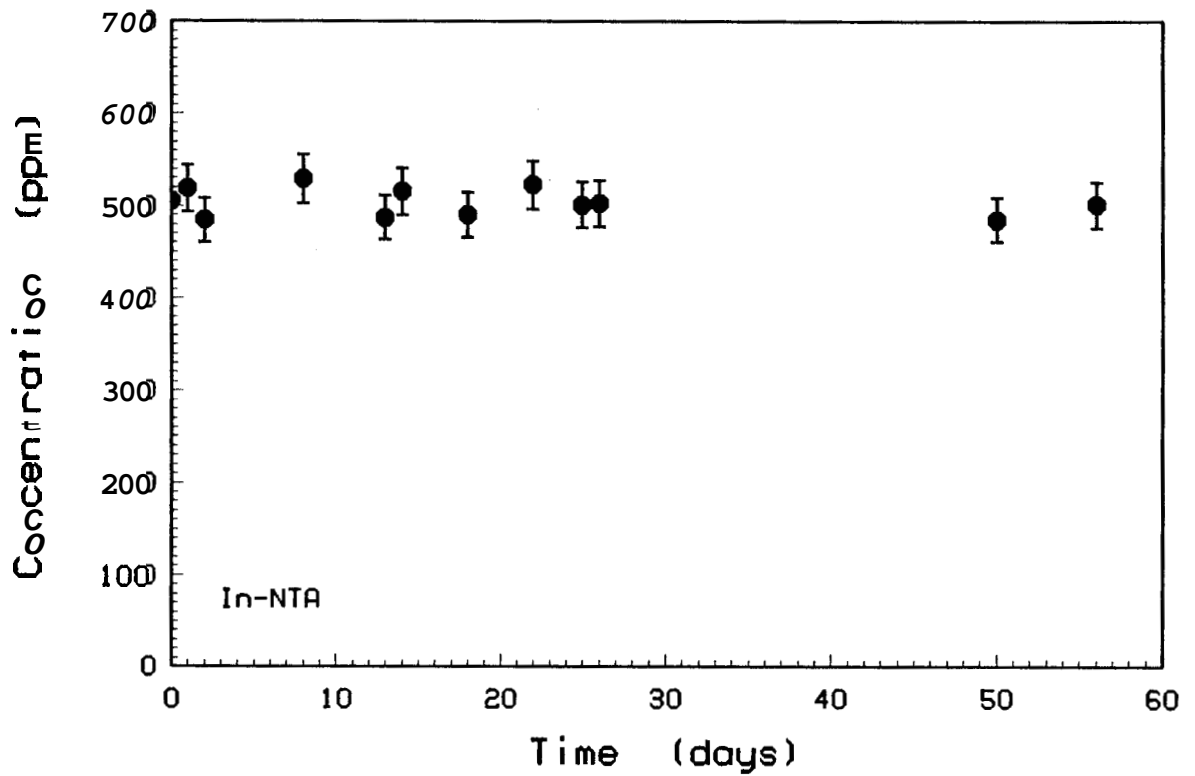


FIGURE XVIII. InNTA Solubility Time Function



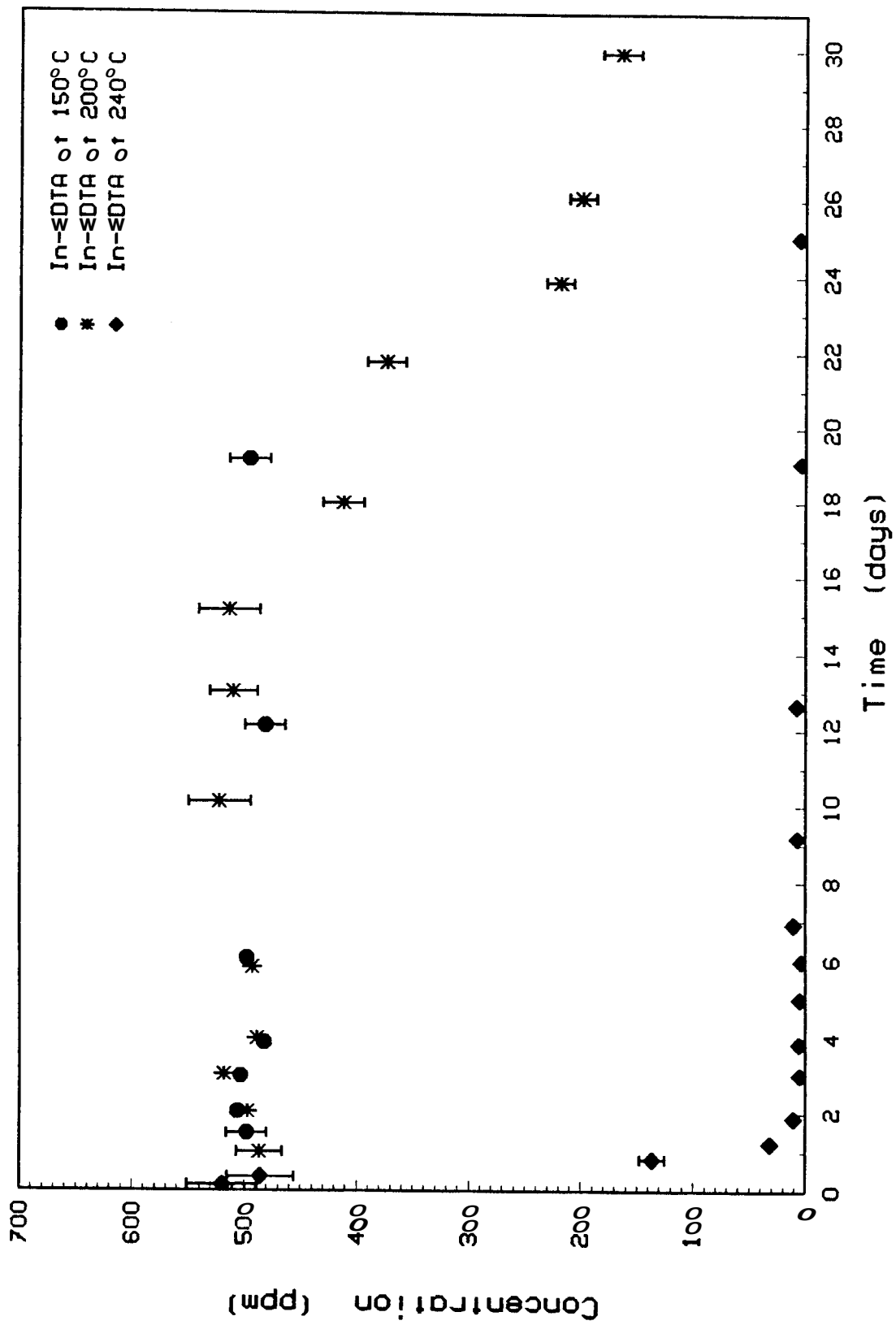


FIGURE XIX. Effect of Temperature and Time on InEDTA Stability

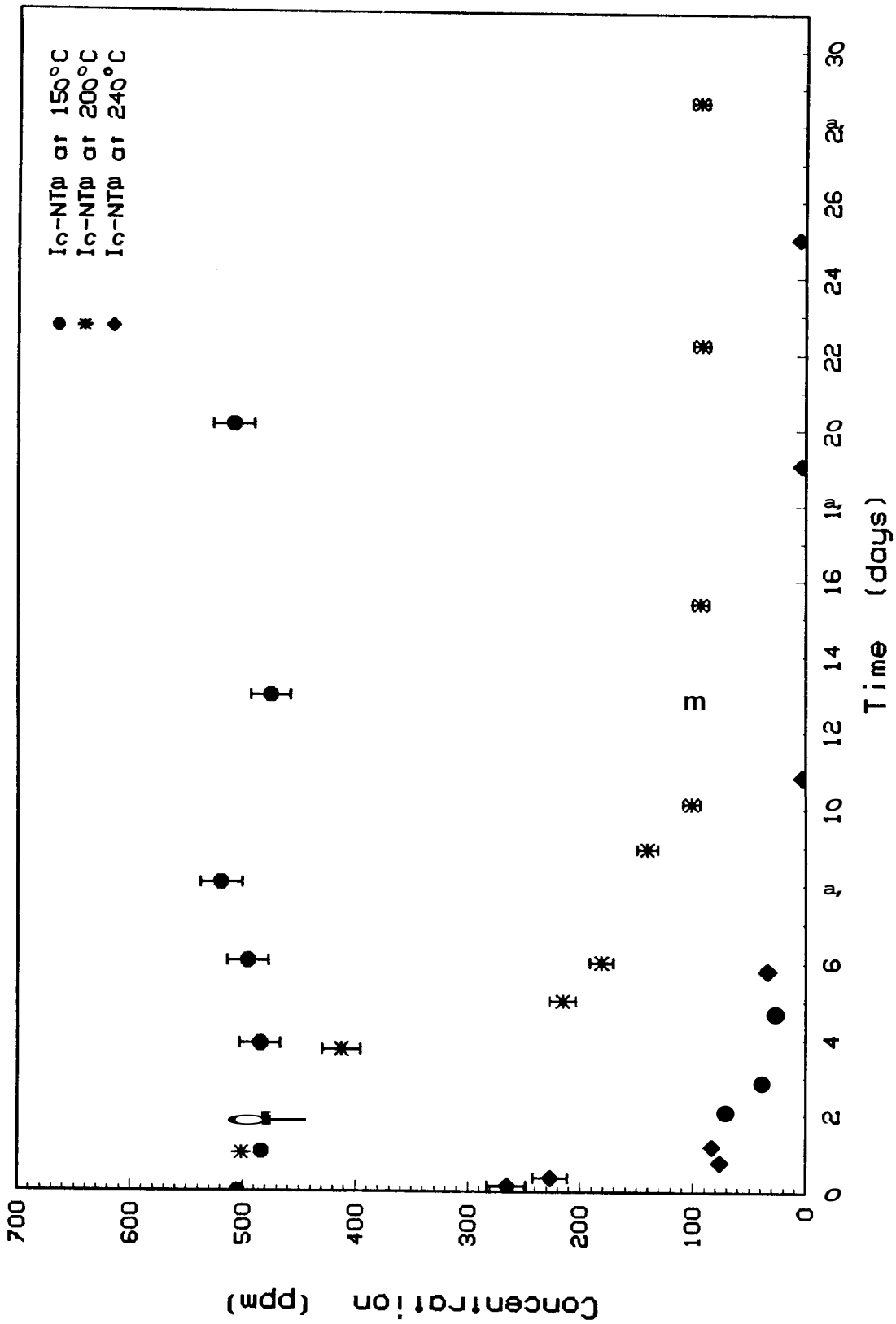


FIGURE XX. Effect of Temperature and Time on InNTA Stability

At 200°C the soluble indium concentration of the InEDTA tracer solution remained constant for 16 days, and then decreased to a level 32 percent of its initial value within 14 additional days. The time lag before the Occurrence of any significant change in the total soluble indium concentration can be attributed to the chelating characteristics of the intermediate thermal decomposition products of EDTA. The chelating ability of EDTA degradation products at 200°C has also been observed by Venezky and Moniz (1969). A mathematical expression of the first order type was used to describe the complex degradation process of InEDTA at 200°C after the initial time lag period. The experimental data were fairly consistent with the proposed rate expression, and a rate constant of $k_{obs} = 0.09d^{-1}$ was calculated (Appendix D).

The results obtained from the InNTA run at 200°C, show that the decrease in soluble indium concentration started simultaneously with the initiation of the experiment. The indium concentration decreased steadily from 505 ppm to approximately 95 ppm within a period of 11 days, with $k_{obs} = 0.17d^{-1}$, and then remained uniform at 95 ppm for the rest of the experimental duration. An additional experiment was run at 200°C with InNTA initial concentration of 321.5 ppm. The purpose of this experiment was to examine the dependence of the equilibrium indium concentration on the initial tracer concentration. The results of this investigation are shown in Figure XXI. The indium concentration decreased from 321.5 ppm to 35 ppm within 5 days. The data obtained during the following 12-day period show a uniform indium concentration with an average value of 32.5 ppm. The scatter of the experimental data is attributed to indium detection limitations of the available apparatus. Obviously the equilibrium indium concentration at 200°C is strongly dependent on the initial InNTA concentration.

Martell et al. (1975) observed that NTA does not undergo hydrolytic cleavage below 260°C. Therefore, the decrease in InNTA concentration at 200" was caused by an equilibrium shift to the left as shown by the following reaction:



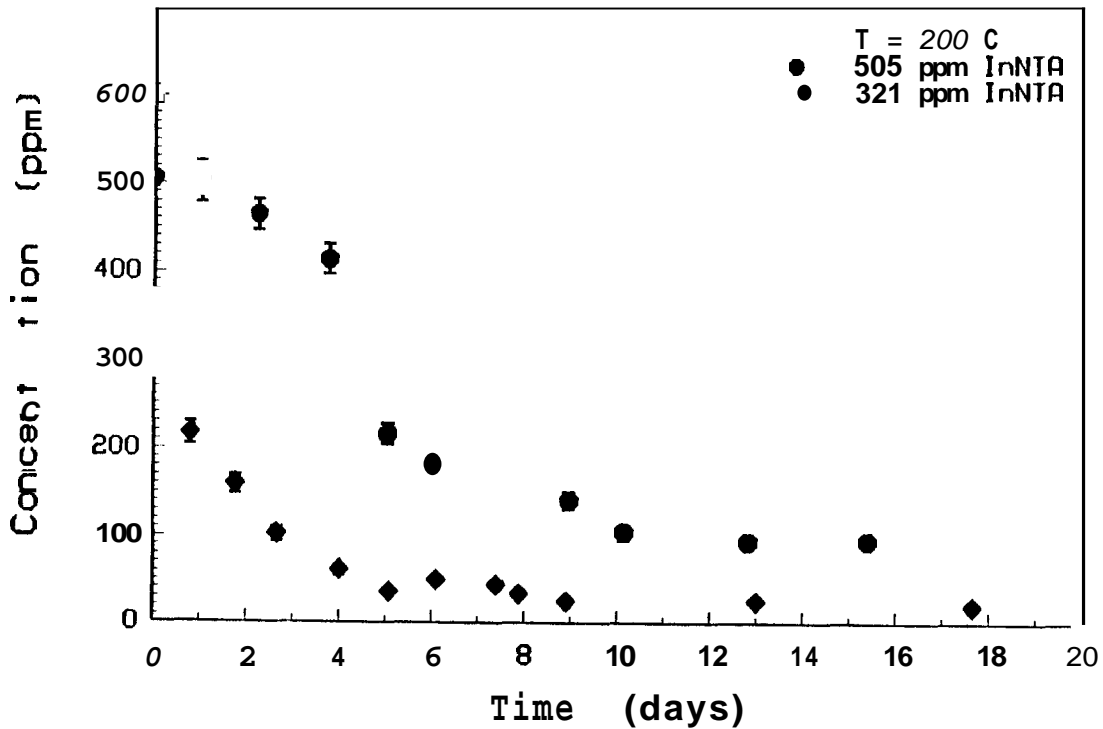
This implies that the logarithm of the InNTA formation constant at 200°C is much lower than 15.9, as reported in literature for 20°C.

The formation constant of InNTA at 200°C can be estimated by the following equation:

$$k_{200} = \frac{[(InNTA)_{20} - \xi]}{[(In^{3+})_{20} + \xi] [(NTA^{3-})_{20} + \xi]} \quad (4.2)$$

Where ξ is the extend of reaction or the amount of [InNTA] which has been decomposed to $[In^{3+}]$ and $[NTA^{3-}]$ due to the temperature increase. The technique of neutron activation provides total indium concentrations and can not differentiate between oxidation state, chemical form or physical location of indium. Since the experimental data obtained for the equilibrium InNTA concentration are overestimated by the amount of soluble indium in any other form, such as $In(OH)_2$, $In(OH)_3$ and $In(OH)_4$, the calculation of InNTA formation constant at 200°C has not been attempted.

FIGURE XXI. Effect of Initial InNTA Conc. on the Equilibrium Conc. at 200°C



At 240°C the data were not suitable for quantitative analysis because the time required for the first few pressure vessels to reach air-bath temperature was an appreciable fraction of each heating period. Nonetheless, both indium chelated tracers showed rapid decomposition. Assuming that the thermal decomposition of InEDTA and the equilibrium shift of InNTA at 240°C can be described by a first order reaction, a rate constant of $k_{obs} = 1.76d^{-1}$ and $k_{obs} = 0.41d^{-1}$ for InEDTA and InNTA were calculated respectively.

4.2. TRACER ADSORPTION RESULTS

The results from the chelated tracer thermal stability experimentations provided convincing evidence that the ability of the organic ligand EDTA to enhance indium solubility at elevated temperatures is superior compared to the ability of NTA. For this reason the InNTA tracer was excluded from the adsorption investigations.

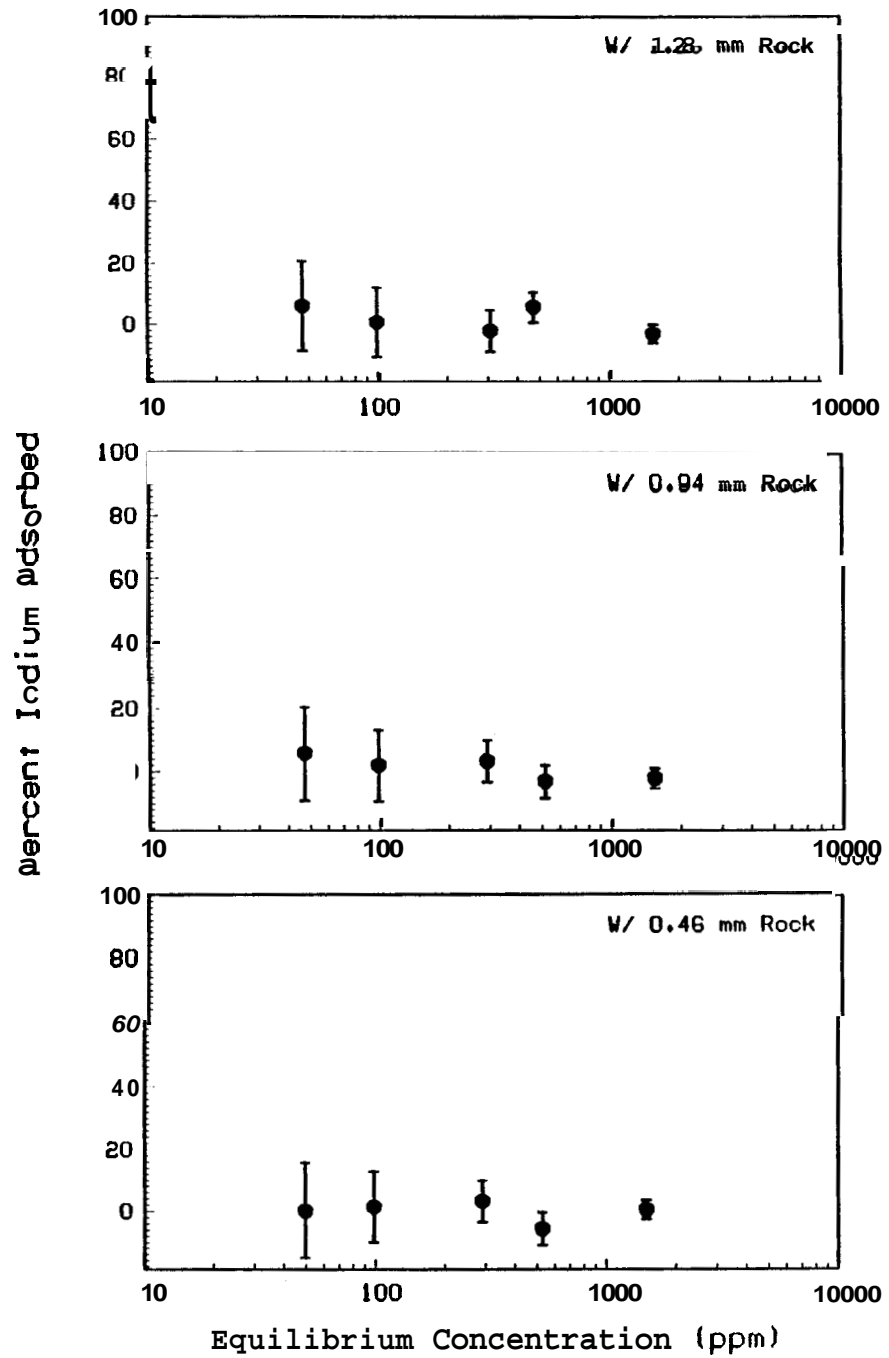
Tracer Adsorption Evaluation at Room Temperature

The results from the adsorption experiments of InEDTA in contact with graywacke sandstone of 1.28, 0.94 and 0.46-mm average rock size distributions at room temperature are shown in Figure XXII. The experimental data are presented in a graphical form of equilibrium tracer concentration versus percent of tracer adsorbed. The results indicate that for all three rock size distributions, and for tracer concentrations ranging from 50 to 1,500 ppm no detectable indium was adsorbed.

Although the excess of EDTA present in solution could remove metals from the rock structure, thus creating a charge imbalance that could be satisfied by In^{3+} adsorption, the high affinity of EDTA for indium did not permit this to take place.

In order to examine the effect of potassium phosphate buffer on the adsorption of InEDTA onto graywacke sandstone, additional experiments were run with **500** ppm InEDTA solution without buffer and all three rock size distributions. The data of these experiments are displayed in Table XV, together with the corresponding data of

FIGURE XXII. InEDTA Adsorption Onto 1.28, 0.94 and 0.46 mm Graywacke Sandstone Rock sizes



the runs employing 0.2-M potassium phosphate buffer. A comparison between the two sets of data suggests that the presence of buffer did not affect the adsorption process.

TABLE XV. Effect of Potassium Phosphate Buffer On 500 ppm InEDTA Adsorption

Percent InEDTA in Solution for Adsorption Experiments at 22°C			
	1.28-mm Rock	0.94-mm Rock	0.46-mm Rock
Without Buffer	99.9± 5.2	92.6± 4.9	98.4± 5.9
With Buffer	94.5± 5.0	103.3± 5.2	105.8± 5.3

The 3-day equilibration period is considered adequate because the adsorption mechanism of chelated indium involves either an ion exchange of elements in the rock structure for cations in solution, or physical adsorption. Ion exchange has a low activation energy and the approach to equilibrium is rapid. Also, physical adsorption of indium complexes is a quick process. The fast kinetics of equilibrium cation adsorption onto clays have been studied by Maest et al. (1985). The investigators reported that equilibrium adsorption of U, Co, Sr and Cs in the presence of EDTA in contact with either kaolinite or montmorillonite, two of the main constituents of graywacke sandstone, was attained within 30 minutes. Therefore, the 3-day equilibration period for the adsorption experiments is justified.

Effect of Temperature

The effect of temperature on InEDTA adsorption onto graywacke sandstone for the 500 ppm tracer solution and 0.94-mm rock size is presented in Figure XXIII. The results show that little adsorption of the tracer occurred up to 175°C. At 200°C the soluble indium concentration dropped sharply to 52.5 ppm. At temperatures above 200°C the detectable indium concentration had been decreased to low levels. From the thermal stability studies of InEDTA it was determined that primary thermal degrada-

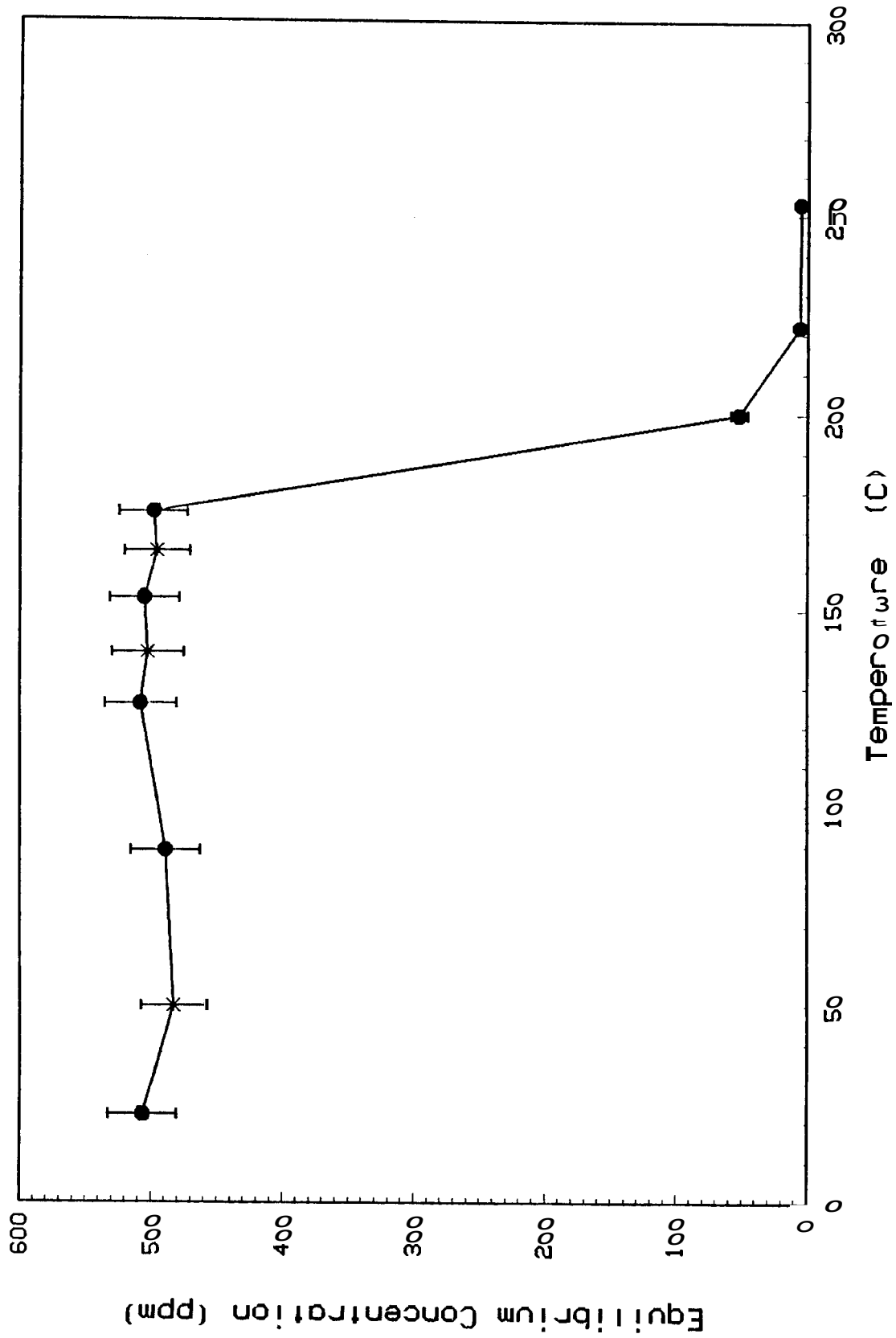


FIGURE XXIII. Effect of T(°C) on InEDTA Adsorption Onto Graywacke Sandstone

tion of EDTA occurs at and above 200°C. In particular the thermal stability data of InEDTA at 200°C had a 16-day time lag before any significant change in the soluble indium concentration occurred. This time lag was attributed to the chelating characteristics of the intermediate thermal decomposition products of EDTA. The results from the adsorption experiments at 200°C indicate that a sharp drop in the soluble indium concentration occurred within a 3-day equilibration period. A comparison of the two experimental results indicate that either the presence of graywacke sandstone acts as catalyst increasing the rate of InEDTA thermal decomposition, or the indium chelated intermediate thermal decomposition products of EDTA adsorb significantly on graywacke rock. Therefore, the sharp change in soluble indium concentration at and above 200°C was caused mainly by the thermal degradation of the organic ligand.

The effect of the potassium phosphate buffer on the adsorption of InEDTA onto graywacke sandstone was investigated by conducting experiments with tracer solutions without buffer. The data from these experiments do not differentiate from the results obtained from the runs employing buffered tracer solutions. This implies that InEDTA adsorption was not affected by either the presence of potassium phosphate or the pH fluctuations of the aqueous solutions.

CHAPTER 5

CONCLUSIONS AND RECOMMENDATIONS

5.1. CONCLUSIONS

The optimization analysis for several potential external tracers, based on a literature survey on the chemical composition of geothermal effluents taking into account the criteria for activable tracers and laboratory sensitivity requirements, indicated that indium is a promising activable tracer for liquid-dominated geothermal reservoirs. The chief reason that makes indium an excellent activable tracer is the unique combination of good detection sensitivity and relatively high energy of major gamma-ray emission of its activation product 54.12 minute-^{116m}In.

The organic ligands ethylenediaminetetraacetic acid (EDTA) and nitrilotriacetic acid (NTA), employed to enhance indium solubility in the pH range of geothermal interest, form stable time persistent complexes with indium at laboratory temperatures. The results from the tracer thermal stability studies showed that InEDTA and InNTA are thermally degraded at and above 200°C. The experimental data suggested that EDTA is more favorable than NTA for indium chelation at elevated temperatures.

The adsorption experimental results of InEDTA tracer solution in contact with graywacke sandstone, indicated that adsorbate concentration, particle size, and buffer concentration did not effect the tracer adsorption process. In fact, the data indicate that tracer adsorption occurred after the initiation of thermal decomposition of the organic ligand EDTA which takes place at 200°C.

The indium chelated complexes InEDTA and InNTA are excellent activable tracers for low temperature liquid-dominated geothermal reservoirs. However, **InEDTA** can be used effectively in geothermal reservoirs with temperatures up to 200°C for transit times of at least 20 days.

5.2. RECOMMENDATIONS

Further study of indium chelated tracers should include an investigation of the effect of metal cations present in geothermal liquids with the ability to displace indium from its chelates. In particular, the ferric cation may be an important displacing reactant because of its higher EDTA stability constant. Further research should include the development of a rapid analytical procedure for InEDTA preconcentration from geothermal effluents. A rigorous tracer separation scheme should be designed before on-line tracer activation analysis can be implemented.

APPENDIX A

Derivation of Radioactivity Correction Factors for Decay During Counting

The disintegration rate, D , of the radioisotope produced at the end of irradiation period, τ , is given by the radioactivity equation (Eq. 2.5) and is schematically represented in Figure A.1. The amount of species present at the end of irradiation, N , diminish with time and the activity at any time, D , is given by the rate of depletion of the original number of species, $-dN/dt$, so that we have:

$$D = - \frac{dN}{dt} = \lambda N \quad (\text{A.1})$$

where λ is the decay constant expressed in units of reciprocal time. Equation A.1 represents one statement of the fundamental law of radioactive decay. It can be integrated to give:

$$\frac{N_t}{N_o} = e^{-\lambda t} \quad (\text{A.2})$$

or

$$\frac{D_t}{D_o} = e^{-\lambda t} \quad (\text{A.3})$$

Usually the decay rate of radionuclides is characterized by the half-life, $T_{1/2}$, instead of the decay constant λ . By setting $D_t/D_o=0.5$, Eq. A.3 gives $\ln 0.5 = -\lambda T_{1/2}$, which is equivalent to the following expression:

$$\lambda = \frac{\ln 2}{T_{1/2}} \quad (\text{A.4})$$

Equations A.2 and A.3 are independent of starting time and any instant may be chosen as zero time, provided that N and D are taken as the values appearing at that particular instant. When the half-life of an isotope is short compared to the counting time t' , the counting rate $A = N_{obs}/t'$ is not accurate because considerable decay occurs during the counting period.

The disintegration rate at the beginning of counting can be calculated by integrating Equation A.3 over the counting time t' :

$$\int_0^{t'} D_t dt = D_o \int_0^{t'} e^{-\lambda t} dt \quad (\text{A.5})$$

substituting A.1 into A.5 yields:

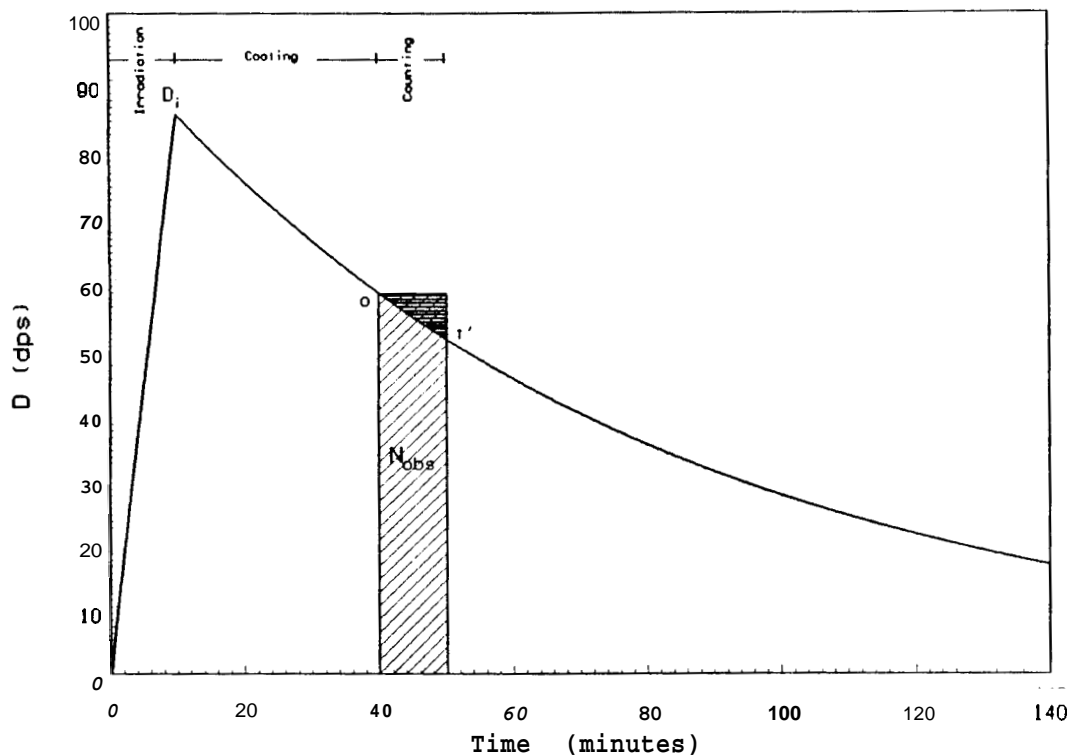
$$-\int_{N_o}^{N_t} dN = D_o \int_0^{t'} e^{-\lambda t} dt \rightarrow$$

$$D_o = \frac{\lambda(N_o - N_t)}{1 - e^{-\lambda t}} = \frac{\lambda N_{obs}}{1 - e^{-\lambda t'}} \quad (\text{A.6})$$

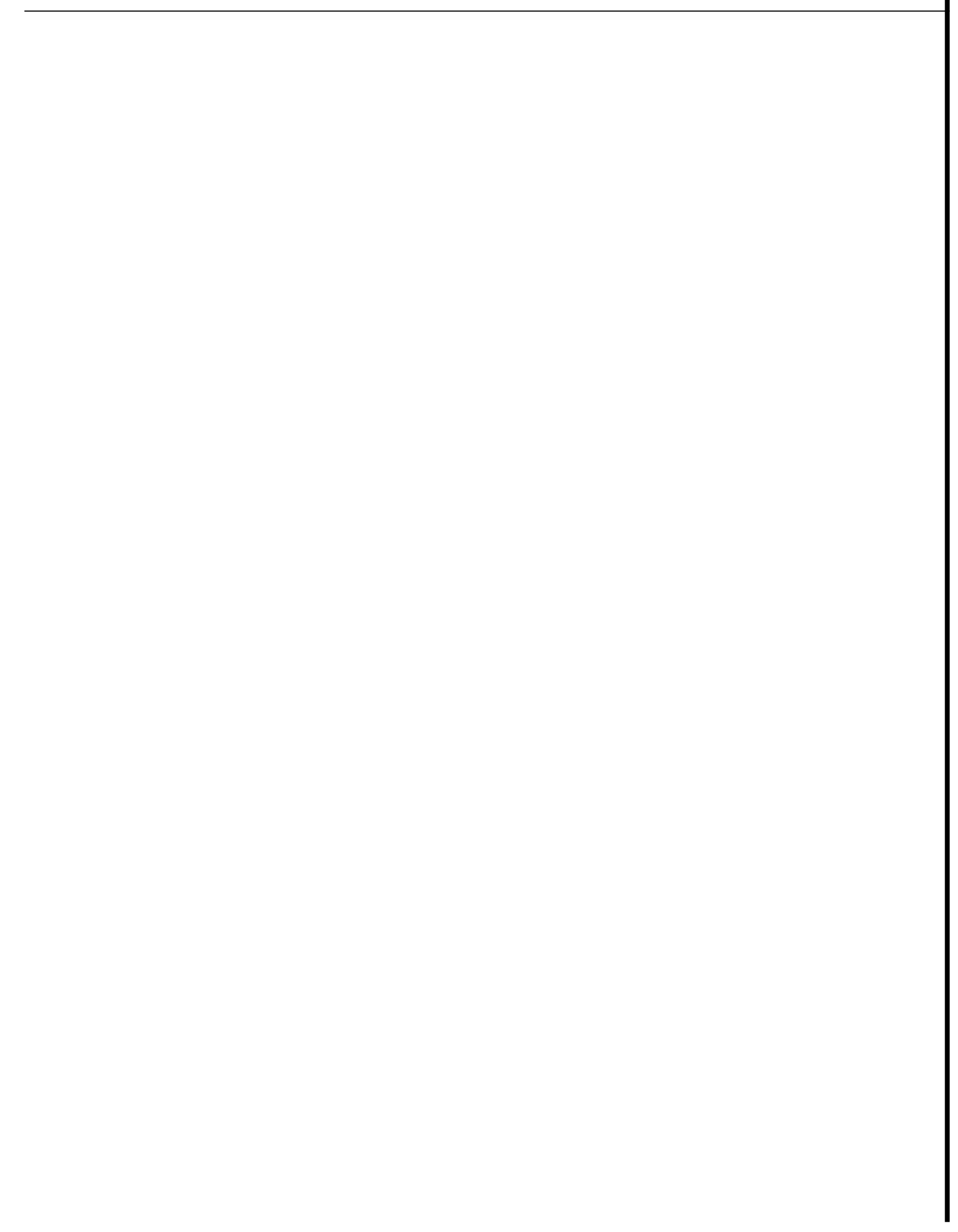
Substituting A.4 into A.6 and multiplying by the counting period t' yields the correct number of counts, N_{corr} , assuming that the activity remains constant over the counting period:

$$N_{corr} = \frac{N_{obs}}{1 - \exp\left(-\frac{\ln 2}{T_{1/2}} t'\right)} \left[\frac{\ln 2}{T_{1/2}} \right] t' \quad (\text{A.7})$$

FIGURE A.1. Illustration of activity change during irradiation and decay periods.



The heavy shaded area in Figure A.1 illustrates the underestimation of total counts when corrections are not made for a 2-ml sample of 0.0044-M indium irradiated in a thermal neutron flux of 2×10^6 n/cm²sec for ten minutes with 30-minute cooling period till measurement and 10-minute counting period. Actually, a 10-minute counting period corresponds to 18.48% of one half-life of the activation product ^{116m}In.



APPENDIX B

DATA LISTINGS • STABILITY EXPERIMENTS

TABLE B-1

InEDTA Time Stability Data		InNTA Time Stability Data	
Time (days)	Concentration (ppm)	Time (days)	Concentration (ppm)
0	505.0	0	505.0
1	488.4±23.9	1	519.5f25.4
9	525.2±25.6	2	484.5±23.8
11	521.2f25.5	8	529.2±26.6
13	485.1±23.1	13	487.2k23.9
14	482.1±23.7	14	515.5k25.3
17	513.8±24.8	18	490.3f24.4
18	483.4±23.0	22	522.9k26.0
22	519.1f25.0	25	500.9±24.8
26	497.1f23.5	26	502.7f24.8
65	523.0±25.2	65	484.9k23.8
67	508.1±24.6	67	501.4k24.8

TABLE B-2

InEDTA Thermal Stability Data					
150°C		200°C		240°C	
Time	Conc. (ppm)	Time	Conc. (ppm)	Time	Conc. (ppm)
0.00	505.0	0.00	505.0	0.00	505.0
1.50	498.1k18.1	1.00	486.5±20.6	0.14	519.8±31.4
2.04	506.5±18.3	2.04	496.9±20.4	0.36	485.7±29.6
3.00	503.3f18.3	3.04	517.8±21.4	0.81	136.7f11.3
3.88	482.1k17.8	4.00	488.8±20.6	1.22	31.7± 4.6
6.06	497.7k18.1	5.83	493.0±20.7	1.88	10.9± 2.6
12.13	481.2f17.8	10.13	521.9±27.6	3.01	4.8± 1.7
19.17	495.0±18.1	13.01	509.3±21.2	3.85	5.9± 1.9
		15.13	513.4±27.3	5.01	4.8± 1.7
		17.99	411.8f18.4	5.98	3.4± 1.4
		21.75	373.3k17.3	9.17	6.8± 2.0
		23.84	218.8f12.4	12.64	7.9± 2.2
		26.05	198.6f11.7	19.08	3.7± 1.5
		29.92	163.9k17.2	25.00	4.7± 1.7

TABLE B-3

InNTA Thermal Stability Data					
150°C		200°C		240°C	
Time	Conc. (ppm)	Time	Conc. (ppm)	Time	Conc. (ppm)
0.00	505.0	0.00	505.0	0.00	505.0
1.04	483.4k17.8	1.00	501.3±23.3	0.14	265.6k17.3
1.91	496.6f18.1	2.23	464.5k17.6	0.36	227.1f15.4
3.88	484.6k17.9	3.75	413.W16.7	0.76	76.2± 7.4
6.06	495.5k18.1	5.02	215.9k11.5	1.17	83.5± 7.9
8.07	519.4k18.6	6.01	181.3f10.5	2.09	70.7± 7.1
12.96	475.4f17.8	8.96	140.55 9.2	2.88	39.2± 5.0
20.08	508.4k18.4	10.13	101.6± 7.8	4.69	26.7± 4.1
		12.81	99.9± 7.7	5.81	33.6± 4.6
		15.38	93.8± 7.4	10.83	3.W 1.3
		22.22	92.52 7.4	19.08	3.6± 1.4
		28.63	94.w 7.5	25.00	5.2± 1.7

TABLE B-4

InNTA Thermal Stability Data Obtained at 200°C	
Time (days)	Concentration (ppm)
0.00	321.5
0.79	216.4k12.4
1.77	154.6k10.2
2.65	109.9± 8.4
4.01	60.2± 6.1
5.08	34.62 4.6
6.10	49.0± 5.5
7.38	44.1± 5.2
7.88	33.w 4.4
8.90	25.0± 3.9
13.00	24.72 3.8
17.65	19.4± 3.4

APPENDIX C

DATA LISTINGS • ADSORPTION EXPERIMENTS

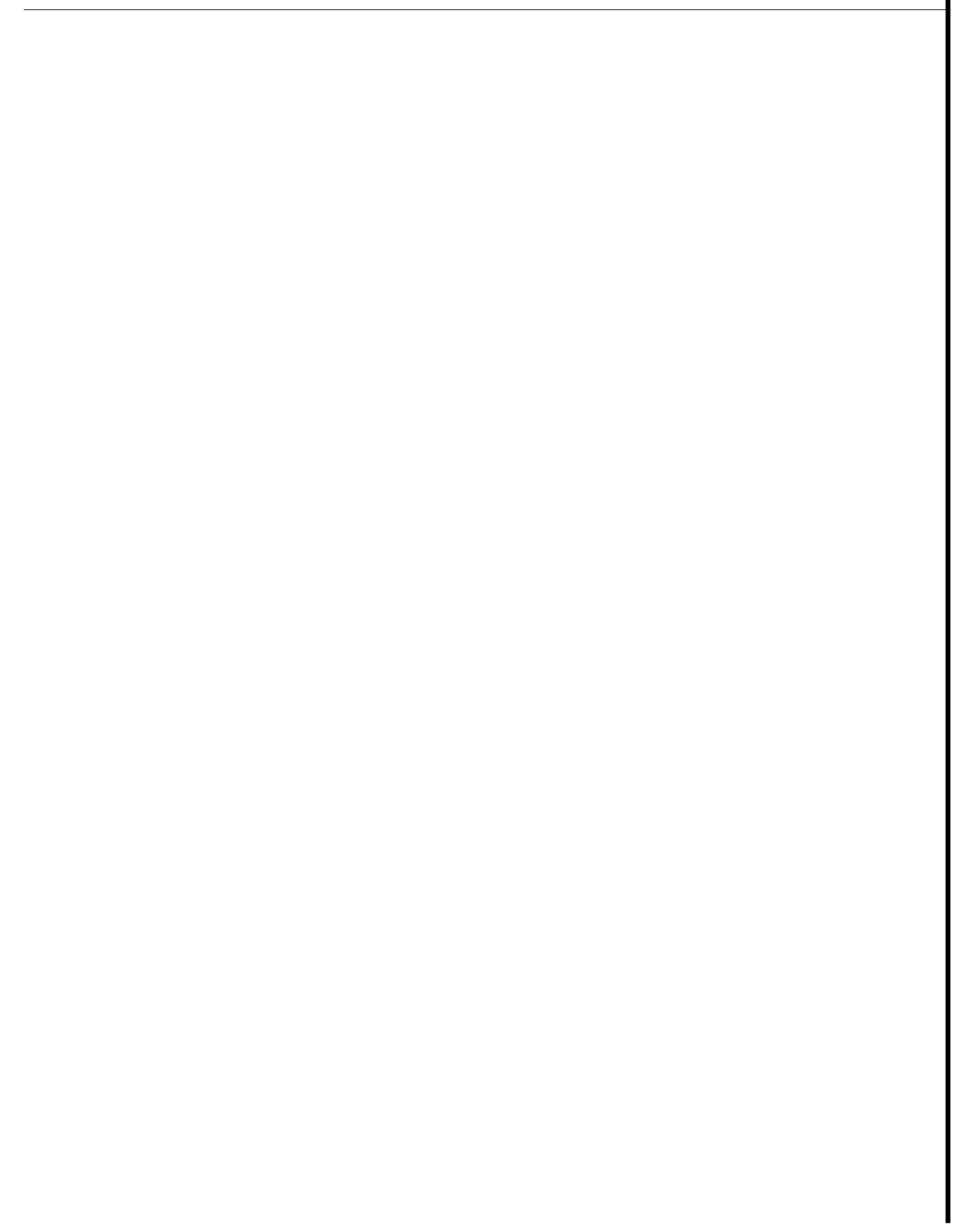
TABLE C-1

Percent InEDTA in Solution for Adsorption Experiments at 22°C			
Adsorbate Conc. (ppm)	1.28-mm Rock	0.94-mm Rock	0.46-mm Rock
50	94.2±14.7	94.5k14.7	99.9±15.3
100	99.4±11.4	98.2rt11.3	98.8k11.3
300	102.2± 6.8	97.W 6.6	97.W 6.6
500	94.5± 5.0	103.3± 5.2	105.8± 5.3
1500	103.2± 3.1	102.3± 3.1	99.7± 3.0

TABLE C-2

InEDTA Conc. as a Function of Temp. in contact with 0.94-mm Rock	
Temperature (°C)	Equilibrium Conc. (ppm)
22	506.7±26.1
50 *	483.0-124.6
89	489.1k26.4
126	508.1k27.2
139 *	502.6±27.4
153	505.4rt26.4
165 *	495.5k24.9
175	498.2k26.0
200	52.2± 6.2
222	6.3± 2.1
253	5.3± 1.9

* Solutions without potassium phosphate buffer



APPENDIX D

Rate constant calculation

The first order rate equation is:

$$-\frac{dC}{dt} = kC \quad (\text{D.1})$$

where, C is the concentration of reactant and k is the rate constant. Separating and integrating we obtain

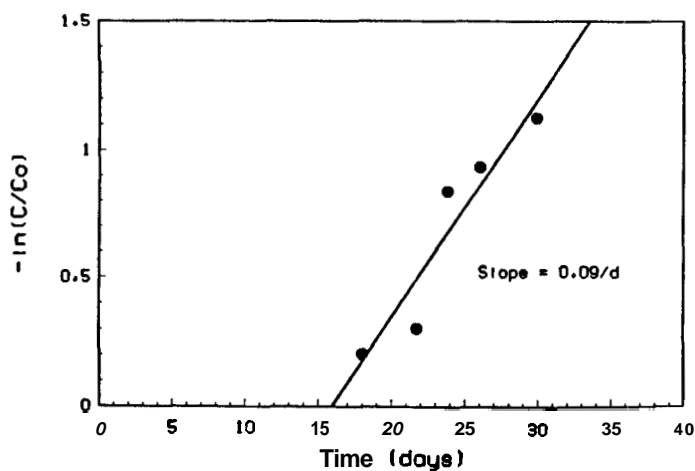
$$-\int_{C_0}^C \frac{dC}{C} = k \int_0^t dt$$
$$-\ln \frac{C}{C_0} = kt. \quad (\text{D.2})$$

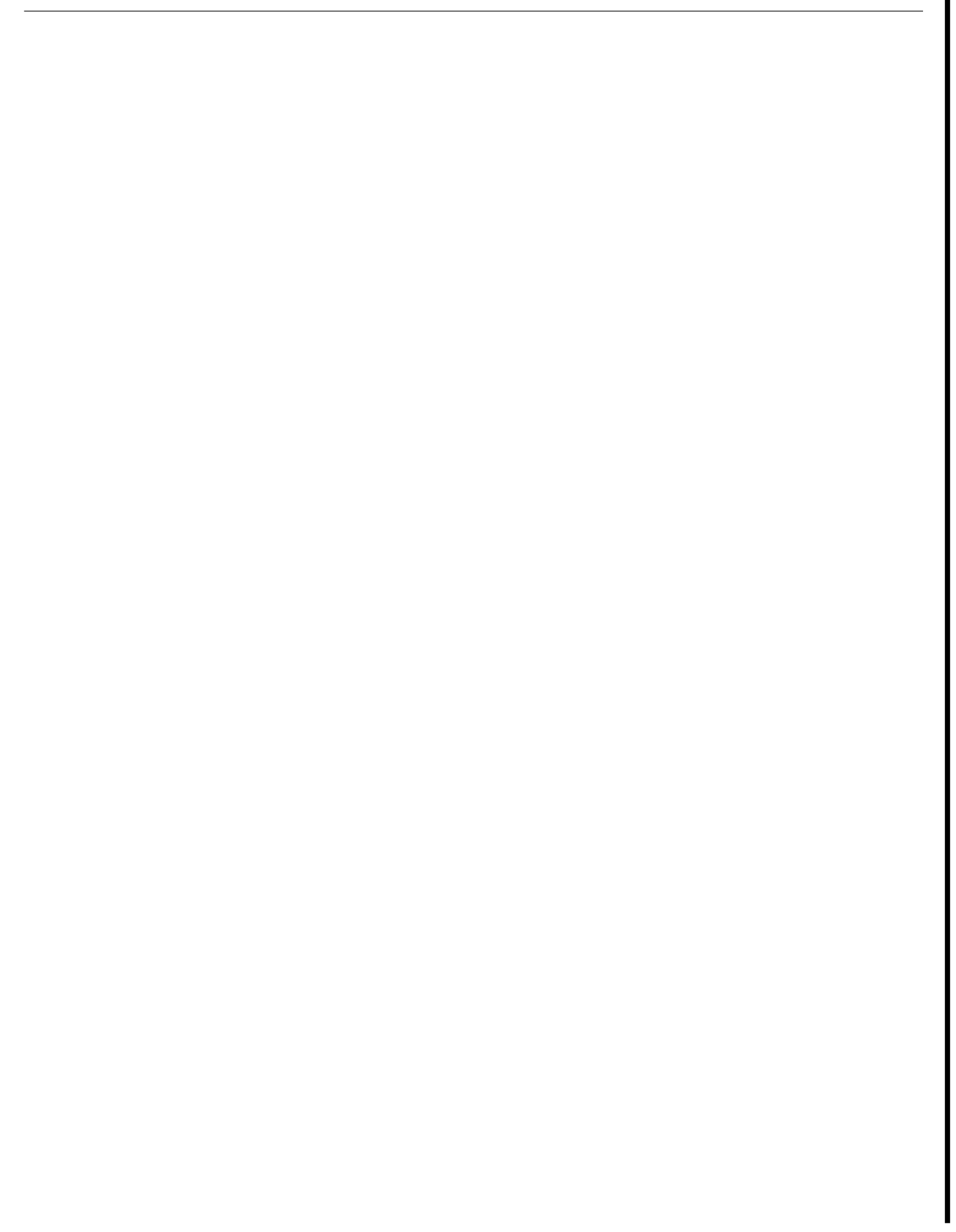
A plot of $-\ln(C/C_0)$ versus time gives a straight line with slope equal to the rate constant, k . For the thermal degradation of **InEDTA** at 200°C



the observed reaction rate constant is calculated by plotting the data after the initial time-lag period and evaluating the slope of the line, as shown in Figure D.1. Observed reaction rates, k_{obs} , at other temperatures are calculated similarly.

FIGURE D.1. Calculation of first order reaction rate constant





REFERENCES

- Al-Riyami, Y. (1986), Personal Communication
- Andersen, T. and Knutsen, B. (1962), "Anion-Exchange Study: I. Adsorption of Some Elements in HBr Solutions," *Acta Chem. Scand.* **16** , pp. 849-854.
- Armstead, H. C. H. (1983), *Geothermal Energy*, E. & F. N. Spon Ltd, New York, NY.
- Baes, C. F. and Mesmer, R. E. (1976), *The Hydrolysis of Cations*, Wile Interscience, New York, NY.
- Behrens, H., Moser, H. and Wildner, E. (1977), "Investigation of Groundwater Flow with the Aid of Indium-EDTA-Complex Using Neutron Activation for the Determination of the Tracer," *J. Radioanal. Chem.*, **38** , pp. 491-498.
- Belous, R. (1974), "Westinghouse Mulling Plans to Up Output Capacity at Nuclear Plant," *Am. Metal Market*, **81** , pp. 23-28.
- Biedermann, G. (1956), "Studies on the Hydrolysis of Metal Ions. Part 14. The Hydrolysis of the Indium(III) Ion, In^{3+} ," *Arkiv For Kemi*, **9** , pp. 277-292.
- Brady, J. E. and Humiston, G. E. (1975), *General Chemistry: Principles and Structure*, Wiley Interscience, New York, NY.
- Brunauer, S., Emmett, P. H. and Teller, E. (1938), "The Adsorption of Gasses in Multimolecular Layers," *J. Am. Chem. Soc.*, **60** , pp. 309-316.
- Burke, D. P. (1972), "Catalysts Part 1. Petroleum Catalysts," *Chem. Week*, **111** , pp. 23-33.
- Busheina, I. S. and Headridge, J. B. (1981), "Determination of Indium by Hydride Generation and Atomic Absorption Spectrometry," *Talanta*, **29** , pp. 519-520.
- Butler, J. N. (1964), *Ionic Equilibrium A Mathematical Approach*, Addison Wesley, Menlo Park, CA.
- Butler, E. W. and Pick, J. B. (1982), *Geothermal Energy Development*, Plenum Press, New York, NY.
- Carty, A. J. and Tuck, D. G. (1975), "Coordination Chemistry of Indium," *Prog. Inorg. Chem.* **19** , pp. 243-337.

- Channell, J. K. (1970), *Activable Rare Earth Elements as Estuarine Water Tracers*, Ph.D. Dissertation, Civil Engineering Department, Stanford University, Stanford, CA.
- Chow, T. J. and Snyder, C. B. (1969), "Indium Content of Sea Water," *Earth and Planetary Science Letters*, **7** , pp. 221-223.
- Chynoweth, A. G. (1976), "Electronic Materials: Functional Substitutions," *Science*, **191** , pp. 725-732.
- Collie, M. J., Ed. (1978), *Geothermal Energy: Recent Developments*, Noyes Data Corporation, Park Ridge, NJ.
- Connolly, T. J. (1978), *Foundations of Nuclear Engineering*, Wiley Interscience, New York, NY.
- Cosner, S. R. and Apps, J. A. (1978), "Compilation of Data on Fluids from Geothermal Resources in the United States," U. S. Dept of Energy, W-7405-ENG-48.
- D'Amore, F., Celati, R., Calore, C. and Bertrami, R. (1983), "Effects of Natural Recharge on Gas Composition in the Larderello-Castelnuovo Area," *Proceedings Ninth Workshop on Geothermal Reservoir Engineering*, SGP-TR-74, Stanford University, Stanford, CA.
- De, A. K. and Sen, A. K. (1967), "Solvent Extraction and Separation of Gallium(III), Indium(III) and Thallium(III) with Tributylphosphate," **14** , pp. 629-635.
- DeGroot, M. H. (1975), *Probability and Statistics*, Addison-Wesley, Menlo Park, CA.
- DeVoe, J. R. and LaFleur, P. D., Eds. (1969), *Modern Trends in Activation Analysis*, National Bureau of Standards Special Publication 312, Vols. I & II, National Bureau of Standards, Washington, D. C.
- Drabaek, I. (1982), "Analysis and Time Stability of Activable Hydrospheric Tracers," *J. Radioanal. Chem.*, **75** , pp. 97-106.
- Dwyer, F. P. and Mellor, D. P. (1964), *Chelating Agents and Metal Chelates*, Academic Press, New York, NY.
- Dybczynski, R., Polkowska-Motrenko, H. and Shabana, R. M. (1977), "Influence of Temperature and Degree of Resin Crosslinking on the Anion Exchange of Phosphate Complexes of Ga(III) and In(III)," *J. Chromatogr.*, **134** , pp. 285-297.
- Dybczynski, R. and Sterlinska, E. (1974), "The Use of the Amphoteric Ion-Exchange Resin Retardion 11A8 for Inorganic Separations," *J. Chromatogr.*, **102** , pp. 263-271.
- Edwards, L. M., Chilingar, G. V., Rieke III, H. H. and Fertl, W. H. (1982), *Handbook of Geothermal Energy*, Gulf Publishing Co, Houston, TX.

- Ellis, A. J. and Mahon, W. A. J. (1977), *Chemistry and Geothermal Systems*, Academic Press, New York, NY.
- Erickson, S. J., Maloney, T. E. and Gentile, J. H. (1970), "Effect of Nitrilotriacetic Acid on the Growth and Metabolism of Estuarine Phytoplankton," *J. Water Pollut. Contr. Fed.*, **42** , pp. 329-335.
- Feitknecht, W. and Schinder, P. (1963), "Solubility Constants of Metal Oxides, Metal Hydroxides and Metal Hydroxide Salts in Aqueous Solution," *Pure and Applied Chemistry*, **6** , pp. 125-199.
- Ferri, D. (1972a), "On the Complex Formation Equilibria Between Indium(III) and Chloride Ions," *Acta Chem. Scand.*, **26** , pp. 733-746.
- Ferri, D. (1972b), "On the Hydrolysis of the Indium(III) Ion in Chloride Solutions," *Acta Chem. Scand.*, **26** , pp. 747-759.
- Florence, T. M., Batley, G. E. and Farrar, Y. J. (1974), "The Determination of Indium by Anodic Stripping Voltammetry," *Electroanal. Chem. and Interf. Electrochem.*, **56** , pp. 301-309.
- Forrester, P. G. (1964), "Materials for Plain Bearings," in *Modern Materials Advances in Development and Applications*, Vol. 4, Gosner, B. W. and Hausner H. H., Eds., Academic Press, New York, NY.
- Friedlander, G., Kennedy, J. W., Macias, E. S. and Miller, J. M. (1981), *Nuclear and Radiochemistry*, Wiley Interscience, New York, NY.
- Garvan, F. L. (1964), *Metal Chelates of Ethylenediaminetetraacetic Acid and Related Substances*, in "Chelating Agents and Metal Chelates," Edited by Dwyer, F. P. and Mellor, D. P., Academic Press, New York, NY.
- Gary, M., McAfee, R. and Carol, L. (1972), *Glossary of Geology*, American Geological Institute, Washington, D.C.
- Gudmundsson, J. S., and Hauksson, T. (1984), "Tracer Survey in Svartsengi Field 1984," Stanford Geothermal Program, Draft Paper.
- Gudmundsson, J. S., Johnson, S. E., Horne, R. N., Jackson, P. B. and Culver, G. G. (1983), "Doublet Tracer Testing in Klamath Falls, Oregon," *Proceedings, Ninth Workshop on Geothermal Reservoir Engineering*, SGP-TR-74, Stanford University, Stanford, CA.
- Gulati, M. S., Lipman, S. C. and Strobel, C. J. (1978), "Tritium Tracer Survey at the Geysers," *Geothermal Resources Council, Trans.*, **2** , pp. 237-240.
- Gupta, H. K. (1980), *Geothermal Resources: an Energy Alternative*, Elsevier Scientific, Amsterdam, The Netherlands.

- Hayashi, M., Mimura, T. and Yamasaki, T., (1978), "Geological Setting of ReInjection Wells in the Otake and the Hatchobaru Geothermal Field, Japan," *Geothermal Resources Council Trans.*, **2** , pp. 263-266.
- Holman, J. P. (1978), *Experimental Methods for Engineers*, McGraw-Hill, New York, NY.
- Home, R. N. (1981), "Tracer Analysis of Fractured Geothermal Systems," *Geothermal Resources Council, Trans.*, **5** , pp. 291-294.
- Home, R. N. (1982), "Geothermal ReInjection Experience in Japan," *J. Pet. Tech.*, **34** pp. 495-503.
- Home, R. N. (1984), "Reservoir Engineering Aspects of ReInjection," Prepared for the Seminar on Utilization of Geothermal Energy for Electric Power Production and Space Heating, Florence, Italy.
- Hunsbedt, A., Kruger, P. and London, L. (1975), "A Laboratory Model of Simulated Geothermal Reservoirs," Stanford Geothermal Program, SGP-TR-7, Stanford University, Stanford, CA.
- Irving, H. and Damodaran A. D. (1970), "The Extraction of Indium From Aqueous Halide and Thiocyanate Media by Solutions of Liquid Anion Exchangers in Organic Solvents," *Anal. Chim. Acta*, **50** , pp. 277-285.
- Irving, H. and Lews, D. (1967), "The Extraction of Indium Halides into Organic Solvents: Part VII. The Distribution of Indium Between Hydrochloric and Binary Solvent Mixtures Containing Isobutyl Ketone," *Arkiv For Kemi*, **28** , pp. 131-143.
- Ito, J., Kubota, Y. and Kurosawa, M. (1978), "The Tracer Tests Applied at the Onuma Geothermal Power Station, and the Considerations about the Geothermal Reservoir and Water Shielding of the Wells," *J. Jpn. Geotherm. Energy Assoc.*, **15** , pp. 25-33. (in Japanese, with English abstract)
- Jacklin, C. (1965), "Chelating Agents for Boiler Treatment - Research and Actual Use," *Proceedings Amer. Power Conf.*, **27** , pp. 807-816.
- Katz, S. A. (1981), "Neutron Activation Analysis: A Powerful Technique Becomes Available to Chemists," *Chem. Internat.*, **5** , pp. 13-19.
- Koenig, J. B. (1973), "Worldwide Status of Geothermal Resources Development," in *Geothermal Energy*, pp. 15-68. Kruger, P. and Otte, C., Eds., Stanford University Press, Stanford, CA.
- Korkish, J. and Hazan, I. (1964), "Anion Exchange Separation of Gallium, Indium and Aluminum," *Anal. Chem.* **36** , pp. 2308-2311.
- Kruger, P. (1971), *Principles of Activation Analysis*, Wiley Interscience, New York, NY.

- Kruger, P. and Otte, C., Eds. (1973), *Geothermal Energy*, Stanford University Press, Stanford, CA.
- Kruger, P. (1983), in *Geothermal Reservoir Engineering Research at Stanford University*, Third Annual Report, DOE Contract No DE-ATO3-80SF11459, Stanford Geothermal Program, **SGP-TR-76**, Stanford University, Stanford, CA.
- Lederer, C. M. and Shirley, V. S., Eds. (1978), *Table of Isotopes*, Wiley Interscience, New York, NY.
- Lee, M. and Burrell, D. C. (1972), "Extraction of Cobalt, Iron, Indium and Zinc from Seawater by Means of the Trifluoacetylaceton-Toluene System," *Anal. Chim. Acta*, **62** , pp. 153-161.
- Lin, S. R. and Feng, Q. S. (1984), "Indirect Polarographic Determination of Indium(III) in the Presence of Cadmium(II) by Utilising the Difference in their Kinetic Effects in an Appropriate Substitution Reaction," *Analyst*, **109** , pp. 97-98.
- Linn, T. A. and Schmitt, R. A. (1972), "Indium," in *Handbook of Geochemistry* Vol. 2, Wedepohl, K. H., Ed., Springer-Verlag, Berlin, Heidelberg.
- Lyle, S. J. and Shendrikar, A. D. (1965), "A Separation Scheme for Gallium, Indium, Thallium, Germanium, Tin and Lead by Solvent Extraction with N-Benzoyl-N-Phenylhydroxylamine," *Anal. Chim. Acta*, **32** , pp. 575-582.
- Macias-Chapa, L. (1981), "Radon Emanation in Geothermal Reservoirs," Engineers Thesis, Civil Engineering Department, Stanford University, Stanford, CA.
- Martell, A. E. and Smith, R. M. (1974), *Critical Stability Constants, Volume-I: Amino Acids*, Plenum Press, New York, NY.
- Martell, A. E., Motekaitis, R. J., Fried, A. R., Wilson, J. S. and MacMillan, D. T. (1975), "Thermal Decomposition of EDTA, NTA, and Nitrilotrimethylenephosphonic Acid in Aqueous Solution," *Can. J. Chem.*, **53** , pp. 3471-3476.
- Matthews, A. D. and Riley, J. P. (1970), "The Determination of Indium in Sea Water," *Anal. Chim. Acta*, **5** , pp. 287-294.
- Mazor, E. (1977), "Geothermal Tracing with Atmospheric and Radiogenic Gases," *Geothermics*, **5** , pp. 21-36.
- Mazor, E. and Truesdell, A. H. (1984), "Dynamics of a Geothermal Field Traced by Noble Gases: Cerro Prieto, Mexico," *Geothermics*, **13** , pp. 91-102.
- Means, J. L., Crerar, D. A. and Duguid, J. O. (1978), "Migration of Radioactive Wastes: Radionuclide Mobilization by Complexing Agents," *Science*, **200** , pp. 1477-1481.

- Means, J. L., Kucak, T. and Crerar, D. A. (1980), "Relative Degradation Rates of NTA, EDTA and DTPA and Environmental Implications," *Environ. Pollut. (Series-B)*, **1** , pp. 45-60.
- Means, J. L., Meast, A. S. and Crerar, D. A. (1985), "Role of Organics in Radionuclide Transport in Deep Groundwaters," *Scientific Basis for Nuclear Waste Management*, **3**
- McCabe, W. J., Barry, B. J. and Manning, M. R. (1983), "Radioactive Tracers in Geothermal Underground Water Flow Studies," *Geothermics*, **12** , pp. 83-110.
- Moeller, T. (1975), *The Lanthanides* , in "Comprehensive Inorganic Chemistry," Edited by Bailar, J. C., Emeleus, H. J., Sir Nyholm, R. and Trotman-Dickerson, A. F., Pergamon Press, Oxford, Great Britain.
- Muzzarelli, R. A., Raith, G. and Tubertini, O. (1970), "Separations of Trace Elements from Sea Water, Brine and Sodium and Magnesium Salt Solutions by Chromatography on Chitosan," *J. Chromatog.*, **47** , pp. 414-420.
- Navada, S. V., Kulkarni, V. P. and Rao, S. M. (1981), "Study of Tracer Analysis of Iodide by the Cerium(IV)-Arsenic(III) Catalytic Method and Indium-EDTA Neutron Activation Method for Hydrological Investigation," in *Trace Analysis and Technological Development*, Spec. Contrib. Pap. Int. Symp., pp. 257-271. Sankar, D. M., Ed., Wiley Interscience, New York, NY.
- Pribil, R. (1972), *Analytical Applications of EDTA and Related Compounds*, Pergamon Press, Oxford, Great Britain.
- Rakevic, M. (1970), *Activation Analysis*, CRC Press, Cleveland, OH.
- Rattonetti, A. (1974), "Determination of Soluble Cadmium, Lead, Silver, and Indium in Rainwater and Stream Water with the Use of Flameless Atomic Absorption," *Anal. Chem.*, **46** , pp. 739-742.
- Rees, H. D. and Gray, K. W. (1976), "Indium Phosphide: A Semiconductor for Microwave Devices," *IEE J. Solid-state Electron Devices*, **1** , pp. 1-8.
- Riley, J. P. and Taylor, D. (1968), "Chelating Resins for the Concentration of Trace Elements from Sea Water and their Analytical Use in Conjunction with Atomic Absorption Spectrometry," *Anal. Chim. Acta*, **40** , pp. 479-485.
- Rossotti, F. J. C. and Rossotti, H. (1956), "Studies on the Hydrolysis of Metal Ions: XV. Partition Equilibria in the System $^{114}\text{In}/\text{TTA}/\text{Benzene}$," *Acta Chem. Scand.*, **10** , pp. 779-792.
- Rudd, J. W. M. and Hamilton, R. D. (1972), "Biodegradation of Trisodium Nitrilotriacetate in a Model Aerated Sewage Lagoon," *J. Fish Res.*, **29** , pp. 1203-1207.
- Ryan, V. A., Ed. (1973), *Contemporary Activation Analysis*, Marcel Dekker, Inc., New York, NY.

- Satomi, K. (1982), "Radon Emanation Mechanism from Finely Ground Rocks," Engineers Thesis, Civil Engineering Department, Stanford University, Stanford, CA.
- Semprini, L. (1981), "Radon and Ammonia Transects in Geothermal Reservoirs," Engineers Thesis, Civil Engineering Department, Stanford University, Stanford, CA.
- Shaw, D. M. (1952), "The Geochemistry of Indium," *Geochemica and Cosmochemica Acta*, **2** , pp. 185-206.
- Shibata, S. (1960), "Solvent Extraction Behavior of Some Metal-1-(2-Pyridylazo)-Naphthol Chelates," *Anal. Chim. Acta*, **23** , pp. 367-369.
- Shibata, S. (1961), "Solvent Extraction and Spectrophotometric Determination of Metals with 1-(2-Pyridylazo)-2-Naphthol," *Anal. Chim. Acta*, **25** , pp. 348-359.
- Shumate, K. S., Thompson, J. E., Brookhart, J. D. and Dean C. L. (1970), "NTA Removal by Activated sludge - Field Study," *J. Water Poflut. Contr. Fed.*, **42** , pp. 631-640.
- Smith, C. I. and Carson, B. L. (1981), *Trace Metals in the Environment, Vol. 6-Cobalt*, Ann Arbor Science, Ann Arbor, MI.
- Smith, C. I., Carson, B. L. and Hoffmeister, F. (1978), *Trace Metals in the Environment, Vol. 5-Indium*, Ann Arbor Science, Ann Arbor, MI.
- Sniegowski, P. J. and Venezky, D. L. (1974), "GLC Analysis of Organic Chelating Agents in Steam Propulsion Systems," *J. Chromatogr. Sci.*, **12** , pp. 359-361.
- Sary, J. and Hladky, E. (1963), "Systematic Study of the Solvent Extraction of Metal β -Diketonates," *Anal. Chim. Acta*, **28** , pp. 227-235.
- Strelow, F. W. E. (1980), "Quantitative Separation of Galium from Uranium, Cobalt, Aluminum and Many Other Elements by Cation Exchange Chromatography in Mixtures of Hydrochloric or Hydrobromic Acid with Acetone," *Anal. Chim. Acta*, **113** pp. 323-329.
- Strelow, F. W. E. and Victor, A. H. (1971), "Quantitative Separation of Al, Ga, In and Tl by Cation Exchange Chromatography in Hydrochloric Acid-Acetone," *Talanta*, **19** pp. 1019-1023.
- Stumm, W. and Morgan, J. J. (1981), *Aquatic Chemistry*, 2nd Edition, Wiley Interscience, New York, NY.
- Sunderman, D. N. and Townley, C. W. (1960), *The Radiochemistry of Nuclear Science Series*, National Academy of Sciences-National Reserch Council, Washington, D.C.

- Thompson L. C. A. and Pacer, R. (1963), "The Solubility of Indium Hydroxide in Acidic and Basic Media at 25°C," *J. Inorg. Nucl. Chem.*, **25** , pp. 1041-1044.
- Tiedje, J. M. (1977), "Influence of Environmental Parameters on EDTA Biodegradation in Soils and Sediments," *J. Environ. Qual.*, **6** , pp. 21-26.
- Tsai, F., Juprasert, S. and Sayal, S. K. (1978), "A Review of the Chemical Composition of Geothermal Effluents," *Proceedings Second Workshop on Sampling Geothermal Effluents*, 600/7-78-121, EPA.
- Tyree, S. Y., Jr. (1967), "The Nature of Inorganic Solute Species in Water," in *Equilibrium Concepts in Natural Water Systems*, pp. 183-195, Gould, R. F., Ed., American Chemical Society, Washington, D. C.
- Venezky, D. L. and Moniz, W. B. (1969), "Nuclear Magnetic Resonance Study of the Thermal Decomposition of Ethylenedinitrilotetraacetic Acid and its Salts in Aqueous Solutions," *Anal. Chem.*, **41** , pp. 11-16.
- Venezky, D. L. and Moniz, W. B. (1970), NRL Report 7192, Naval Research Laboratory, Washington, D. C.
- Warren, C. B. and Malec, E. J. (1972), "Biodegradation of Nitrilotriacetic Acid and Related Imino and Amino Acids in River Water," *Science*, **176** , pp. 277-279.
- Weast, R. C., Ed. (1984), *Handbook of Chemistry and Physics*, CRC Press, Boca Raton, FL.
- Wendlandt, W. W. (1960), "Thermogravimetric and Differential Thermal Analysis of (Ethylenedinitrilo)tetraacetic Acid and Its Derivatives," *Anal. Chem.*, **32** , pp. 848-850.
- White, D. E. (1973), "Characteristics of Geothermal Resources," in *Geothermal Energy*, pp. 69-94. Kruger, P. and Otte, C., Eds., Stanford University Press, Stanford, CA.
- Wodkiewicz, L. and Dybczynski, R. (1974), "Anion-Exchange Behaviour of Some Elements on a Weakly Basic Anion Exchanger in Hydrobromic Acid Medium," *J. Chromatogr.*, **102** , pp. 277-285.
- Wylie, A. W. (1984) *Nuclear Assaying of Mining Boreholes, Methods in Geochemistry and Geophysics*, **21**, Elsevier Science Publishers B. V., Amsterdam, The Netherlands.